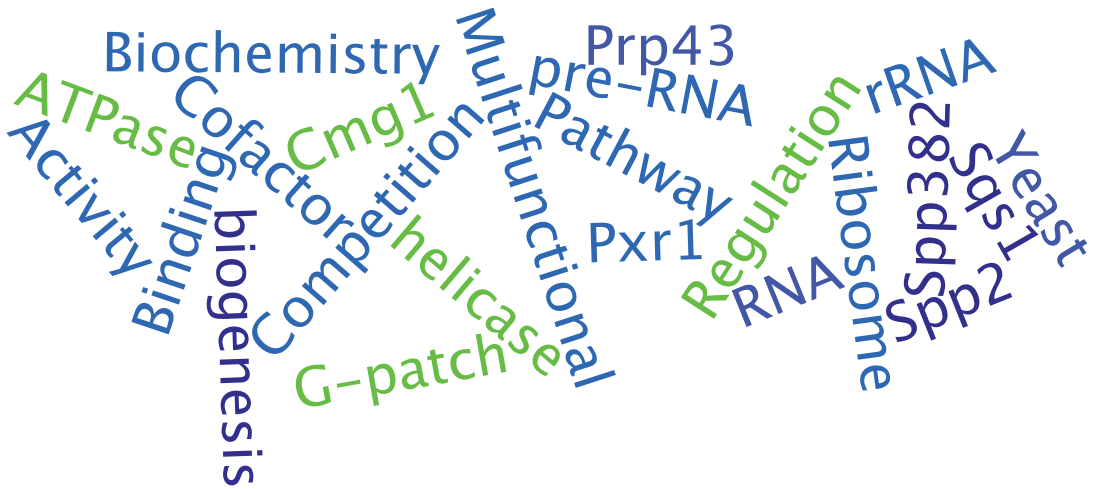


Annika Heininger

Characterisation of the yeast RNA helicase Prp43



Universitätsverlag Göttingen

Annika Heininger

Characterisation of the yeast RNA helicase Prp43

This work is licensed under a [Creative Commons Attribution-ShareAlike 4.0 International License](https://creativecommons.org/licenses/by-sa/4.0/).



Published by Universitätsverlag Göttingen 2016

Annika Heininger

Characterisation of the yeast RNA helicase Prp43



Universitätsverlag Göttingen
2016

Bibliographic information published by the Deutsche Nationalbibliothek
The Deutsche Nationalbibliothek lists this publication in the Deutsche
Nationalbibliografie; detailed bibliographic data are available on the Internet at
<http://dnb.dnb.de>

Address of the Author

Annika Heininger
Email: heininger.annika@t-online.de

Dissertation
for the award of the degree
“Doctor rerum naturalium”
of the Georg-August-Universität Göttingen
within the doctoral program Molecular Biology of Cells
of the Georg-August University School of Science (GAUSS)

Thesis Committee:

Prof. Dr. Markus T. Bohnsack	Department of Molecular Biology University Medical Centre Göttingen
Prof. Dr. Jörg Enderlein	III. Institute of Physics Georg-August-University Göttingen
Prof. Dr. Jörg Stülke	Department of General Microbiology Georg-August-University Göttingen

Members of the Examination Board:

Referee: Prof. Dr. Markus T. Bohnsack, 2nd Referee: Prof. Dr. Jörg Enderlein

Further members of the Examination Board:

Prof. Dr. Jörg Stülke; Prof. Dr. Peter Rehling; Prof. Dr. Detlef Doenecke;
PhD Nuno Raimundo

Date of the oral examination: 23. April 2015

This work is protected by German Intellectual Property Right Law.
It is also available as an Open Access version through the publisher's homepage and
the Göttingen University Catalogue (GUK) at the Göttingen State and University
Library (<http://www.sub.uni-goettingen.de>).
The license terms of the online version apply.

Set and layout: Annika Heininger
Cover design: Jutta Pabst
Cover picture: wordle.net

© 2016 Universitätsverlag Göttingen
<http://univerlag.uni-goettingen.de>
ISBN: 978-3-86395-237-2

INDEX

INDEX	I
INDEX OF TABLES	III
INDEX OF FIGURES	III
INDEX OF ABBREVIATIONS	IV
SUMMARY	VII
1. INTRODUCTION	1
1.1. RNA helicases	1
1.1.1. Families and architecture	1
1.1.2. RNA helicase function	2
1.1.3. RNA helicases in cellular pathways	3
1.1.4. Multifunctional RNA helicases	4
1.2. Pre-mRNA splicing	4
1.2.1. Spliceosome function and RNA helicases	5
1.2.2. The spliceosomal function of Prp43	7
1.3. Ribosome biogenesis	7
1.3.1. Ribosomal RNA processing and modification	8
1.3.2. Ribosome assembly and assembly factors	10
1.3.3. RNA helicases in ribosome biogenesis	11
1.4. G-patch proteins	12
1.4.1. Pxr1	13
1.4.2. Spp382	13
1.4.3. Sqs1	14
1.4.4. Spp2	14
1.5. Aims	15
2. MATERIALS AND METHODS	17
2.1. Materials	17
2.1.1. Chemicals	17
2.1.2. Media and buffers	17
2.1.3. Enzymes and kits	18
2.1.4. Antibodies	18
2.1.5. RNA oligonucleotides	18
2.1.6. DNA oligonucleotides	19
2.1.7. Plasmids	23
2.1.8. Bacterial strains	24
2.1.9. Yeast strains	24
2.2. Methods	25
2.2.1. Standard molecular biological and biochemical methods	25
2.2.2. Expression and purification of recombinant proteins	25
2.2.3. Pull-down assays from yeast	26
2.2.4. Protein interaction analysis	28
2.2.5. <i>In vitro</i> competition assay	28
2.2.6. Electromobility shift assay (EMSA)	29

Index

2.2.7.	Anisotropy measurements	29
2.2.8.	Steady-state ATP hydrolysis	30
2.2.9.	Preparation of yeast strains	31
2.2.10.	Serial dilution growth assay	32
2.2.11.	Survival assay	32
2.2.12.	Fluorescence microscopy	32
2.2.13.	RNA isolation	32
2.2.14.	Northern blots	33
2.2.15.	Preparation of enriched mitochondria	33
2.2.16.	Preparation of mitochondrial extracts	34
2.2.17.	Mitochondrial sublocalisation assay	34
2.2.18.	Mitochondrial localisation assay	35
3.	RESULTS	37
3.1.	Identification of Cmg1-interacting helicases	37
3.2.	Analysis of the Cmg1 - Prp43 interaction <i>in vitro</i>	38
3.3.	Identification of Cmg1 and Prp43 interacting domains	39
3.4.	Effect of Cmg1 on the RNA binding affinity of Prp43	42
3.5.	Prp43 ATPase activity in the presence of Cmg1	44
3.6.	Cmg1 cellular localisation	45
3.7.	Submitochondrial localisation of Cmg1	47
3.8.	Analysis of mitochondrial metabolism upon <i>cmg1</i> deletion or overexpression	48
3.9.	Cell growth and survival in <i>cmg1</i> deletion and overexpression strains	49
3.10.	Relocalisation of Cmg1 and Prp43 under apoptotic conditions	50
3.11.	Mitochondrial binding partners of Prp43 in apoptosis	52
3.12.	Prp43 localisation in the complex III deficient strain	54
3.13.	Localisation of Prp43 upon G-patch protein overexpression	55
3.14.	G-patch proteins compete for Prp43 binding	57
3.15.	Overexpression of G-patch proteins affects precursor ribosomal RNA processing	58
4.	DISCUSSION	61
4.1.	Characterisation of the orphan G-patch protein Cmg1	61
4.2.	Prp43 at mitochondria in apoptosis	64
4.3.	Recruitment of helicases to their target sites	66
4.4.	Regulation of RNA helicases by cofactor competition	67
4.5.	Conclusions	71
5.	REFERENCES	73
	PUBLICATION	83
	ACKNOWLEDGMENTS	85
	CURRICULUM VITAE	87

Index

INDEX OF TABLES

Table 1: <i>S. cerevisiae</i> G-patch proteins	13
Table 2: Media used for growth of yeast cultures	17
Table 3: Antibodies used in this study	18
Table 4: RNA oligonucleotides used in this study	18
Table 5: Oligonucleotides used for cloning	19
Table 6: Oligonucleotides used for mutagenesis	20
Table 7: Oligonucleotides used for DNA sequencing	20
Table 8: Oligonucleotides used for genomic GFP or RFP tagging	21
Table 9: Oligonucleotides used for promoter exchange and genomic protein-tagging	22
Table 10: Oligonucleotides used for pre-rRNA detection	23
Table 11: Plasmids used in this study	23
Table 12: List of strains used in this study	24
Table 13: Proteins with their tags for the appropriate experiment	29
Table 14: Determined dissociation constants of the anisotropy measurements	43
Table 15: Determined Michaelis-Menten constants and rate constants of the ATPase assays	45
Table 16: Mitochondrial Prp43 binding partners identified by mass spectrometry	53

INDEX OF FIGURES

Figure 1: SF1 and SF2 domain organisation and subclasses	2
Figure 2: Schematic representation of the two-step mechanism of pre-mRNA splicing	5
Figure 3: Overview of a pre-mRNA splicing cycle	6
Figure 4: Overview of yeast pre-rRNA processing	9
Figure 6: Schematic overview of ribosome assembly in <i>S. cerevisiae</i>	10
Figure 7: TAP-tagged Cmg1 co-precipitates Prp43 from yeast cells	37
Figure 7: Cmg1 interacts directly with Prp43	38
Figure 8: Scheme of Prp43 domain truncations and their functionality	40
Figure 9: Cmg1 G-patch domain interacts with both the N- and C-terminal domain of Prp43	42
Figure 10: Cmg1 stimulates the RNA affinity of Prp43	43
Figure 11: Cmg1 stimulates the ATPase activity of Prp43	45
Figure 12: Cmg1 colocalisation with a mitotracker	46
Figure 14: Submitochondrial localisation of Cmg1	47
Figure 15: Cmg1 is not required for mitochondrial metabolism	49
Figure 15: Cell growth and survival in <i>cmg1</i> deletion and overexpression strains	50
Figure 16: Cmg1 and Prp43 localisation to mitochondria in apoptosis	52
Figure 17: Prp43 associates with complex III	54
Figure 18: Prp43 is recruited to complex III under apoptotic conditions	55
Figure 19: Prp43 relocalisation upon G-patch protein overexpression	56
Figure 20: G-patch protein competition for Prp43 binding	58
Figure 21: Influence of G-patch protein overexpression on ribosome biogenesis	59
Figure 23: Scheme of Prp43 and G-patch protein localisation in exponential growth and apoptosis	63
Figure 23: Alignment of yeast protein G-patch domains	70

Index

INDEX OF ABBREVIATIONS

Abbreviation	Meaning	kDa	Kilodalton
%	Percent	l	Litre
(w/v)	Weight per volume	LB	Lysogeny broth
°C	Degrees Celsius	LSU	Large ribosomal subunit
2xYT	Two times yeast extract, tryptone/peptone medium	MES	2-(N-morpholino)ethanesulfo nic acid
A	Alanine	min	Minutes
aa	Amino acid	ml	Millilitres
Ala	Alanine	mM	Millimolar
APS	Ammonium persulfate	mm	millimetre
Asp	Aspartic acid	mRNA	Messenger RNA
ATP	Adenosine triphosphate	mV	Millivolt
bp	Base pair	ng	Nanogram
BSA	Bovine serum albumin	NLS	Nuclear localisation signal
cDNA	Complementary DNA	nm	Nanometre
DAPI	4', 6-diamidino-2- phenylindole	nmol	Nanomole
ddH ₂ O	Double-distilled water	NMR	Nuclear magnetic resonance
DNA	Deoxyribonucleic acid	NPC	Nuclear pore complex
dNTP	Deoxynucleoside triphosphate	nt	Nucleotide
dsRNA	Double stranded RNA	NTP	Nucleoside triphosphate
DTT	Dithiothreitol	OD ₆₀₀	Optical density at 600 nm
ECL	Enhanced chemiluminescence	OMM	Outer mitochondrial membrane
EDTA	Ethylenediaminetetraacet ic acid	P	Phosphate
EtBr	Ethidium bromide	PAGE	Polyacrylamide gel electrophoresis
EtOH	Ethanol	PBS	Phosphate buffered saline
g	Gram	PCR	Polymerase chain reaction
G	Glycine	PEG	Polyethylene glycol
GFP	Green fluorescent protein	PMSF	Phenylmethylsulfonyl fluoride
Glu	Glutamic acid	Pol I/II/III	RNA polymerase I/II/III
GTP	Guanosine-5'- triphosphate	Pre-mRNA	Precursor mRNA
h	Hours	Pre-rRNA	Precursor rRNA
H ₂ O ₂	Hydrogen peroxide	rcf	Relative centrifugal force
HCl	Hydrochloric acid	RFP	Red fluorescent protein
His	Histidine	RNA	Ribonucleic acid
HRP	Horseradish peroxidase	RNP	Ribonucleoprotein particle
IMM	Inner mitochondrial membrane	RP	Ribosomal protein
IMS	Mitochondrial intermembrane space	rpm	Revolutions per minute
IPTG	Isopropyl β-D-1- thiogalactopyranoside		
kb	Kilobases		

Index

rRNA	Ribosomal RNA
RT	Room temperature
s	Seconds
SDS	Sodium dodecyl sulphate
SDS-PAGE	SDS polyacrylamide gel electrophoresis
sec	Seconds
SEM buffer	Sucrose, EDTA, MOPS-KOH buffer
SF	superfamily
snoRNA	Small nucleolar RNA
snoRNP	Small nucleolar ribonucleoprotein particle
snRNA	Small nuclear RNA
snRNP	Small nuclear ribonucleoprotein particle
SSC	Saline-sodium citrate
ssDNA	Single stranded DNA
SSU	Small ribosomal subunit
TAE	Tris/Acetate/EDTA
TBE	Tris/Borate/EDTA
TBS	Tris-Buffered Saline
TBS-T	Tris-Buffered Saline-Tween
TEMED	Tetramethyl-ethylenediamine
Tris	Tris(hydroxymethyl)-aminomethane
tRNA	Transfer RNA
UV	Ultraviolet
V	Voltage
x	Times
YPD	Yeast extract, peptone/tryptone, dextrose medium
YPG	Yeast extract, peptone/tryptone, glycerol medium
YPGal	Yeast extract, peptone/tryptone, galactose medium
YPL	Yeast extract, peptone/tryptone, lactate medium
µg	Microgram
µl	Microlitre
µm	Micrometre
µM	Micromolar

SUMMARY

RNA helicases have many important roles in cell metabolism and are involved in numerous pathways, e.g. translation, pre-mRNA splicing and ribosome biogenesis. They function in remodelling of RNA-protein complexes by unwinding or annealing RNA duplexes or displacing proteins. Interestingly, an increasing number of RNA helicase have been shown to be required for more than one cellular pathway. Therefore, how these proteins are distributed between their different targets is a key question.

Protein cofactors have been suggested to recruit multifunctional RNA helicases to their substrates and regulate their activity. The best characterised family of helicase cofactors are the G-patch proteins, which all contain a glycine-rich domain. In yeast, five G-patch proteins have been identified, Spp382, Sqs1, Pxr1, Spp2 and the orphan G-patch protein YLR271W. Three of the G-patch proteins (Spp382, Sqs1 and Prx1) interact with Prp43, a multifunctional DEAH-box RNA helicase that is involved in the maturation of both ribosomal subunits and in several steps of pre-mRNA splicing, while Spp2 binds to the spliceosomal RNA helicase Prp2.

In this work the fifth G-patch protein YLR271W (Cmg1) was also found to interact with Prp43 and increase the RNA-dependent ATPase activity and the RNA affinity of the helicase. Localisation analysis revealed that Cmg1 is present in the mitochondrial intermembrane space as well as in the cytoplasm. Consistent with this, *Cmg1* overexpression leads to reduced cell survival implying that Cmg1 is a novel proapoptotic factor. Interestingly upon induction of apoptosis, Prp43 is sequestered in mitochondria, where it interacts with the complex III of the respiratory chain.

The finding that four G-patch proteins interact with the C-terminal region of Prp43 raised the possibility that they compete for binding to the helicase and by using *in vitro* assays such cofactor competition could be demonstrated. Consistent with this, overexpression of different yeast G-patch proteins leads to mislocalisation of Prp43 and defects in its target pathway of ribosome biogenesis. Together, these data suggest that protein cofactors can regulate the distribution and activity of RNA helicases in different pathways.

1. INTRODUCTION

1.1. RNA helicases

Helicases are enzymes that are generally thought to mainly unwind double-helical nucleic acids in a nucleoside triphosphate dependent (NTP) manner. RNA and DNA helicases are closely related and are found in all kingdoms of life.

1.1.1. Families and architecture

Based on their structure and function, helicases can be classified into six superfamilies (Singleton *et al.*, 2007). Eukaryotic RNA helicases are only found in SF1 and SF2. Furthermore, the superfamilies are subclassified based on typical sequences, structural and mechanistic features. The SF1 includes only one RNA helicase subclass, the Upf1-like family (Fairman-Williams *et al.*, 2010), whereas the SF2 contains five subclasses, namely DEAD-box, DEAH/RHA, NS3/NPH-II, Ski2-like and RIG-I-like (Fairman-Williams *et al.*, 2010). All share a conserved helicase core domain consisting of two RecA-like domains, which contain eight conserved motifs (Pyle, 2008; Fairman-Williams *et al.*, 2010; Cordin and Beggs, 2013). These motifs are necessary for RNA binding (motifs Ia, Ib, and IV) and unwinding, NTP/ATP binding and hydrolysis (motifs Q, I, II, V, and VI), and coupling the NTP/ATPase activity to RNA unwinding and remodelling (motif III; Cordin *et al.*, 2006; Cordin *et al.*, 2012). The largest SF2 RNA helicase subclass are the DEAD-box proteins, whose name derives from the amino-acid sequence (Asp-Glu-Ala-Asp) in motif II (Linder *et al.*, 1989; Cordin *et al.*, 2004). A special feature of DEAD-box helicases is their N-terminal Q-motif, which is essential for their ATP-binding (adenosine triphosphate-binding) and -hydrolysis function (Tanner *et al.*, 2003; Cordin *et al.*, 2004). Furthermore, the Ski2-like and DEAH-box RNA helicases share large C-terminal domains, which all include a winged helix and a ratchet domain that is also named the seven helix bundle (Walbott *et al.*, 2010; He *et al.*, 2010; Kudlinzki *et al.*, 2012; Johnson and Jackson, 2013). The winged helix domain may function as the central hub of the ring-like structure of the helicases and ensures structural stability (Woodman and Bolt, 2011; Johnson and Jackson, 2013). The ratchet domain is functionally important as it was shown that the deletion of the domain leads to reduction or even loss of the RNA unwinding activity (Small *et al.*, 2006; Büttner *et al.*, 2007; Pena *et al.*, 2009; Zhang *et al.*, 2009).

Introduction

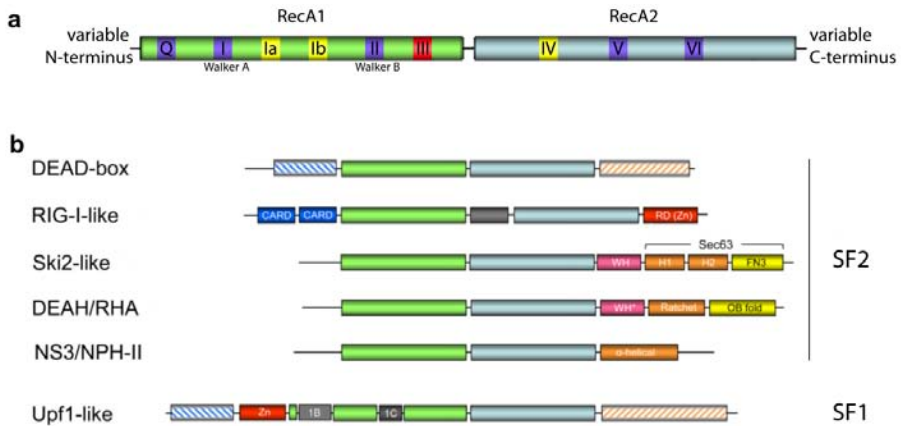


Figure 1: SF1 and SF2 domain organisation and subclasses

a) The helicase core is formed of two RecA-like domains (RecA1 and RecA2), which contain the Q-motif (only DEAD-box proteins), motifs I, II, Ia, Ib, III, IV, V, and VI. Motifs shown in purple are responsible for ATP/NTP binding and hydrolysis, motifs shown in yellow are necessary for RNA binding and the motif shown in red connect the NTP hydrolysis with RNA unwinding (Bleichert and Baserga, 2007; Cordin *et al.*, 2012). **b)** Examples of RNA subclasses and domain organisation. Modified from Fairman-Williams *et al.*, 2010. Domains are not drawn to scale.

Moreover, it is proposed that this domain also functions in regulating the directionality and the processivity of the DEAD-box RNA helicases (Büttner *et al.*, 2007; Pyle, 2008; Pena *et al.*, 2009; Cheung *et al.*, 2012; Jia *et al.*, 2012). The DEAH-box proteins are defined by the specific amino-acid sequence (Asp-Glu-Ala-His) in motif II (He *et al.*, 2010).

1.1.2. RNA helicase function

As the name helicase implies, one of their main function is duplex unwinding and indeed, many RNA helicases have been shown to unwind RNA duplexes *in vitro* (Pyle, 2008; Jankowsky and Putnam, 2010; Linder and Jankowsky, 2011). Two types of unwinding mechanisms are known: processive duplex unwinding and unwinding by local strand separation (Jankowsky, 2011).

Processive unwinding means that a helicase first binds to a single stranded RNA region close to its dsRNA target and then separates the RNA/RNA double strands by multiple NTP-dependent steps, often until it reaches the end of the duplex (Jankowsky, 2011). This type of unwinding is performed by the NS3/NPH-II RNA helicases, which possess an unwinding polarity in either the 3' to 5' or the 5' to 3' direction (Singleton *et al.*, 2007; Pyle, 2008; Jankowsky,

Introduction

2011). Unwinding polarity is also suggested for the Ski2-like, the RIG-I-like, the DEAH/RHA, and the Upf1-like helicases and they are therefore also thought to function by a processive unwinding mechanism (Singleton *et al.*, 2007; Pyle, 2008; Jankowsky, 2011). This hypothesis is supported by structural analysis of RNA helicases and in comparison to processive DNA helicases, for example in the case of the DEAH-box protein Prp43 and the DNA helicase Hel308 (Büttner *et al.*, 2007; Walbott *et al.*, 2010).

In contrast, DEAD-box proteins are non-processive RNA helicases. These helicases are directly loaded onto the RNA duplex and separate the dsRNA by local strand unwinding (Singleton *et al.*, 2007; Pyle, 2008; Jankowsky, 2011). For this process ATP binding is required but not ATP hydrolysis (Singleton *et al.*, 2007; Pyle, 2008; Jankowsky, 2011).

Besides the unwinding function, RNA helicases also participate in other aspects of RNA metabolism like remodelling and folding. Here, helicases serve as RNA chaperones by regulating RNA-protein interactions, disassembling ribonucleoprotein complexes (RNPs), and by promoting RNA annealing (Chamot *et al.*, 2005; Yang and Jankowsky, 2005; Jankowsky and Bowers, 2006; Yang *et al.*, 2007; Bhaskaran and Russell, 2007; Jankowsky, 2011). Furthermore, it was shown that RIG-I-like proteins translocate on dsRNA in an ATP-dependent manner without unwinding the strands, which is thought to reflect their role in RNA recognition (Yoneyama and Fujita, 2008; Myong *et al.*, 2009).

1.1.3. RNA helicases in cellular pathways

Since RNA is involved in multiple cellular processes the same is true for RNA helicases. During gene expression RNA helicases are required for transcription regulation (e.g. Sen1; Steinmetz *et al.*, 2001; Fuller-Pace, 2006), translation initiation (e.g. eIF4A), and termination (Linder and Slonimski, 1988; Blum *et al.*, 1989; Bleichert and Baserga, 2007). Furthermore, RNA helicases are involved in RNA quality control (e.g. Dbp2; Cloutier *et al.*, 2012), degradation (e.g. Ski2; Anderson and Parker, 1998) and small RNA processing (e.g. Sen1 and Mtr4; Ursic *et al.*, 1997; Jia *et al.*, 2012), where it is proposed that they unwind RNA duplexes to allow exonucleases access to their target sites. In addition, the RNA helicases Dbp5 and Sub2 have been shown to play a role in the export of mRNAs from the nucleus to the cytoplasm (Tseng *et al.*, 1998; Jensen *et al.*, 2001). Mitochondria possess their own RNA processing machinery and three RNA helicases, Mss116, Mrh4 and Suv3 are found in these organelles (Cordin

Introduction

et al., 2006; Bleichert and Baserga, 2007). However, the cellular processes involving most RNA helicases are pre-mRNA splicing and ribosome biogenesis. In yeast eight helicases are required for pre-mRNA splicing (Sub2, Prp5, Prp28, Brr2, Prp2, Prp16, Prp22, and Prp43; Cordin *et al.*, 2006; Cordin *et al.*, 2012; Cordin and Beggs, 2013). Moreover, in ribosome biogenesis 19 RNA helicases are involved, seven (Dbp4, Dbp8, Dhr1, Dhr2, Fal2, Rok1, and Rrp3) in the maturation of the small ribosomal subunit (SSU), ten (Dbp2, Dbp3, Dbp6, Dbp7, Dbp9, Dbp10, Drs1, Mak5, Mtr4, and Spb4) in the synthesis of the large ribosomal subunit (LSU) and two (Has1 and Prp43) helicases are involved in biogenesis of both subunits (Martin *et al.*, 2013; Rodriguez-Galan *et al.*, 2013).

1.1.4. Multifunctional RNA helicases

Interestingly, many of the RNA helicases have been found to have multiple cellular functions. At least six of the 39 putative yeast RNA helicases seem to be required for more than one pathway. Dbp2 and Mtr4 have functions in RNA decay as well as in ribosome biogenesis (Gross *et al.*, 2007; Cloutier *et al.*, 2012; Nag and Steitz, 2012; Martin *et al.*, 2013). Nuclear RNA export and translation termination have both been suggested to involve the RNA helicase Dbp5 (Tseng *et al.*, 1998; Bleichert and Baserga, 2007; Gross *et al.*, 2007). As already mentioned, Sub2 is connected to RNA export and pre-mRNA splicing (Jensen *et al.*, 2001; Cordin and Beggs, 2013), while Ded1 takes part in splicing and in translation initiation (Bleichert and Baserga, 2007). Last but not least, the DEAH-box RNA helicase Prp43, which is involved in several aspects of biogenesis of both the large and small ribosomal subunits and plays various roles in pre-mRNA splicing (Arenas and Abelson, 1997; Combs *et al.*, 2006; Bohnsack *et al.*, 2009; Martin *et al.*, 2013). However, how helicases are directed to their target pathways has remained elusive so far, but cofactors could play a crucial role. Moreover, whether multifunctionality of helicases allows co-regulation of pathways is not yet known.

1.2. Pre-mRNA splicing

Most eukaryotic genes are transcribed to produce precursor messenger RNAs (pre-mRNAs) that contain multiple non-coding sequences (introns) and coding sequences (exons). During mRNA maturation, introns have to be removed and the correct exons have to be joined. Introns almost always have a GU nucleotide sequence at their 5' end, which is called the 5' splice site and an AG

Introduction

sequence at their 3' end named the 3' splice site. The branch point is located upstream of the 3' splice site and contains an invariant sequence including an adenine nucleotide. Intron removal is achieved by a transesterification reaction that consists of two steps. First, the 5' splice site phosphodiester bond is attacked by the 2'-hydroxyl group of the conserved branch point adenosine (Figure 2). In the second step, the 3'-hydroxyl group of the free 5' exon attacks the phosphodiester bond at the intron lariat-3' exon.

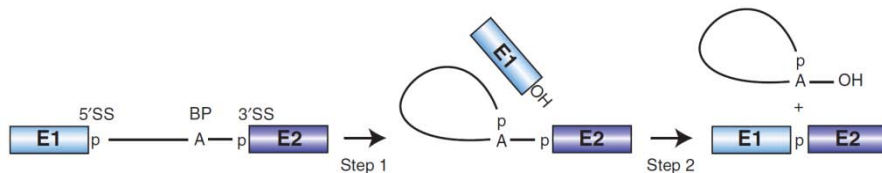


Figure 2: Schematic representation of the two-step mechanism of pre-mRNA splicing

Boxes represent exons (E1, E2) and lines represent the intron. The branch point (BP) adenosine is indicated by the letter A and the phosphate groups (p) at the 5' and 3' splice sites (5'SS and 3'SS) are marked. (Will and Lührmann, 2011)

Although the chemical reaction is rather simple, this critical process involves five small nuclear ribonucleoprotein particles (snRNPs; U1, U2, U4, U5, and U6) and many protein cofactors, which form together the major spliceosome. SnRNPs are composed of small nuclear RNAs (snRNAs), Sm and Lsm-proteins and complex specific proteins (Will and Lührmann, 2011; van der Feltz, Clarisse *et al.*, 2012; Matera and Wang, 2014).

1.2.1. Spliceosome function and RNA helicases

Splicing is a highly ordered processes with multiple steps and a number of intermediates, e.g. the spliceosomal E, A, B, B*, and C complexes, have been identified (Figure 3). First, complex E forms by the recognition of the 5' splice site of the pre-mRNA by the U1 snRNP. In the next step, the U2 snRNP joins the pre-spliceosome at the branch point to form the exon-defined complex (complex A). This process is facilitated by the DEAD-box helicases Sub2 and Prp5, which function by displacing spliceosomal cofactors and bring about RNP remodelling in an energy dependent manner. After complex A assembly, the pre-assembled tri-snRNP complex U4/U6.U5 is recruited to form the pre-catalytic spliceosome (complex B). In this step the U1 snRNP at the 5' splice site is replaced by U6 snRNP with the help of the DEAD-box protein Prp28. Furthermore, the Ski2-like helicase Brr2 disrupts the U4/U6 snRNP interaction

Introduction

enabling a new U6-U2 interaction to be formed. The release of the U4 and U1 snRNPs completes formation of the B^{act} complex. The DEAH-box helicase Prp2 is essential for remodelling the B^{act} complex into the activated spliceosome (B^* complex). The catalytically activated B^* complex catalyses the first transesterification reaction, which generates the complex C, containing the 5' exon and a 3' intron-exon lariat intermediate.

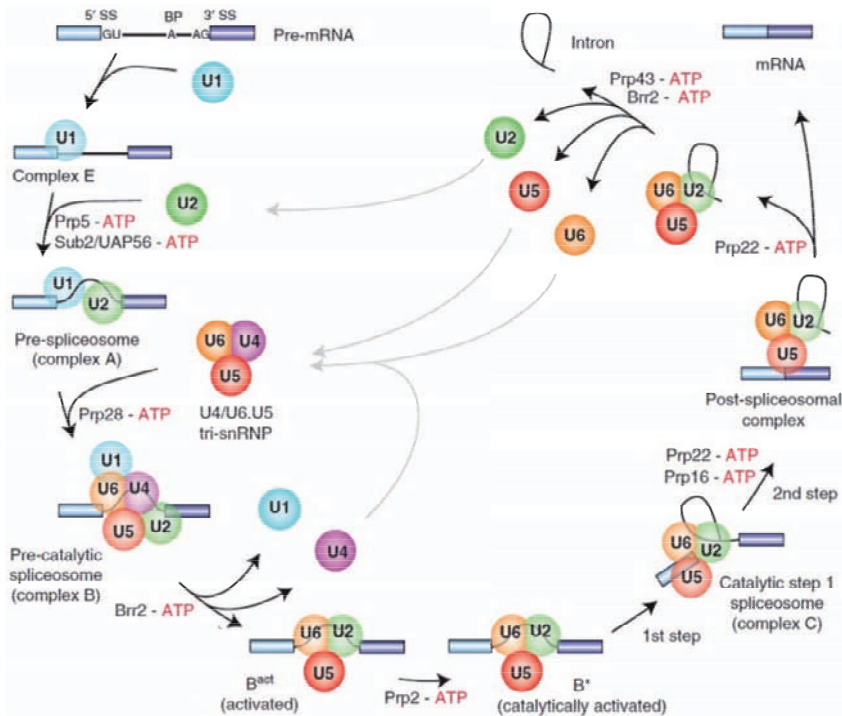


Figure 3: Overview of a pre-mRNA splicing cycle

Stepwise assembly of spliceosomal intermediate complexes is shown. SnRNPs are indicated by colored circles. Boxes represent exons (E1, E2) and the black line represents an intron. For each step the required RNA helicases are shown. (Will and Lührmann, 2011)

In the last step of pre-mRNA splicing, the second transesterification reaction occurs, forming the spliced mRNA in the post-spliceosomal complex. This process is dependent on rearrangements within the spliceosome by the helicases Prp16 and Prp22. In addition, Prp22 releases the mature mRNA from the U5 snRNP. Finally, all snRNPs have to be recycled in order to be functional in the next round of splicing. For this spliceosome disassembly the two RNA helicases Brr2 and Prp43 are necessary (Will and Lührmann, 2011; van der Feltz, Clarisse *et al.*, 2012; Matera and Wang, 2014).

1.2.2. The spliceosomal function of Prp43

The role of Prp43 in post-spliceosomal complex disassembly was first identified using a thermosensitive, catalytically inactive Prp43 mutant (G395E; Arenas and Abelson, 1997). This mutation was shown to increase the levels of pre-mRNAs and intron lariats while mature mRNA levels were not affected. Based on these data, it was concluded that Prp43 could play a role in spliceosome disassembly after mRNA release. Furthermore, it was shown that the RNA-dependent ATPase activity of Prp43 is necessary to make the lariat-intron RNA accessible for the debranching enzyme Dbr1 (Martin *et al.*, 2002). Subsequently, Prp43 was found to be part of the NTC-related proteins complex (NTR complex, Ntr1/Spp382, Ntr2, and Prp43; Tsai *et al.*, 2005), which together function in the recycling of the U2, U6 and U5 snRNPs (Boon *et al.*, 2006). In this context, Spp382 is important for the enzymatic function of Prp43 (Tanaka *et al.*, 2007) and Ntr2 targets Prp43 to the U5 snRNP by interacting with Brr2 (Tsai *et al.*, 2007). Furthermore, Prp43 is involved in the proofreading of the 5' splice site cleavage together with the DEAH-box protein Prp16 and is there necessary for discarding suboptimal spliceosomal substrates (Koodathingal *et al.*, 2010; Mayas *et al.*, 2010).

1.3. Ribosome biogenesis

Ribosomes are macromolecular RNA-protein complexes that are responsible for protein synthesis in every cell through all kingdoms of life. They translate the genetic information, encoded in DNA sequences and mRNAs into polypeptides and proteins. The ribosome, which is a ribozyme, is composed of a small (SSU, 40S) and large (LSU, 60S) ribosomal subunit (Nissen *et al.*, 2000). While the LSU of *Saccharomyces cerevisiae* contains three ribosomal RNAs (rRNAs; 5S, 5.8S, 25S rRNA) and 46 ribosomal proteins (RPs), the SSU contains the 18S rRNA and 33 RPs (Lafontaine and Tollervey, 2001; Kressler *et al.*, 2010; Woolford and Baserga, 2013). These two ribonucleoprotein particles (RNPs) have different functions within the ribosome; the SSU contains the decoding centre that monitors the codon:anticodon base pairing of the mRNA and transfer RNAs (tRNAs), while the LSU contains the peptidyl-transferase activity that is required for peptide bond formation within the nascent polypeptide chain (Lafontaine and Tollervey, 2001; Woolford and Baserga, 2013).

1.3.1. Ribosomal RNA processing and modification

During exponential growth a yeast cell produces approximately 2000 ribosomes per minute and therefore ribosome biogenesis is one of the most energy consuming processes in the cell (Warner, 1999). The synthesis of eukaryotic ribosomes is best studied in the yeast *Saccharomyces cerevisiae*. Ribosome biogenesis starts in the nucleolus with the transcription of the 35S precursor rRNA (pre-rRNA) by RNA polymerase I and the transcription of the 5S rRNA precursor by polymerase III (Venema and Tollervey, 1999; Warner, 1999). There are 100-200 copies of the rDNA coding for these rRNAs arranged in a tandem array on chromosome XII, which form the RDN locus (Long and Dawid, 1980). Within the 35S pre-rRNA transcript the 5' and 3' external transcribed regions (ETS) flank 18S, 5.8S and 25S rRNAs, which are separated by two internal transcribed spacers, ITS1 and ITS2 (Venema and Tollervey, 1999; Woolford and Baserga, 2013). An overview of the organisation of a single rDNA repeat and the pathway of pre-rRNA processing is given in Figure 4. Pre-rRNA cleavages at sites A₀, A₁ and A₂ can occur co-transcriptionally and lead to removal of the 5' ETS and separation of the precursors of the SSU rRNA (18S) and the LSU pre-rRNAs (5.8S and 25S). These cleavages generate the 20S pre-rRNA, which is exported to the cytoplasm where it is processed to the mature 18S rRNA by cleavage at site D, as well as the 27A₂ pre-rRNA. The processing of the 27SA₂ pre-rRNA is continued in the nucleus following two alternative pathways. The majority of the 3' product of A₂ cleavage is processed by cleavage at site A₃ in the ITS1 resulting in a 27SA₃ precursor. This short-lived intermediate is trimmed by a 5'-3' exoribonuclease to produce the 27SB_S rRNA precursor. In the minor pathway, the 27SB_L intermediate is produced by direct cleavage at site B_{1L}. These two pre-rRNA intermediates are further processed in an identical manner at sites C₁ and C₂ in ITS2, releasing the mature 25S rRNA and the 7S_S or 7S_L pre-rRNAs. Finally, the mature 5.8S_S and 5.8S_L rRNAs are produced by exonucleolytic digestion from the 3' end of the 7S intermediates (Venema and Tollervey, 1999; Fromont-Racine *et al.*, 2003; Woolford and Baserga, 2013). As well as removal of transcribed spacer regions by numerous endonucleolytic cleavages (e.g. Rnt1; Kufel *et al.*, 1999) and exonucleolytic processing (e.g. Rat1; Henry *et al.*, 1994), the maturation of the rRNAs also involves chemical modifications, mostly dedicated by the action of 75 small nucleolar RNPs (snoRNPs). These modifications are mainly added co-transcriptionally in the nucleolus. The box H/ACA snoRNPs mediate site-specific pseudouridylations (Ψ), whereas the box C/D snoRNPs perform

Introduction

methylation of the 2'-hydroxyl group of riboses (2'-O-methylation; Watkins and Bohnsack, 2012).

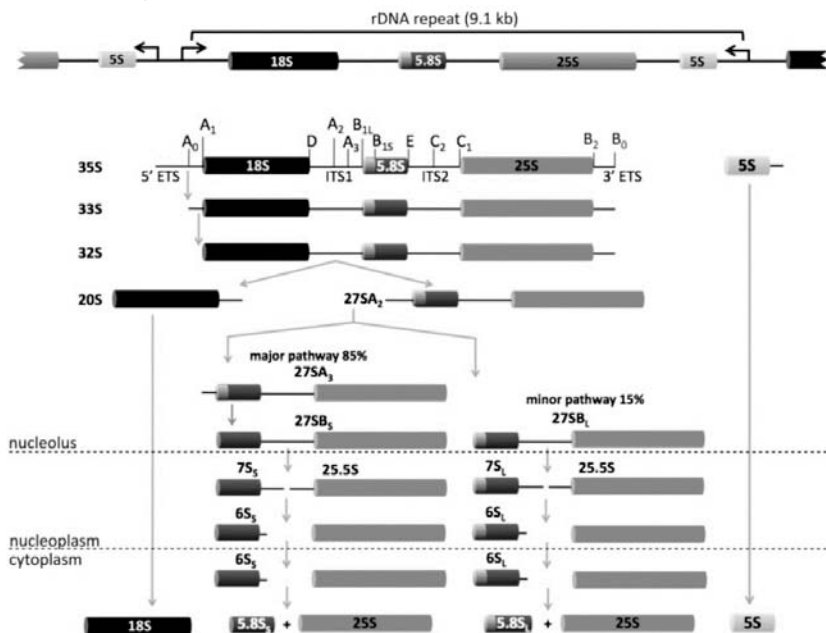


Figure 4: Overview of yeast pre-rRNA processing

The 35S pre-rRNA contains sequences for 18S, 5.8S, and 25S rRNAs (black, dark grey, and light grey cylinders). Separating external and internal transcribed spacers (ETS and ITS, solid lines) are removed during pre-rRNA processing. Pre-5S rRNA (white cylinder) is transcribed and processed independently. Endonucleolytic and exonucleolytic processing sites are indicated with letters. Pre-rRNA processing starts in the nucleolus, continues in the nucleoplasm and finishes in the cytoplasm. (Woolford and Baserga, 2013)

The small nucleolar RNA (snoRNA) component of the snoRNPs basepairs with the pre-rRNA target sites, while the snoRNP proteins provide the catalytic activity that is essential for the chemical reactions (Watkins and Bohnsack, 2012). Such modifications are important for ribosome maturation and functionality (Henras *et al.*, 2008; Watkins and Bohnsack, 2012; Woolford and Baserga, 2013). In addition to their functions in guiding rRNA modifications, some snoRNPs are required for pre-rRNA folding and processing (Watkins and Bohnsack, 2012).

1.3.2. Ribosome assembly and assembly factors

The processing and modifications of the rRNAs are coordinated with the assembly of the 79 ribosomal proteins (RPs). All RPs directly interact with the rRNA and their assembly is hierarchical. The 35S pre-rRNA transcript is co-transcriptionally bound by RPs and assembly factors, which forms the 90S pre-ribosome. Early pre-rRNA processing steps separate the 90S pre-ribosome into 43S and 66S pre-ribosomal particles. The pre-40S and pre-60S particles follow separate maturation pathways and are independently exported through the nuclear pore complex to the cytoplasm, where they undergo the final processing steps and rejoin to form a mature 80S ribosome (Figure 5; Woolford and Baserga, 2013).

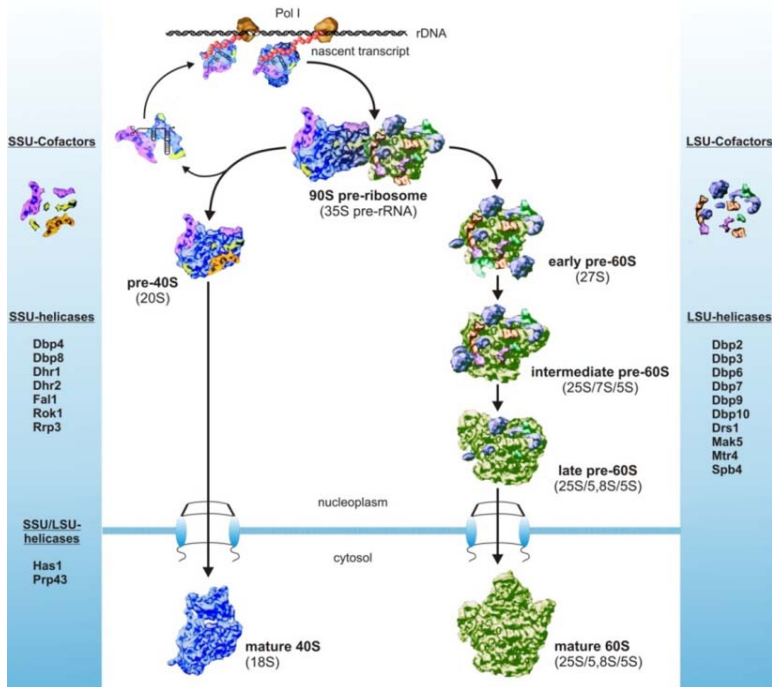


Figure 5: Schematic overview of ribosome assembly in *S. cerevisiae*

The 35S pre-rRNA is transcribed by RNA polymerase I and co-transcriptional assembly of RPs and cofactors leads to the formation of the 90S pre-ribosome. Early pre-rRNA cleavages separate precursors of the small (blue) and the large (green) subunits. RNA helicases involved in maturation of the SSU are listed to the left and those required for the maturation of the LSU are given on the right. Helicases involved in the maturation of both ribosomal subunits are given in the lower left. (PhD Thesis R. Martin, 2015)

Introduction

More than 200 proteinaceous non-ribosomal assembly factors coordinate ribosome assembly (Venema and Tollervey, 1999; Woolford and Baserga, 2013). As well as nucleases involved in pre-rRNA processing these cofactors include AAA-ATPases, GTPases, kinases, phosphatases, RNA-binding proteins, putative scaffolding proteins, methyltransferases, and RNA helicases (Venema and Tollervey, 1999; Kressler *et al.*, 2010; Woolford and Baserga, 2013). Together, these cofactors also function in pre-ribosome rearrangement, protein exchange, protein release, post-translational protein modification, rRNA modification, and subunit export (Venema and Tollervey, 1999; Henras *et al.*, 2008; Kressler *et al.*, 2010; Woolford and Baserga, 2013).

1.3.3. RNA helicases in ribosome biogenesis

Most RNA helicases involved in ribosome biogenesis are essential for cell survival (Martin *et al.*, 2013). Depletion of individual RNA helicases causes pre-rRNA processing defects implying that these DEAH- and DEAD-box proteins have important functions in ribosome synthesis. Based on these pre-rRNA processing defects ten helicases (Dbp2, Dbp3, Dbp6, Dbp7, Dbp9, Dbp10, Drs1, Mak5, Mtr4, Spb4) are proposed to participate in synthesis of LSU particles, seven (Dbp4, Dbp8, Dhr1, Dhr2, Fal1, Rok1, Rrp3) are implicated in 40S biogenesis, and two RNA helicases, namely Has1 and Prp43, contribute to the biogenesis of both subunits (Figure 5; Martin *et al.*, 2013). These RNA helicases are proposed to function in structural remodelling of rRNA secondary structure/pre-ribosomal complexes and several (Rok1, Dbp4, Prp43 and Has1) have been shown to be required for the release of particular snoRNAs from pre-ribosomes (Kos and Tollervey, 2005; Liang and Fournier, 2006; Bohnsack *et al.*, 2008; Bohnsack *et al.*, 2009). Of these, Prp43 is the best studied RNA helicase involved in ribosome biogenesis. Mutational and depletion analysis of Prp43 revealed 35S and 23S pre-rRNA accumulation, while downstream pre-rRNA levels were reduced (Lebaron *et al.*, 2005; Combs *et al.*, 2006; Leeds *et al.*, 2006). These findings are in line with the association of TAP-tagged Prp43 with the 35S, 27S and 20S pre-rRNAs (Lebaron *et al.*, 2005; Leeds *et al.*, 2006). Furthermore, UV cross-linking and analysis of cDNA (CRAC; Granneman *et al.*, 2009; Bohnsack *et al.*, 2012) identified interaction sites of Prp43 with 18S rRNA, 25S rRNA and snoRNA species (Bohnsack *et al.*, 2009). At the sites in 25S pre-rRNA Prp43 was found to be necessary for release of a cluster of box C/D snoRNAs (snR39, snR39b, snR50, snR55, snR59, snR60, and snR72) from pre-ribosomes. Interestingly, the levels of two snoRNAs, snR64 and snR67, which guide modifications close to Prp43 crosslinking sites, were

reduced on pre-ribosomes. Together with the 25S rRNA C₂₃₃₇ methylation defect reported in a *prp34-Q423N* mutation strain (Leeds *et al.*, 2006), this suggests that Prp43 also functions in remodelling of pre-ribosomal complexes enabling snoRNAs to access their target sites. Prp43 is also implicated in structural remodelling in late SSU particles, where it is proposed to unwind rRNA structures to enable the endonuclease Nob1 to gain access to its target site at the 3' end of the 18S rRNA sequence (Pertschy *et al.*, 2009). Strikingly, for some functions in ribosome biogenesis, Prp43 appears to act together with cofactors such as Sqs1 and Pxr1 (Lebaron *et al.*, 2009; Pertschy *et al.*, 2009; sections 1.4.1 and 1.4.3 for further details).

1.4. G-patch proteins

Several RNA helicases have been shown to be regulated by specific cofactors. For example, in ribosome biogenesis the helicase Rok1 is suggested to be regulated by Rrp5 (Young *et al.*, 2013), while both the activity of Dbp8 and its recruitment to its targets are proposed to be stimulated by Esf2 (Granneman *et al.*, 2006). In addition, the translation initiation factor eIF4G binds to the DEAD-box protein eIF4A and stimulates its unwinding activity (Dominguez *et al.*, 1999; Hilbert *et al.*, 2011). Furthermore, the RNA export factor Gle1 activates the RNA helicase Dbp5 (Alcázar-Román *et al.*, 2006), while the function of the DEAD-box protein Ded1 is inhibited by Gle1 (Bolger and Wentz, 2011).

A specific group of RNA helicase cofactors are the G-patch proteins. By systematic studies of protein sequences a highly conserved element of approximately 48 amino acids (aa), containing six specifically distributed glycine residues, was discovered. Proteins with this element are called G-patch proteins and are found in eukaryotes and type D retroviruses. Most G-patch proteins are thought to be RNA-associated proteins although these interactions are not necessarily mediated by the G-patch domain (Aravind and Koonin, 1999).

In the yeast *S. cerevisiae* five proteins containing this G-patch motif have been identified (Table 1). Interestingly, four out of five of these G-patch proteins function as RNA helicase cofactors. However, the fifth G-patch protein (YLR271W) is so far uncharacterised.

Introduction

Table 1: *S. cerevisiae* G-patch proteins

Name	Alias	Systematic name	Pathway
Pxr1	Gno1	YGR280C	Ribosome biogenesis
Sqs1	Pfa1	YNL224C	Ribosome biogenesis
Spp382	Ntr1	YLR424W	Pre-mRNA splicing
Spp2	-	YOR148C	Pre-mRNA splicing
-	-	YLR271W	uncharacterised

1.4.1. Pxr1

Based on the identification of C-terminal KK(E/D) repeats and its nucleolar localisation, Pxr1 was suggested to be a ribosome biogenesis cofactor (Guglielmi and Werner, 2002). Pxr1 has also been shown to be required for pre-rRNA processing steps downstream of the 27SA₂ intermediate (Guglielmi and Werner, 2002; Chen *et al.*, 2014). Interestingly, the G-patch domain of Pxr1 was found to be necessary for pre-rRNA processing as well as mediating interactions with the RNA helicase Prp43 (Guglielmi and Werner, 2002; Lebaron *et al.*, 2005; Chen *et al.*, 2014). Moreover, this interaction stimulates the Prp43 ATPase activity (Chen *et al.*, 2014). These findings lead to the suggestion that the functions of Pxr1 in ribosome biogenesis are coupled to those of Prp43 (Chen *et al.*, 2014). In addition, Pxr1 has been suggested to be involved in processing of the snoRNAs U18 and U24 (Guglielmi and Werner, 2002). Furthermore, the human homologue of Pxr1, PINX1, has been shown to play a role in telomere regulation (Zhou and Lu, 2001; Cheung *et al.*, 2012), but it is not yet known if this function involves interaction with an RNA helicase.

1.4.2. Spp382

Spp382 was first identified as a protein that interacts with Ntr2 and Prp43 in the NTR complex (NTC-related complex; Tsai *et al.*, 2005; Boon *et al.*, 2006). This complex is required for the post-catalytic step of intron-lariat release in pre-mRNA splicing (Tsai *et al.*, 2005). The name Spp382 derives from its function as a suppressor of *prp38-1* mutation, in which Prp38 is a protein required for U4/U6 snRNA dissociation from B^{act} complexes (Xie *et al.*, 1998; Pandit *et al.*, 2006). It was shown that the G-patch domain (aa 51-110) of Spp382 is sufficient for interaction with the DEAH-box protein Prp43 (Tsai *et al.*, 2005; Tanaka *et al.*, 2007; Christian *et al.*, 2014). Furthermore, the Spp382 G-patch domain enhances the RNA unwinding and ATPase activity of Prp43 *in vitro* by binding the C-terminal part of the helicase (Tanaka *et al.*, 2007; Christian *et al.*, 2014). Besides its role in pre-mRNA splicing, Spp382 and its human homologue TFIP11 are suggested to function in the regulation of non-

Introduction

homologous end joining (NHEJ) by sequestering the DNA ligase cofactor Lif1p in an inactive complex (Herrmann *et al.*, 2007).

1.4.3. Sqs1

The YNL224C-encoded protein impairs *spp382-1*-based suppression and was therefore named Sqs1 (squelch of splicing suppression; Pandit *et al.*, 2006). A direct interaction between Sqs1 and Prp43 was identified (Lebaron *et al.*, 2005; Lebaron *et al.*, 2009; Walbott *et al.*, 2010). In detail, the N-terminal (aa 1-202) and C-terminal (aa 574-767) region of Sqs1 were shown to interact independently with the C-terminal part of Prp43 (Lebaron *et al.*, 2009; Walbott *et al.*, 2010). Only the Sqs1 C-terminus, containing the G-patch domain, is necessary to stimulate the Prp43 ATPase and unwinding activity (Lebaron *et al.*, 2009). Furthermore, a genetic interaction between Sqs1, the pre-40S factor Ltv1, Prp43, and the nuclease Nob1 was shown (Lebaron *et al.*, 2009; Pertschy *et al.*, 2009). Immunoprecipitations showed that Sqs1 is associated with 20S pre-rRNA, together with Prp43, indicating a role in SSU biogenesis (Lebaron *et al.*, 2005; Lebaron *et al.*, 2009). Further studies showed that Sqs1 overexpression reduces levels of 23S pre-rRNA, while deletion of Sqs1 protein leads to 20S pre-rRNA accumulation (Pandit *et al.*, 2009; Pertschy *et al.*, 2009). In addition, tandem affinity purification with TAP-tagged Sqs1 identified not only proteins of pre-40S particles, but also of pre-60S and 90S pre-ribosomal particles (Lebaron *et al.*, 2009). This is in line with the findings that Sqs1 overexpression reduces levels of 27SA₂ pre-rRNA of the LSU (Pandit *et al.*, 2009). Interestingly, in Δ *pxr1* cells the steady-state levels of Sqs1 are strongly decreased and Sqs1 is truncated at the N-terminal part of the protein (Lebaron *et al.*, 2009). Moreover, an interaction between the G-patch proteins Spp382 and Sqs1 is proposed (Herrmann *et al.*, 2007; Pandit *et al.*, 2009).

1.4.4. Spp2

The only G-patch protein that was not shown to interact with Prp43 so far is Spp2. This protein is required for the first catalytic step in pre-mRNA splicing (Roy *et al.*, 1995). Spp2 enters the spliceosome independently (Roy *et al.*, 1995). It physically interacts with the C-terminal fragment of the DEAH-box protein Prp2, which is also necessary for the first transesterification reaction (Yean and Lin, 1991; Roy *et al.*, 1995; Silverman *et al.*, 2004). The leucine at position 109 of Spp2, which is part of the G-patch domain, is critical for this interaction (Silverman *et al.*, 2004). Like the interactions of Pxr1, Sqs1 and Spp382 with

Prp43, the interaction of Spp2 with Prp2 stimulates the ATPase activity of the helicase (Roy *et al.*, 1995).

1.5. Aims

RNA helicases are involved in many processes within the cell, e.g. transcription, translation, ribosome biogenesis, and pre-mRNA splicing. It has emerged that several RNA helicases function in more than one pathway. A key example is the DEAH-box protein Prp43 that is involved in the synthesis of the large and the small ribosomal subunit as well as in pre-mRNA splicing. This raises the question how helicases are recruited to their RNA targets and how their activity in the different pathways is regulated, but cofactors are likely to play a major role. Relatively few RNA helicase cofactors have been identified so far, but a family of proteins called the G-patch proteins have been shown to interact with RNA helicases. In yeast, five G-patch proteins are known: three interact with the multifunctional RNA helicase Prp43, one interacts with the RNA helicase Prp2 and the fifth is uncharacterised so far.

The objectives of this study were to characterise the orphan G-patch protein YLR271W (here named Cmg1) and to study the interaction between the ATP-dependent RNA helicase Prp43 and the five G-patch proteins in yeast *S. cerevisiae*.

This work therefore aimed to:

- Identify the RNA helicase interaction partner of Cmg1
- Characterise the helicase-cofactor interaction biochemically
- Determine the sub-cellular localisation of Cmg1
- Study the role of G-patch protein cofactors in recruiting and regulating Prp43 in its target pathways

2. MATERIALS AND METHODS

2.1. Materials

2.1.1. Chemicals

Chemicals used for experiments were purchased from Sigma-Aldrich Chemie GmbH (Munich, Germany), VWR International GmbH (Darmstadt, Germany), Carl Roth GmbH + Co. KG (Karlsruhe, Germany), and AppliChem GmbH (Darmstadt, Germany). Complete™ Protease Inhibitor Cocktail was ordered from Roche (Penzberg, Germany), ³²P-γ-ATP (6000Ci/mmol) was purchased from Perkin Elmer (Waltham, MA, USA) and chemiluminescence HRP substrate was bought from Merck Chemicals GmbH (Schwalbach, Germany).

2.1.2. Media and buffers

For bacterial growth 2xYT (2x Yeast Extract Tryptone) medium was prepared as described by Sambrook *et al.*, 1989. Media listed in Table 2 and drop-out media, for selective yeast growth, were prepared according to Treco and Lundblad, 2001. Yeast extract without amino acids and supplements were purchased from ForMedium™ (Norfolk, United Kingdom). All components were solubilised in ultrapure water and sterilised for 20 min at 120 °C.

Table 2: Media used for growth of yeast cultures

Acronym	Recipe
YPD	1 % yeast extract, 2 % peptone/tryptone, 2 % dextrose
YPG	1 % yeast extract, 2 % peptone/tryptone, 3 % glycerol
YPL	1 % yeast extract, 2 % peptone/tryptone, 3 % lactate pH 5.5 with NaOH
YPGal	1 % yeast extract, 2 % peptone/tryptone, 2 % galactose
Synthetic glucose medium	1.9 g/l yeast nitrogen base without amino acids and ammonium sulphate, 5 g/l ammonium sulphate, 0.79 g/l Complete supplement mixture drop out: complete
Drop-out media:	1.9 g/l yeast nitrogen base without amino acids and ammonium sulphate, 5 g/l ammonium sulphate and:
-His	0.77 g/l complete supplement mixture drop out: -His
-Leu	0.69 g/l complete supplement mixture drop out: -Leu
-Ura	0.77 g/l complete supplement mixture drop out: -Ura

Materials and methods

2.1.3. Enzymes and kits

Restriction enzymes were purchased from Fisher Scientific - Germany GmbH (Schwerte, Germany) or New England Biolabs GmbH (Frankfurt a. M., Germany). DNA purification from agarose gels was performed with a gel extraction kit from QIAGEN GmbH (Hilden, Germany).

2.1.4. Antibodies

Primary antibodies were used to identify specific proteins, while secondary antibodies fused to HRP enable detection by chemiluminescence. A list of antibodies used in this study is given in Table 3.

Table 3: Antibodies used in this study

Antibody target	Detection of/Marker for	Source
Atp5	Mitochondrial complex V	P. Rehling
Cox2	Mitochondrial complex IV	P. Rehling
HA	HA-tagged proteins	Convance Inc.
Mic10	Mitochondrial intermembrane space	P. Rehling
Mouse antigen HRP	secondary antibody	Jackson ImmunoResearch Europe Ltd.
PAP	ProteinA-tagged proteins	Sigma-Aldrich Chemie GmbH
Pgk1	Cytoplasm	Life Technologies GmbH
Prp43	Prp43	R. Lühmann
Qcr8	Mitochondrial complex III	P. Rehling
Rabbit antigen HRP	secondary antibody	Jackson ImmunoResearch Europe Ltd.
Tim21	Inner mitochondrial membrane	P. Rehling
Tim44	Inner mitochondrial membrane	P. Rehling
Tom70	Outer mitochondrial membrane	P. Rehling

2.1.5. RNA oligonucleotides

RNA oligonucleotides used in this study were purchased from Integrated DNA Technologies (Leuven, Belgium). Names and sequences of RNA oligonucleotides can be found in Table 4.

Table 4: RNA oligonucleotides used in this study

Name	Sequence 5' to 3'
18S H29 32nt	GUAAUGAAAGUGAACGUAAAAACAAAAACAAAAAC
18S H29 11nt fl.	GUAAUGAAAGU-Atto647
18S H29 11nt	GUAAUGAAAGU

Materials and methods

2.1.6. DNA oligonucleotides

DNA oligonucleotides used in this study were purchased from Sigma-Aldrich Chemie GmbH (Munich, Germany). Furthermore, oligonucleotides were used for several different purposes and are grouped accordingly. Oligonucleotides listed in Table 5 were used for PCR amplification of genes for cloning.

Table 5: Oligonucleotides used for cloning

Name	Sequence 5' to 3'
RP Gno1_XhoI	ATATACTCGAGATCATTGGTGATCATGAAGATTTC
FP Gno1_NcoI	ATATACCATGGGACTGGCAGCAACCCG
RP A5 Cmg1 1-85	TTCCATCATTTTATAACCCCTGGGC
FP A5 Cmg1 1-85	TGACCCGGGGAGATCTCATCACC
FP Spp382 51-110 NcoI	TATATCCATGGGTAATGCCCAACGATCTCAAAATTAAC
RP Spp382 51-110 HindIII A5	TATATAAGCITTCTAGTTGGTATTTGAAAACATTCCTAGACC
RP Spp382 51-110 BamHI A15	ATATAGGATCCGTTGGTATTTGAAAACATTCCTAGACC
FP Spp2 92-157 NcoI	TATATGCCATGGTCACCGAAAAAGAATATAATGAG
RP Spp2 92-157 BglII	TATATAGATCTCAGTTTATTGCCTTATTTAACTGGC
RP Sqs1 705-767 A101	CATGGACCCTTGGAAGTAGAGGTTTTC
FP Sqs1 705-767	GTTAAAGAAGGTGAGATTGTTGGTCAAAAC
FP Gno1 1-72 A8 Stop	TAAAAGCTTAATTAGCTGAGCTTGG
RP Gno1 1-72	TAATTTAGCACCGAGCCCAAC

Materials and methods

Table 6 provides the primers used in this study for mutagenesis of plasmids for recombinant protein expression.

Table 6: Oligonucleotides used for mutagenesis

Name	Sequence 5' to 3'
FP Prp43 1-657/752	ATATATCCCGGGGAGATCTCATCACCATCAC
FP Prp43 92-767	ATATATCCATGGAATTGCCAGTACATGCCCAG
RP Prp43 1-657	ATATATCCCCGGGCTACTAGAAAAACCCAGACGCAAGAGCC
RP Prp43 1-752	ATATATCCCGGGCTACTCGTTTAATCTATCAACTTTTTCCTTGATCC
RP Prp43 92-767	TATATACCATGGATCCCTGAAAAATAAAGGTTTTCTC

In Table 7 the list of sequencing primers that were used in this study is given. Further sequencing primers were provided directly by GATC Biotech AG (Konstanz, Germany).

Table 7: Oligonucleotides used for DNA sequencing

Name	Sequence 5' to 3'
FSP A5 RFP	CGAGGGTTCGCCACTCCACCG
FSP Prp43 110	ATCCAAAACAGCATCCTCTTCC
FSP Prp43 1256	TTGTTTCCCCTATCTCCAAG
FSP Prp43 1403	AATTTATCCTCCACCGTTCTAG
FSP Prp43 1786	TCAAATCGGATGAAGCTTATG
FSP Prp43 1952	TTTGACAACATCAGAAAAGGC
FSP Prp43 34	GAAGATTCTCGTCCGAACACC
FSP Prp43 505	AGGAAATGGATGTCAAGTTGG
FSP Prp43 592	ATATGACTGATGGTATGTTGTTG
FSP Prp43 716	TGAAGCAAGTAGTCAAGAGGAG
FSP Prp43 962	ATGAAATTGAAGACGCTGTCAG
FSP Spp382 1428	AGACATAATGACCCCATCTACG
FSP Spp382 423	AAGTCAAATTCAAATAAACCTCC
FSP Spp382 927	CTCGCATATAGAATGGATACAAC
FSP Sqs1 1424	CAGATATTCCGATTTCTGATTC
FSP Sqs1 400	TACGATCCATCCCACAATATG
FSP Sqs1 872	TCCAACGTATTACATGGTATGC

Materials and methods

In Table 8 and Table 9 oligonucleotides are listed that were used for PCR amplification of tag/promoter cassettes used in the preparation of yeast strains.

Table 8: Oligonucleotides used for genomic GFP or RFP tagging

Name	Sequence 5' to 3'
F2_Gno1_Lt	GGGCCGCGTTGATGGACTCCAAGGCACTGAATGAGAT CTTTATGATAACAAACGACCGGATCCCCGGGTTAATTA A
R1_Gno1_Lt	CTTGCTGCGTGTGCAGACTGGCCAGCTGCTCACACAAT GAAACGCAATGGAATGTGAATTCGAGCTCGTTTAAAC
F2_Spp382_Lt	GGGTGGAGGATTCAGTGGGACCTTTAAGCCAATTTAT TTATGGGCCCTTGACCTCCGGATCCCCGGGTTAATTA CAATTTTGTTTTTCGACAATAATATATAAATCGTGCCTA TCTCACCTCTTTTATAGGTACTTTGAATTCGAGCTCGTT TAAAC
FP Prp43g Y	GATTAAACGAGTTGAAACAAGGTAAAAACA AAAAGAA GAGTAAAGCACTCCAAGAAACGGATCCCCGGGTTAATTA A
RP Prp43g Y	CTATGAAATAGTCTTATAAAATTTATATAAATCTATTTTTT TTTTTTTTTCGACACAAAATGTGAATTCGAGCTCGTTT AAC
FP Cmg1-GFP_Anpl1-cRFP	CGACAAGAACAAGAAAAACATCCTAAAGAAGTTCCAT TAGACTTCGACCCTGATAGAAACCGGATCCCCGGGTTA ATTAA
RP Cmg1-GFP_Anpl1-cRFP	CGGTATATATGTACAACATATATGAATTCGTA CTTCATAT GTAGGTCACTAAAAAACCGAGCGAATTCGAGCTCGTTT AAAC
FP Cmg1-GFP_Ape1-cRFP	GTTCTTCAACGGATTTTTTCAAGCACTGGAGATCAGTCTA CGATGAATTCGGCGAGTTGCGGATCCCCGGGTTAATTA A
RP Cmg1-GFP_Ape1-cRFP	GTATTTTTAGAAAAAGGATAAAAGAAACAGAAATCAAAA GAAATAAAAAGAGTGTGGCAAAAAGAAATTCGAGCTCGTT TAAAC
FP Cmg1-GFP_Chcl1-cRFP	GATGGCCAACCTTTGATGCTGATGAACAGCGCGATGAA CGTTCAACCCACAGGATTTTCGGATCCCCGGGTTAATTA A
RP Cmg1-GFP_Chcl1-cRFP	CGGTAAAAA AAAAAAAAAAATACACGATGGGGTACAGCAA ACGAAATTAATTTTATCCACGTCAATTCGAGCTCGTTTAA AC
FP Cmg1-GFP_Dcp1-cRFP	GACAAAATATCTACGAACTAATAAAAATATCTTCTGAAAA ATGAGCCAAAAGATTTCTTTTGCTCGGATCCCCGGGTTA ATTAA
RP Cmg1-GFP_Dcp1-cRFP	GTATTAAGTACATCATTATTTAAAAA AATTCCTCACTT GGGCATCTCACCTCTGTGCGAATTCGAGCTCGTTTAA C
FP Cmg1-GFP_Pex3-cRFP	GAGCGCCAGCGTATACAGCAACTTTGGCGTCTCCAGCT CGTTTTCTTCAAGCCTCGGATCCCCGGGTTAATTA
RP Cmg1-GFP_Pex3-cRFP	GATTACGCTATATATATATATATATTCTGGTGTGAGTGCA GTACTTATTCAGAGAGAATTCGAGCTCGTTTAAAC
FP Cmg1-GFP_Snf7-cRFP	GGATGAAGAAGATGAAGATGAAAAAGCATTAAAGAGAA CTACAAGCAGAAATGGGGCTTCGGATCCCCGGGTTAAT TAA

Materials and methods

RP Cmg1-GFP_Snf7-cRFP	CAGAACATGGAAAAGTAAGAACACCTTTTTTTTTTCTTTT ATCTAAACCCGCATAGAACACGTGAATTCGAGCTCGTTT AAAC
FP Cmg1-GFP_Ssa2-cRFP	CCCAGGTGGTGCTCCTCCAGCTCCAGAAGCTGAAGGTC CAACTGTGGAAGAAGTTGATCGGATCCCCGGGTTAATT AA
RP Cmg1-GFP_Ssa2-cRFP	CAGAGGAAAAGCAAAAAGTAAAACTTTTCGGATATTTTTAC AGGGCGATCGCTAAGCGAATTCGAGCTCGTTTAAAC
FP Cmg1g Y	GGATGAAGGTGATCTCTACGAGCATTGCCCAGGAGTG AATGAAGACGACCACAAACGGATCCCCGGGTTAATTAA
RP Cmg1g Y	AAAAGCTGTTCATTTCTTTCTTTCTTGAAATATGACTTTA CCTATCTCGATAAAAATGAATTCGAGCTCGTTTAAAC
FP Cmg1g Y mC	GGATGAAGGTGATCTCTACGAGCATTGCCCAGGAGTG AATGAAGACGACCACAAAGGATCCATGGAAAAAGAGAA G

Table 9: Oligonucleotides used for promoter exchange and genomic protein-tagging

Name	Sequence 5' to 3'
FP TAP-Cmg1_pTEF	ACGGACAATAAGAGGTACGCTACACATCTACCATCACCTT TCAGGGAGGGCATAAAGAACAAGGCTGGAGCTCAT
RP TAP-Cmg1_pTEF	GTGTATTCTTCAAATCTATGCGATCCTCTTTTCTTTTTGT CTTACTCTCCTCCATCTTATCGTCATCATCAAAGTG GAATAAGAGGACGGACAATAAGAGGTACGCTACACAT CTACCATCACCTTCAGGGAGGAATTCGAGCTCGTTTAA AC
FP Cmg1_pGal	CGGTGTATTCTTCAAATCTATGCGATCCTCTTTTCTTTTT GTCTTACTCTCCTCCATGCACTGAGCAGCGTAATCTG GAAGGAAGAAGTGATTTAATCGCAGAGTCAAATATAA GCATAAATTTGTTGTAACCGTGAATTCGAGCTCGTTTAA AC
RP Cmg1_pGal	GCTACCACGTGCATGCCTACGTCCTGCTTCCTTGATAATG ACTATGCCTTTTTGCCATGCACTGAGCAGCGTAATCTG GTTATTAAGGTAATAATGCACGTCGAGCGATGGTAGGT AAAATGTCTAGAGGCATATCTAGGAATTCGAGCTCGTT TAAAC
FP Spp2_pGal	CTTGAAAATATTTTTTTTCAAGGTCTTACTCCCCAACTTA AGTGAAAACITGCTCATGCACTGAGCAGCGTAATCTG CCAAAATTCGAAAATAGTACAACCGAGAGAGGTGGAAG AACTTAAAGCCTTCAGTACGAATTCGAGCTCGTTTAAAC CGATTCTTTTTTTTTGAAAAAGAACTTTTTATCTGTGTT GGAGTCCGAATCCTCCATGCACTGAGCAGCGTAATCTG GAAGCGATGAGATGAGTACTCAATAGTAAACATATAGGC AGCTTACACCAATTAACAAGAAATTCGAGCTCGTTTAAA C
RP Spp2_pGal	CCGTATTCTGGGGTCTAAACCAAACCGCTGTTTGGTTT TTGTAGCTGCCAAACCATGCACTGAGCAGCGTAATCT G

Materials and methods

For Northern blotting, oligonucleotides (Table 10) were radioactively labelled (section 2.2.14) and used as probes.

Table 10: Oligonucleotides used for pre-rRNA detection

Name	Sequence 5' to 3'
P004	CGGTTTTAATTGTCCTA
P020	TGAGAAGGAAATGACGCT
P250 (scR1)	ATCCCGGCCGCCCTCCATCAC

2.1.7. Plasmids

Plasmids served as templates for PCR amplification of genes for cloning or tag/promoter cassette amplification for preparation of yeast strains. Furthermore, plasmids were generated for recombinant protein expression in *E. coli*. A list of the plasmids used in this study is shown in Table 11.

Table 11: Plasmids used in this study

Name	Usage	Source
A 101	Empty vector for H ₁₀ -MBP-tagging (N-term.) and protein expression in <i>E. coli</i>	M. Bohnsack
A 101 Gno1 1-72	Recombinant protein expression in <i>E. coli</i>	This study
A 101 Spp382 51-110	Recombinant protein expression in <i>E. coli</i>	This study
A 101 Spp2 92-157	Recombinant protein expression in <i>E. coli</i>	This study
A 101 Sqs1 705-767	Recombinant protein expression in <i>E. coli</i>	This study
A 101 Cmg1 1-85	Recombinant protein expression in <i>E. coli</i>	This study
A 15	Empty vector for ProteinA-tagging (N-term.), H ₆ -tagging (C-term.) and protein expression in <i>E. coli</i>	M. Bohnsack
A 15 Spp382 51-110	Recombinant protein expression in <i>E. coli</i>	This study
A 21	Empty vector for H ₁₀ -ProteinA-tagging (N-term.) and protein expression in <i>E. coli</i>	M. Bohnsack
A 21 Gno1s	PCR template for cloning	This study
A 21 Spp382	PCR template for cloning	M. Bohnsack
A 21 Prp43 1-657	Recombinant protein expression in <i>E. coli</i>	This study
A 21 Prp43 92-767	Recombinant protein expression in <i>E. coli</i>	This study
A 21 Prp43 d753	Recombinant protein expression in <i>E. coli</i>	This study
A 21 Prp43 FL	Recombinant protein expression in <i>E. coli</i>	M. Bohnsack
A 21 Spp2	PCR template for cloning	M. Bohnsack
A 21 Sqs1	PCR template for cloning	M. Bohnsack
A 21-Cmg1	Recombinant protein expression in <i>E. coli</i> and PCR template for Cloning	M. Bohnsack
A 4	Empty vector for GFP-tagging (N-term.) in <i>E. coli</i>	M. Bohnsack
A 4 Prp43	Recombinant protein expression in <i>E. coli</i>	This study
A 5	Empty vector for RFP-tagging (N-term.) in <i>E. coli</i>	M. Bohnsack
A 5 Cmg1	Recombinant expression <i>E. coli</i>	This study
A 5 Cmg1 1-85	Recombinant expression <i>E. coli</i>	This study
A 8	Empty vector for His ₈ -tagging (N-term.)	M. Bohnsack

Materials and methods

	and protein expression in <i>E. coli</i>	
A 8 Gno1 1-72	Template restriction digest and for cloning	This study
A 8 Spp2 92-157 G	Template restriction digest and for cloning	This study
pBS1761 pTEF Ura3	Protein overexpression in <i>S. cerevisiae</i>	M. Bohnsack
pFA6a KanMX6 pGal1 3HA	pGal1 insertion/ genomic HA-tagging (C-term.) in <i>S. cerevisiae</i>	M. Bohnsack
pFA6a RFP NatMx6	Genomic RFP-tagging (C-term.) in <i>S. cerevisiae</i>	Longtine <i>et al.</i> , 1998
pUN100 mRFP-Nop1	Nuclear marker for <i>S. cerevisiae</i>	M. Bohnsack

2.1.8. Bacterial strains

For cloning or plasmid preparation, the *E. coli* strains DH5 α or TOP10 F' (Life Technologies) were used. In case of protein expression, the *E. coli* strains BL21 Codon Plus or BL21 Rosetta Star (Life Technologies) were chosen.

2.1.9. Yeast strains

Yeast strains that were used in this study are listed in Table 12. The strain preparation is described in section 2.2.3.

Table 12: List of strains used in this study

Name	Genotype	Source
BY4741	MATa; his3 Δ 1; leu2 Δ 0; met15 Δ 0; ura3 Δ 0	Brachmann <i>et al.</i> , 1998
YMB455	BY4741 with <i>prp43-HTP</i> (Ura3MX)	Bohnsack <i>et al.</i> , 2009
YMB824	MATa; his3 Δ 1; leu2 Δ 0; met15 Δ 0; ura3 Δ 0; YLR271w::KanMX4	Euroscarf
YMB858	BY4741 with <i>prp43-GFP</i> (His3MX6)	Ghaemmaghami <i>et al.</i> , 2003
YMB859	BY4741 with <i>cmg1-GFP</i> (His3MX6)	Ghaemmaghami <i>et al.</i> , 2003
YMB884	BY4741 with <i>P_{TEF}-TAP-cmg1</i> (Ura3MX)	This study
YMB886	YMB455 with <i>P_{GALI}-3HA-spp2</i> (KanMX6)	This study
YMB890	YMB455 with <i>P_{GALI}-3HA-spp382</i> (KanMX6)	This study
YMB894	YMB455 with <i>P_{GALI}-3HA-pxr1</i> (KanMX6)	This study
YMB900	YMB455 with <i>P_{GALI}-3HA-cmg1</i> (KanMX6)	This study
YMB936	YMB455 with <i>P_{GALI}-3HA-sqs1</i> (KanMX6)	This study
YMB915	YMB859 with <i>dcp1-RFP</i> (NatMX6)	This study
YMB918	YMB859 with <i>snj7-RFP</i> (NatMX6)	This study
YMB920	YMB859 with <i>pex3-RFP</i> (NatMX6)	This study
YMB921	YMB859 with <i>ssa2-RFP</i> (NatMX6)	This study
YMB923	YMB859 with <i>cbc1-RFP</i> (NatMX6)	This study
YMB926	YMB859 with <i>anp1-RFP</i> (NatMX6)	This study
YMB932	YMB858 with <i>P_{GALI}-3HA-cmg1</i> (KanMX6); pRS415 RFP-nop1 (Leu2MX)	This study
YMB933	YMB859 with pMS124 (<i>mCherry-sbb2</i>) (Leu2MX)	Powis <i>et al.</i> , 2013
YMB948	YMB858 with <i>P_{GALI}-3HA-sqs1</i> (KanMX6); pRS415 RFP-nop1 (Leu2MX)	This study

Materials and methods

YMB950	YMB858 with <i>P_{G.ALI}-3HLA-spp382</i> (KanMX6); pRS415 RFP-nop1 (Leu2MX)	This study
YMB952	YMB858 with <i>P_{G.ALI}-3HLA-spp2</i> (KanMX6); pRS415 RFP-nop1 (Leu2MX)	This study
YMB954	YMB858 with <i>P_{G.ALI}-3HLA-pxr1</i> (KanMX6); pRS415 RFP-nop1 (Leu2MX)	This study
YMB1000	MA1a; ade2-101; his3Δ200; leu2Δ1; ura3-520; trp1-Δ63; lys2-801;	Frazier <i>et al.</i> , 2006
YMB1002	MA1a; ade2-101; his3Δ200; leu2Δ1; ura3-520; trp1-Δ63; lys2-801; cox4::His3MX6	Frazier <i>et al.</i> , 2006
YMB1001	MA1a; ade2-101; his3Δ200; leu2Δ1; ura3-520; trp1-Δ63; lys2-801; cyt1::His3MX6	Vukotic <i>et al.</i> , 2012

2.2. Methods

2.2.1. Standard molecular biological and biochemical methods

The preparation of plasmids involved PCR amplification, restriction enzyme digestion, ligation, and *E. coli* transformation and was performed according to standard methods (Sambrook *et al.*, 1989). Sodium dodecyl sulfate polyacrylamide gel electrophoresis (SDS-PAGE) was performed according to standard protocol (Laemmli, 1970). For the detection of specific proteins by antibodies, proteins were transferred from the gel onto a nitrocellulose membrane (Amersham™Protran™ Premium 0.45 μm NC, GE Healthcare) by wet blotting. After incubation with specific primary antibodies (Table 3) followed by incubation with a secondary antibody coupled to a horse radish peroxidase (HRP), HRP was visualised by enhanced chemiluminescence (ECL) with chemiluminescence HRP substrate (Millipore). Stripping of bound antibodies from membranes was done by incubation with 6 M guanidine hydrochloride, 0.2 % nonidet, 0.1 M beta-mercaptoethanol, and 20 mM Tris/HCl pH 7.4 for 10 min.

2.2.2. Expression and purification of recombinant proteins

E. coli expression plasmids containing the open reading frames of the proteins of interest were transformed into *E. coli* BL21 Codon Plus (DE3) or Rosetta star. One to four litres of 2xYT medium, containing 100 μg/ml ampicillin and 34 μg/ml chloramphenicol were inoculated from an overnight culture and maintained in logarithmic growth at 37 °C, shaking at 110 rpm. When the

Materials and methods

OD₆₀₀ reached a value of 0.6-0.8, protein expression was induced by adding 250 μ M IPTG and cultures were incubated for 16 h at 18 °C or 3 h at 37 °C while constantly shaking at 110 rpm. Cells were harvested by centrifugation and stored at -80 °C. The protein purification was carried out at 4 °C. Cell pellets were resuspended in 20 ml lysis buffer (50 mM Tris/HCl, pH 7.4, 300 mM NaCl, 20 mM imidazole, 0.1 mM PMSF, 1 mM MgCl₂) per 5 ml cell pellet. Cells were disrupted by sonication and insoluble material was pelleted by centrifugation at 20,000 rcf for 20 min. The soluble lysate was incubated for 10 min with 0.5 % polyethylenimine to precipitate nucleic acids and was centrifuged at 100,000 rcf for 30 min. The supernatant was mixed for 1 h with 5 ml (for Prp43) or 1 ml (all other proteins) of cComplete His-tag Purification Resin (Roche). Bound protein was eluted using 500 mM imidazole in 50 mM Tris/HCl pH 7.4, 150 mM NaCl, and 1 mM MgCl₂. Proteins were stored in 50 mM Tris/HCl pH 7.4, 120 mM NaCl, 2 mM MgCl₂ and 20 % glycerol at -80 °C.

2.2.3. Pull-down assays from yeast

2.2.3.1. Pull-downs using yeast strains expressing genomically tagged proteins

For pull-down assays 20 ml of YPD was inoculated with wild-type yeast or the pTEF-TAP-*cmg1* strain and grown exponentially for 8 h. Each yeast culture was used to inoculate 6 l fresh YPD medium and was grown exponentially. Cells were harvested and if they were not directly used for pull-down assay, they were frozen in liquid nitrogen and stored at -80 °C. For cell lysis, the pellet was resuspended in one volume of lysis buffer (50 mM Tris/HCl pH 7.4, 100 mM NaCl, 1 mM EDTA, 0.05 % Tween 20) and dropped into liquid nitrogen. The frozen cell drops were crushed with a mortar and pestle. In the next step, the lysate was thawed and mixed with 35 ml of lysis buffer supplemented with cComplete Mini protease inhibitors (Roche). Cell debris were removed by centrifugation (20,000 rcf, 4 °C, 20 min). The supernatant was then incubated for 1 h at 4 °C on a rolling incubator with 500 μ l of IgG Sepahrose (GE Healthcare) that had been pre-equilibrated in lysis buffer. After binding, three washing steps were performed with IgG wash buffer (50 mM Tris/HCl pH 7.4, 100 mM NaCl, 1 mM MgCl₂, 0.05 % Tween 20) in a gravity flow column. Protein bound beads were then equilibrated with TEV cleavage buffer (10 mM Tris/HCl pH 7.4, 1 mM beta-mercaptoethanol) and incubated overnight at 4 °C on a rolling incubator with 1 ml of TEV cleavage buffer

Materials and methods

containing 5 μ l of 90 μ M TEV protease to elute bound complexes. TEV protease was removed by incubation of the first eluate with 150 μ l of Glutathione Sepharose (GE Healthcare) for 1 h at 4 °C on a rolling incubator. The second elution fraction was collected and precipitated with 15 % trichloroacetic acid (TCA) with following centrifugation (15 min, 4 °C, 20,000 rcf). Protein pellets were washed with ice cold acetone and centrifuged (5 min, 4 °C, and 20,000 rcf) to remove residual TCA and air dried. Samples were resuspended in 10 μ l of 4x SDS sample loading buffer (40 % glycerol, 240 mM Tris/HCl pH 6.8, 8 % SDS, 0.04 % bromophenol blue, and 5 % beta-mercaptoethanol) and 2 μ l of Tris/HCl pH 7.4 and were separated on a NuPAGE® Novex® 4-12 % Bis-Tris protein gel (Life technologies). Proteins were transferred to a nitrocellulose membrane and analysed by Western blotting (section 2.2.1). Alternatively, gels were stained with coomassie brilliant blue R250 (0.1 % Coomassie R250, 10 % glacial acetic acid, 40 % methanol, 50 % water) and then destained using destain solution (10 % glacial acetic acid, 20 % methanol, 70 % water). Proteins in eluates were identified by mass spectrometry. In brief, samples were digested with trypsin, treated as previously described (Sloan *et al.*, 2015) and analysed by MS/MS on a MALDI-TOF-TOF instrument. Proteins were identified using the MASCOT software. Mass spectrometry was performed by the groups of Dr. Bernhard Schmidt and Prof. Dr. H. Urlaub.

2.2.3.2. Pull-downs using immobilised recombinant proteins

250 μ l of IgG Sepharose was equilibrated with lysis buffer and pre-incubated with saturating amounts of ProteinA-tagged, recombinantly expressed bait protein and washed with lysis buffer (50 mM Tris/HCl pH 7.4, 100 mM NaCl, 1 mM EDTA, 0.05 % Tween 20) or, in the case of pull-down with solubilised mitochondria, solubili buffer (20 mM Tris/HCl pH 7.4, 0.1 mM EDTA, 100 mM NaCl, 10 % glycerol, 1 % digitonin, 2 mM PMSF). The prepared beads were then incubated with cleared cell lysate or 15 mg of solubilised mitochondria (section 2.2.16) for at least one hour at 4 °C. When beads were incubated with whole cell lysate, washing steps were performed as described in section 2.2.3.1. However, when the beads were incubated with solubilised mitochondria the washing steps were performed with an alternative wash buffer (20 mM Tris/HCl pH 7.4, 0.1 mM EDTA, 100 mM NaCl, 10 % glycerol, 0.3 % digitonin). In both cases, complexes were eluted as described in section 2.2.3.1. Small scale experiments were also performed using 20 μ l of IgG Sepharose and 1 mg solubilised mitochondria.

2.2.4. Protein interaction analysis

2.2.4.1. Gel based assay

4.2 nmol of ProteinA-tagged Cmg1 or Spp2 were bound to 30 μ l of IgG sepharose (GE Healthcare) and incubated for 30 min at 4 °C in buffer A (50 mM Tris/HCl pH 7.4, 100 mM NaCl, 1.5 mM MgCl₂ and 2 mM beta-mercaptoethanol). After three washing steps, 2.6 nmol of GFP-tagged Prp43 was added and again incubated for 2 h at 4 °C. After washing with buffer A, the bound proteins were eluted with 30 μ l of elution buffer (50 mM Tris/HCl pH 7.4 and 2 M MgCl₂). Input and elution samples were separated on a NuPAGE® Novex® 4-12 % Bis-Tris protein gel and stained with coomassie brilliant blue R-250.

2.2.4.2. Fluorescence based assay

One nanomole of full length ProteinA-tagged Prp43 and RFP-tagged Cmg1 G-patch domain (1-85) were incubated with 30 μ l of IgG sepharose (GE Healthcare) for 1 h at 4 °C in buffer A (50 mM Tris/HCl pH 7.4, 100 mM NaCl, 1.5 mM MgCl₂, 2 mM beta-mercaptoethanol) supplemented with 1.5 mg/ml BSA. After three washing steps with buffer A, bound proteins were eluted with 300 μ l of elution buffer (40 mM Tris/HCl pH 7.4, 80 mM NaCl, 1.2 mM MgCl₂, 1.6 mM beta-mercaptoethanol, 1.2 mg/ml BSA, and 150 mM DTT). The fluorescence of elution samples were monitored using a BioTEK Synergy H1 microplate spectrophotometer at excitation wavelength 560 nm and emission wavelength 610 nm and analysed using Gen5 software.

2.2.5. *In vitro* competition assay

One nanomole of ProteinA-tagged Spp382 G-patch domain (51-110) was bound to 30 μ l of IgG sepharose (GE Healthcare) and incubated for 30 min and 4 °C in buffer A (50 mM Tris/HCl pH 7.4, 100 mM NaCl, 1.5 mM MgCl₂, 2 mM beta-mercaptoethanol) supplemented with 1.5 mg/ml BSA. After three washing steps with buffer A, 1 nmol of GFP-tagged Prp43 and 1 nmol or 5 nmol MBP-tagged competing G-patch domains (Table 13; 1) were added to the IgG beads and were incubated for 2 h at 4 °C. After additional three washing steps with buffer A, the bound proteins were eluted with 300 μ l of elution buffer (40 mM Tris/HCl pH 7.4, 80 mM NaCl, 1.2 mM MgCl₂, 1.6 mM beta-mercaptoethanol, 1.2 mg/ml BSA, and 150 mM DTT). Elution samples were analysed using a BioTEK Synergy H1 microplate spectrophotometer at excitation wavelength of 475 nm and emission wavelength of 510 nm and analysed using Gen5 software. In an alternative protocol, 1 nmol of ProteinA-

Materials and methods

tagged Prp43 was immobilized on 30 μ l of IgG sepharose. After three washing steps (performed as described above) 1 nmol of RFP-tagged Cmg1 G-patch domain (1-85) and 1 nmol or 5 nmol of MBP-tagged competing G-patch domains (Table 13; 2) were added. Subsequent steps were performed as described above. Samples were analysed at excitation wavelength of 560 nm and emission wavelength of 610 nm.

Table 13: Proteins with their tags for the appropriate experiment

Experiment	ProteinA tag bait	GFP/RFP tag readout	MBP tag competitor
1	Spp382 51-110	GFP-Prp43	Sqs1 705-767
			Pxr1 1-82
			Cmg1 1-85
			Spp2 92-157
2	Prp43	RFP-Cmg1 1-85	Sqs1 705-767
			Pxr1 1-82
			Spp2 92-157

2.2.6. Electromobility shift assay (EMSA)

Electromobility shift assays were used to detect the RNA affinity of Prp43 in absence or presence of cofactors. Reactions containing 45 mM Tris/HCl pH 7.4, 2 mM MgCl₂, 25 mM NaCl and 2 nM radioactively labelled (³²P) 11 nt RNA (18S H29 11 nt) and increasing amounts of Prp43 (0-500 nM) were incubated at 30 °C for 30 min. This experiment was performed in the absence or in the presence of 2 μ M Cmg1. The bound and unbound RNAs were separated by electrophoresis through a native 5 % polyacrylamide gel containing 22.25 mM Tris-borate, 22.25 mM boric acid, and 0.5 mM EDTA. After drying the gel, the ³²P-labelled RNA was visualised using a phosphorimager and quantified using ImageQuant software (Molecular Dynamics).

2.2.7. Anisotropy measurements

The anisotropy setup (MicroTime 200, PicoQuant GmbH, Berlin, Germany) contains an inverse epi-fluorescence microscope (IX-71, Olympus Europa, Hamburg, Germany), two identical pulsed 635 nm diode lasers (LDH-P-635, PicoQuant GmbH, Berlin, Germany); lasers (PDL 828 “Sepia II”, PicoQuant GmbH, Berlin, Germany), a polarisation-preserving single-mode fibre, four dichroic mirror (FITC/TRITC, Chroma Technology, Rockingham, VT, USA), a microscope’s objective (UPLSAPO 60x W, 1.2 N.A., Olympus Europa,

Materials and methods

Hamburg, Germany), a single circular aperture (diameter 150 μm), a polarising beam splitter cube (Ealing Catalogue, St. Asaph, UK), two single photon avalanche diodes for the red emission (two SPCM-AQR-13, Perkin Elmer, Wellesley, MA, USA), emission bandpass filters HC692/40 (Semrock, USA), and a time-correlated single-photon counting electronics (HydraHarp 400, PicoQuant GmbH, Berlin, Germany). For the anisotropy measurements, 20 μl samples containing 20 nM 11 nt Atto647 labelled RNA (18S H29 11nt fl.), increasing amounts of Prp43 (0-4 μM) and with or without 5 μM cofactor, were inserted into a measurement chamber. The chamber consisted of two glass coverslides connected through a 1 mm silicon spacer (Grace Bio-Labs). Before the experiments, the coverslides were coated with Sigmacote (Sigma-Aldrich), according to the manufacturer's instructions, to avoid unspecific binding during the measurements. At least three independent measurements over 10 min were performed at room temperature for each sample. For each data point, the mean and the standard deviation of three independent measurements were calculated. Finally, dissociation constants were determined using the Origin software to fit the data with Formula 1.

$$r = r_0 + \frac{\Delta r_{\max}}{[\text{RNA}]_{\text{tot}}} \cdot \left(\frac{[\text{Prp43}]_{\text{tot}} + [\text{RNA}]_{\text{tot}} + K_d}{2} - \sqrt{\left(\frac{[\text{Prp43}]_{\text{tot}} + [\text{RNA}]_{\text{tot}} + K_d}{2} \right)^2 - [\text{Prp43}]_{\text{tot}}[\text{RNA}]_{\text{tot}}} \right)$$

Formula 1: Equation for determine RNA dissociation constant of Prp43 in presence of cofactor

Where r_0 is the anisotropy of unbound RNA, r_{\max} is the amplitude, $[\text{Prp43}]_{\text{tot}}$ is the total Prp43 concentration and $[\text{RNA}]_{\text{tot}}$ the total RNA concentration.

Anisotropy measurements were performed in the group of Prof. Jörg Enderlein together with Mira Prior.

2.2.8. Steady-state ATP hydrolysis

The ATPase activity of Prp43 was monitored with an NADH-coupled ATPase assay. The decrease of the reduced β -nicotinamide adenine dinucleotide (NADH) and the increase of its oxidised version (NAD⁺) leads to a decrease of absorption at 340 nm (A_{340}). The assay was performed with 400 nM Prp43 in the absence, or 250 nM Prp43 in the presence of 1 μM cofactor in 45 mM Tris/HCl pH 7.4, 25 mM NaCl, 2 mM MgCl₂, and 4 mM ATP (Sigma) and indicated concentrations of 32 nt RNA (18S H29). The reactions were

Materials and methods

supplemented with 1 mM phosphoenolpyruvate (Sigma), 20 U/ml pyruvate kinase/lactic dehydrogenase (Sigma) and 300 μ M NADH (Sigma). Absorbance data were collected using a BioTEK Synergy HT microplate spectrophotometer equipped with Gen5 software. The reaction velocities were calculated from the change in A_{340} . The ATPase rates relative to the RNA concentrations were determined using the Origin software according to the Michaelis-Menten equation:

$$v = [E_0] \cdot k_{cat} \cdot \frac{[RNA]}{K_M + [RNA]}$$

Formula 2: Michaelis-Menten equation

Where $[E_0]$ means total enzyme concentration of Prp43, $[RNA]$ is the total RNA concentration, v means reaction velocity at certain RNA concentration, k_{cat} is the rate constant and K_M is Michaelis-Menten constant.

2.2.9. Preparation of yeast strains

Promoters and tags were amplified from plasmid templates (Longtine *et al.*, 1998) by PCR using primers containing >50 nt sequence that are complementary to appropriate regions of yeast genomic DNA. Yeast transformations were performed under sterile conditions and with sterile solutions as follows. A 50 ml yeast culture was grown at 30 °C to OD₆₀₀ 0.7. Cells were harvested by centrifugation (5 min, 4165 rcf) and washed with 10 ml of sterile water (5 min, 4165 rcf). Cells were resuspended in 1 ml water and transferred to a 1.5 ml tube and centrifuged (5 min, 4165 rcf). Then cells were washed with 1 ml of 1xTE/LiOAc (10 mM Tris/HCl pH 7.4, 1 mM EDTA pH 7.5, 100 mM lithium acetate pH 7.5) and resuspended in 200 μ l 1xTE/LiOAc (approx. 2×10^9 cells/ml). Next, 50 μ l of cells were mixed with 5 μ l of 10 mg/ml denatured salmon sperm DNA (100 °C, 20 min) and 12 μ l (~5 μ g) of DNA for homologous recombination. Immediately, 300 μ l of 40 % PEG4000 in 1xTE/LiOAc was added. Cells were incubated for 30 min at 30 °C while shaking and heat shocked for 15 min at 42 °C. After addition of 800 μ l of water, cells were pelleted by centrifugation (10 s, 18,000 rcf), resuspended in 100 μ l water and plated on selective media missing specific amino acids (auxotrophic markers). Alternatively for antibiotic selection, cells were grown on YPD plates overnight and replica plated onto selective plates the next day. Cells were grown at 30 °C and streaked out to obtain single colonies. Yeast strains were prepared with the help of Philipp Hackert.

2.2.10. Serial dilution growth assay

Serial dilution growth assays were performed as previously described by Kötter *et al.*, 2009. Saturated cultures of yeast cells were diluted in YPD to an OD₆₀₀ 1 followed by three serial 1:10 dilutions. From the diluted cultures, 5 µl were spotted on YPD (Dextrose), YPG (Glycerol) or YPL (Lactate) plates. Colony sizes were recorded following incubation of the plates for 2 days at 30°C.

2.2.11. Survival assay

Survival assays were performed as previously described by Teng and Hardwick, 2009. Saturated cultures of yeast strains grown in YPD were used to inoculate 5 ml cultures, which were then grown to OD₆₀₀ 0.5. Cultures were split in half and 2 ml of each culture was treated with 199 mM acetic acid and 2 ml was left untreated as a control. Cultures were incubated at 30 °C for a further 4 h. Five 1:5 serial dilutions were made and 5 µl of each dilution were spotted onto YPD plate.

2.2.12. Fluorescence microscopy

For fluorescence microscopy, yeast strains expressing GFP and RFP fusion protein were cultured in synthetic medium to an OD₆₀₀ of 0.5. 4 µl of yeast culture were spread on glass slides and monitored with DeltaVision Spectris (Applied Precision) fluorescence microscope equipped with a 100× objective and GFP, mCherry, and DAPI filter sets (excitation wavelengths of 475/28 nm, 575/25 nm, and 390/18 nm and emission wavelengths of 632/60 nm, 525/50 nm, and 435/48 nm respectively). Captured images were deconvolved using WoRx (Applied Precision) software. Mitochondria were stained with MitoTracker Orange CMTMRos Invitrogen (Eugen, Oregon, USA). Fluorescence microscopy was performed with the help of Philipp Hackert.

2.2.13. RNA isolation

RNA isolation from 30 ml OD₆₀₀ 0.7 yeast cell pellet was performed as previously described by Sambrook in 1989. Cells were lysed by vortexing for 5 min with 0.6 ml glass beads and 0.2 ml GTC mix (6 M guanidinium thiocyanate, 75 mM Tris/HCl pH 8, 0.2 M β-mercaptoethanol, 3 % sarkosyl) and 0.2 ml phenol at 4 °C. A further 3 ml of phenol and 3 ml GTC mix was added and incubated at 65 °C for 5 min, followed by 5 min chilling on ice. After addition of 1.6 ml NaAc Mix (100 mM NaAc pH 5.2, 1 mM EDTA pH 8, 10 mM Tris/HCl pH 8) and 3 ml chloroform samples were centrifuged (25 min, 4165 rcf, 4 °C). The upper aqueous phase was transferred to a fresh

Materials and methods

tube and mixed with 5 ml PCI (phenol:chloroform:isoamyl alcohol, 25:24:1) and centrifuged (5 min, 4165 rcf, 4 °C). The resulting upper phase was mixed with 4.5 ml chloroform, followed by centrifugation (5 min, 4165 rcf, 4 °C). The remaining 4 ml aqueous phase was mixed with 11 ml of ethanol and RNA was precipitated for at least 30 min at -80 °C. After centrifugation at 4165 rcf at 4 °C for 30 min, the RNA pellet was washed with ice cold 70 % ethanol (5 min, 4165 rcf, 4 °C) and air dried. Finally, RNA was resuspended in RNase free water and the concentration was measured using a NanoDrop 2000c. RNA was stored at -80 °C.

2.2.14. Northern blots

4 µg total RNA was mixed with 5 volumes of 0.2x glyoxal loading dye (8.2 % glyoxal, 4.9 % glycerol, 61.2 DMSO, 1.22x BPTE) and denatured at 55 °C for 1 h before separation by electrophoresis on a 1.2 % agarose gel in BPTE buffer (10 mM PIPES, 30 mM Bis-Tris, 10 mM EDTA). After washing steps (20 min in 100 mM NaOH, 2x 15 min in 0.5 M Tris/1.5 M NaCl, 20 min in 6x SSC; 1x SSC: 150 mM NaCl, 15 mM sodium citrate, pH 7 with NaOH), RNA was transferred on a Hybond-N Extra membrane (Amersham Biosciences) by vacuum blotting (200 mbar and 2 h; Sambrook *et al.*, 1989). The transferred RNA was UV cross-linked to the membrane by exposure two times to 0.12 J/cm² in a Stratalinker™ 2400. Mature rRNAs were visualised by methylene blue staining (0.03 % methylene blue (w/v), 0.3 M sodium acetate pH 5.2) for 15 min. Afterwards, the membrane was pre-hybridised for 30 min at 37 °C with SES1 buffer (0.5 M sodium phosphate pH 7.2, 7 % SDS, 1 mM EDTA). Next, membranes were hybridised overnight at 37 °C with ³²P-labelled DNA oligonucleotide probes. Probes were prepared by phosphorylation of DNA oligonucleotides with polynucleotide kinase (PNK, Fermentas) and ³²P-γ-ATP (Perkin-Elmer), for 30 min at 37 °C. Following hybridisation, membranes were washed twice (1: 6x SSC for 30 min; 2: 2x SSC, 0.1 % SDS for 20 min; 1x SSC). Finally, the membrane was dried and exposed to a phosphorimager screen. Pre-rRNAs were visualised using a phosphorimager and were quantified using ImageQuant software.

2.2.15. Preparation of enriched mitochondria

Cultures were maintained in exponential phase for ~24 h. Cells (approx. 5g) were harvested (10 min, 7500 rcf, 18 °C) and washed with 100 ml water. Next, cell pellets were resuspended in 2 ml/g DTT buffer (100 mM Tris/H₂SO₄ pH 9.4, 10 mM DTT) and incubated at 30 °C for 30 min with gentle shaking.

Materials and methods

Cells were pelleted by centrifugation (8 min, 5000 rcf, and 18 °C), the buffer was removed, the pellets were washed with 200 ml 1.2 M sorbitol and again centrifuged. Cell walls were disrupted by incubation of the cell pellets with 7 ml zymolyase buffer per gram of yeast (20 mM potassium phosphate buffer pH 7.4, 1.2 M Sorbitol and 4 mg of zymolyase 20T per gram yeast) for 1.5 h at 30 °C with gentle shaking. Spheroblasts were pelleted by centrifugation (10 min, 500 rcf, and 18 °C). After washing with ice cold zymolyase buffer without zymolyase cells were lysed up by 15 strokes with a homogeniser in 2 ml MES buffer pH 6 (4.22 mM MES, 0.6 M sorbitol, 0.5 mM EDTA, 2 mM KCl, 0.2 M PMSF, cOmplete Mini) per gram yeast, on ice. Then, samples were centrifuged (5 min, 500 rcf, and 4 °C), the supernatants were then centrifuged for 10 min at 4 °C at 2000 rcf and then for 15 min at 15,000 rcf at 4 °C). Next the enriched mitochondrial pellets were washed with ice cold SEM buffer (125 mM SEM pH 7.2, 200 mM PMSF) and resuspended to a concentration of 10 µg/ml in SEM buffer. Finally, mitochondria were frozen in liquid nitrogen and stored at -80 °C. Enriched mitochondria were prepared in the group of Prof. P. Rehling and together with Dr. Markus Deckers.

2.2.16. Preparation of mitochondrial extracts

To prepare mitochondrial extracts for pull-down assays (section 2.2.3.2) 20 mg or 1 mg mitochondria were thawed and centrifuged (10 min, 20,000 rcf, and 4 °C). After removing the supernatant, mitochondria were resuspended in 1 ml/mg ice cold solubili buffer (20 mM Tris/HCl pH 7.4, 0.1 mM EDTA, 100 mM NaCl, 10 % glycerol, 1 % digitonin, 2 mM PMSF) and incubated for 30 min at 4 °C on a rolling incubator. Insolubilised membranes were pelleted (15 min, 20,000 rcf, and 4 °C) and discarded and the supernatant was used for assays.

2.2.17. Mitochondrial sublocalisation assay

The mitochondrial sublocalisation assay was performed following the protocol described in Mick *et al.*, 2007. Isolated mitochondria were converted to mitoplasts by hypotonic swelling in EM buffer (1 mM EDTA, 10 mM MOPS pH 7.2) or lysed in 1% Triton X-100 and then treated with different concentration of Proteinase K (0, 20, and 100 µg/ml) for 15 min and 4 °C. Samples were precipitated with TCA (section 2.2.3) and analysed by SDS-PAGE and Western blotting (section 2.2.1). The mitochondrial sublocalisation assay was performed in the group of Prof. Peter Rehling with the help of Dr. Markus Deckers.

2.2.18. Mitochondrial localisation assay

For mitochondrial localisation assays, yeast strains were treated with 100 mM H₂O₂ for 1 h to induce apoptosis or left untreated. Cells were then treated as described in section 2.2.15 until the step of centrifugation for 5 min at 4 °C with 500 rcf in MES buffer pH 6. The samples were adjusted with MES buffer pH 6 to same protein concentration. Next, 500 µl of each sample were taken as cell extract samples and in addition 1 ml was layered onto an 1.5 ml a 30 % sucrose cushion in a 1.5 ml tube. Samples were centrifuged at 20,000 rcf for 30 min at 4 °C. Then 500 µl of the supernatants were taken as cytosolic samples, while the pellets were washed carefully with MES buffer pH 6 and resuspended in 1 ml MES buffer. Finally, 500 µl samples were taken from the resuspended enriched mitochondrial pellets. All samples were precipitated with 15 % TCA (15 min, 4 °C, and 20,000 rcf). The protein pellets were washed with ice cold acetone (5 min, 4 °C, and 20,000 rcf) to remove residual TCA and air dried. Samples were mixed with 4x SDS sample loading buffer (40 % glycerol, 240 mM Tris/HCl pH 6.8, 8 % SDS, 0.04 % bromophenol blue, and 5 % beta-mercaptoethanol) and separated on a NuPAGE® Novex® 4-12 % Bis-Tris protein gel (Life technologies) and analysed by Western blotting (section 2.2.1).

3. RESULTS

3.1. Identification of Cmg1-interacting helicases

Four of the G-patch proteins in yeast have been shown to interact with an RNA helicase. Pxr1, Sqs1 and Spp382 interact with Prp43 and Spp2 binds to Prp2. Therefore pull-down experiments from yeast lysate were performed to determine if the fifth, uncharacterised G-patch protein Cmg1, also interacts with an RNA helicase. For these experiments a BY4741 wild-type strain was chosen as negative control and a yeast strain overexpressing a TAP-tagged version of Cmg1 was prepared. Identical volumes of cleared yeast lysates (Figure 6a, Input) were incubated with IgG Sepharose and isolated complexes were eluted.

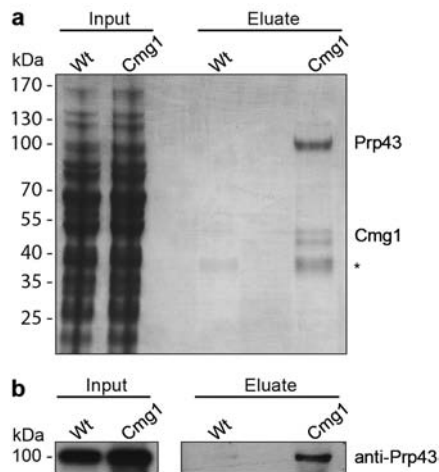


Figure 6: TAP-tagged Cmg1 co-precipitates Prp43 from yeast cells

a) Samples of cleared lysate (Input) from wild-type (Wt) and TAP-*Cmg1* overexpression strains (Cmg1), as well as elution samples of the pull-down experiments were separated on a SDS-PAGE and stained with coomassie brilliant blue. Bands are labelled with the protein name corresponding to proteins identified by mass spectrometry. Asterisk marks the bands also found in the wild-type control. **b)** Samples described in (a) were separated by SDS-PAGE and analysed by Western blotting using an anti-Prp43 antibody.

Inputs and eluates were separated by SDS-PAGE and coomassie staining was used to visualise proteins that co-precipitated with Cmg1 (Figure 6a). The Cmg1 elution lane contains several visible bands. The lower bands between 40 to 55 kDa represent the Cmg1 bait protein, while the bands below 40 kDa, marked with an asterisk, were also found in the negative control suggesting they correspond to non-specific, background interactions. Interestingly, the band

Results

corresponding to a protein of approximately 90 kDa was identified as the RNA helicase Prp43 by mass spectrometry. To support the mass spectrometry findings, a Western blot using the same samples was performed and probed with an anti-Prp43 antibody. The result in Figure 6b confirmed that Prp43 can be co-precipitated with Cmg1 from yeast cells, leading to the conclusion that these two proteins interact *in vivo*.

3.2. Analysis of the Cmg1 - Prp43 interaction *in vitro*

Although the pull-down assays from yeast showed an *in vivo* interaction between Cmg1 and Prp43, it was not clear if the observed interaction is the result of direct binding. Both proteins could be part of a larger protein complex and therefore bind via another protein or both might interact with the same RNA. To exclude these possibilities, an *in vitro* protein-protein interaction assay was performed. The gene sequences coding for the Cmg1 and Spp2 G-patch proteins were cloned into a plasmid that enabled expression of ProteinA-tagged proteins in *E.coli*. Recombinant Cmg1 and Spp2 G-patch proteins were purified and bound in the same amounts to IgG Sepharose (Figure 7, Input lanes 1 and 2).

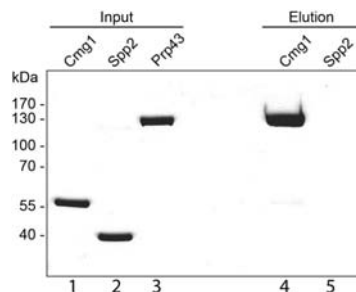


Figure 7: Cmg1 interacts directly with Prp43

Recombinantly expressed ProteinA-tagged Cmg1 and Spp2 (Input) were immobilised on IgG sepharose and incubated with GFP-tagged Prp43. Co-precipitated Prp43 was eluted (Elution) and samples were analysed by SDS-PAGE followed by coomassie staining. Protein size marker is indicated on the left.

The G-patch protein Spp2 was chosen as a negative control because no interaction with Prp43 has been demonstrated so far. Both samples were incubated with an equal amount of recombinant GFP-tagged Prp43 (Figure 7, lane 3). Next, GFP-Prp43 that was co-precipitated with the G-patch proteins

was eluted with high magnesium concentrations that disrupt molecular interactions. Prp43 was only eluted from the Cmg1 bound sepharose beads, which means that Prp43 binds to Cmg1, but not to Spp2 (Figure 7, lanes 4 and 5). Furthermore, this result clearly shows that Cmg1 can directly interact with Prp43.

3.3. Identification of Cmg1 and Prp43 interacting domains

Since Cmg1 and Prp43 interact directly, this raised the question of which part of the helicase Cmg1 binds to. Interestingly, both Spp382 and Sqs1 G-patch proteins were shown to bind to the C-terminal part of Prp43 (Tanaka *et al.*, 2007; Lebaron *et al.*, 2009; Walbott *et al.*, 2010; Christian *et al.*, 2014). Prp43 truncation mutants were created based on the known domain architecture of Prp43 (He *et al.*, 2010) and a crystal structure model of the helicase (Walbott *et al.*, 2010). Prp43 is a DEAH-box protein with two RecA-like domains (Figure 8a, green and light blue), containing eight conserved motifs, a winged helix domain (Figure 8a, pink) and a ratchet domain (Figure 8a, orange). The first truncation mutant (Prp43 92-767) lacks the amino acids 1-91, which form the N-terminal domain (Figure 8a and b) that has no known function, so far. The second truncation mutant (Prp43 1-657) is missing the last 110 amino acids, which are part of the C-terminal domain that contains an oligonucleotide binding motif (OB-motif; He *et al.*, 2010). Both versions of the protein were expressed with an N-terminal ProteinA tag in *E. coli*. As RNA helicases are able to bind RNA when they are recombinantly expressed, they are often co-purified along with *E. coli* RNAs, which can affect subsequent biochemical analyses. In order to prepare RNA-free proteins, the purification procedure was optimised. A polyethyleneimine-based nucleic acid precipitation step and a high salt washing step were successfully tested and included in the protocol. Before investigating interactions between these truncated forms of Prp43 and Cmg1 it was necessary to check whether the purified mutants are able to fold correctly. Therefore, the functionality of the helicase core domain was confirmed using an NADH-coupled ATPase assay. In this assay, the decrease in NADH concentration is directly proportional to the amount of hydrolysed ATP. The decrease in NADH can be measured spectrophotometrically by monitoring the absorbance at 340 nm and the hydrolysis rate (ATP/sec) can then be calculated (section 2.2.8).

Results

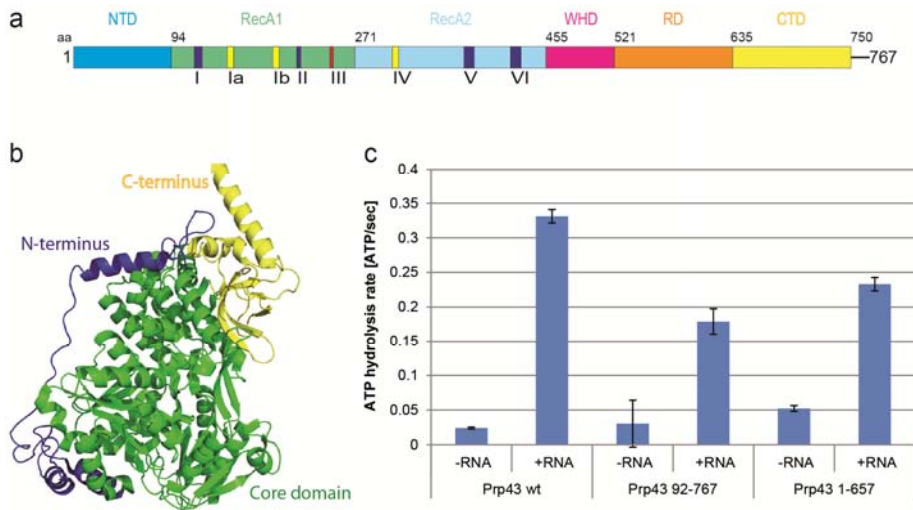


Figure 8: Scheme of Prp43 domain truncations and their functionality

a) Schematic domain organisation of Prp43. The helicase core is formed from two RecA-like domains (green and light blue), which contain eight conserved motifs (I, II, Ia, Ib, III, IV, V, and VI). Blue motifs are responsible for ATP/NTP binding and hydrolysis, motifs in yellow are necessary for RNA binding and the motif shown in red connects the NTP hydrolysis with RNA unwinding. Also shown are the winged helix domain (WHD, pink), the ratchet domain (RD, orange), N-terminal domain (blue) and the C-terminal domain (CTD, yellow). Numbers indicate amino acid (aa) positions. (Walbott *et al.*, 2010; He *et al.*, 2010) **b)** Prp43 crystal structure (Walbott *et al.*, 2010). Amino acids 1-91 are represented in blue (N-terminus), amino acids 92-656 are shown in green (Core domain) and amino acids 657-767 (C-terminus) are depicted in yellow. **c)** NADH-coupled ATPase assay of Prp43 wild-type (wt), Prp43 92-767 and Prp43 1-657 mutants in the absence (-RNA) or presence (+RNA) of RNA. The ATP hydrolysis rate was calculated in three independent experiments and is shown with standard deviation.

Wild-type Prp43 and the N/C-terminal truncation mutants were incubated without and with RNA because the ATPase activity of Prp43 is stimulated by the presence of RNA (Martin *et al.*, 2002; Tanaka and Schwer, 2006). Compared to wild-type Prp43, both truncated versions of Prp43 show slightly impaired ATP hydrolysis in presence of RNA (Figure 8c). Prp43 92-767 has half of the ATPase activity of wild-type protein, while Prp43 1-657 has almost three quarters of the wild-type ATPase rate. These findings mean that the truncation mutants do have a functional helicase core domain, but that both the N- and C-terminal domains of the protein influence the ATPase activity of Prp43. Consistent with this, in a parallel study (Walbott *et al.*, 2010) it was demonstrated that the mutation of single amino acids within the C-terminal

Results

region also lead to reduction of RNA-dependent ATPase activity. This is likely due to the mutation of the OB-motif, since RNA binding is coupled with ATPase function. In the case of Prp43 92-767, the decrease in ATPase activity could be due to the destabilised structure as the N-terminal helix folds back across the core of the protein like a frame (He *et al.*, 2010; Figure 8b, blue part). Having established that the N- and C-terminal truncated forms of Prp43 are functional, they could be used to investigate which region of the helicase binds to Cmg1. Furthermore, the region of Cmg1 that mediates the Prp43-interaction remains to be identified. Interestingly, it was shown for Spp382 and Sqs1 that the G-patch domain of these proteins is sufficient for binding to Prp43 (Tanaka *et al.*, 2007; Lebaron *et al.*, 2009). To test if this is also the case for Cmg1, the gene sequence encoding the N-terminal part (aa 1-85) of the protein, containing the proposed G-patch domain (aa 40-85), was cloned into an *E.coli* expression vector for N-terminal RFP-tagging and the tagged G-patch domain was purified. The purified full length and truncated versions of Prp43 were bound, in saturating amounts, to IgG sepharose and incubated with Cmg1 1-85. RFP-Cmg1 appeared as a double band when analysed by SDS-PAGE. However, this could be abolished by addition of high amounts of DTT suggesting they represent different folding states. Co-precipitated Cmg1 1-85 was eluted and both input and elution samples were analysed by SDS-PAGE, followed by coomassie staining. Alternatively, eluted RFP-Cmg1 1-85 was detected spectrophotometrically using an excitation wavelength of 560 nm and emission wavelength of 610 nm in a microtiter plate. The results in Figure 9a show that the Cmg1 1-85 protein is co-precipitated by wild-type Prp43. This interaction is specific because the negative control without Prp43 (empty beads) shows no co-precipitation of Cmg1 1-85 (Figure 9a). This means that the G-patch domain of Cmg1 is sufficient for Prp43 binding. Furthermore, the absence of any RFP-Cmg1 1-85 co-precipitation with Prp43 92-767 and Prp43 1-657 indicates that the N-terminal, as well as the C-terminal domain, is important for Cmg1 binding. An explanation could be the ring shaped structure of Prp43, so that the N- and C-terminus together form the Cmg1 binding platform.

Results

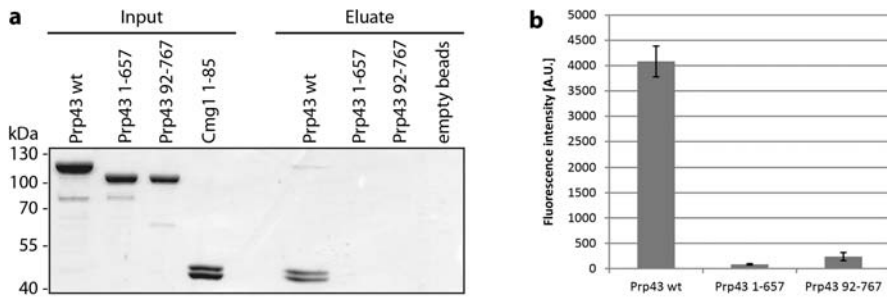


Figure 9: Cmg1 G-patch domain interacts with both the N- and C-terminal domain of Prp43

a) Full length and truncated forms of Prp43 were immobilised on IgG sepharose and incubated with RFP-tagged Cmg1. Inputs and eluted proteins were separated by SDS-PAGE and visualised by coomassie staining. b) Fluorescence-based protein interaction assay. Samples were prepared as in a) and the amount of RFP-Cmg1 eluted was monitored spectrophotometrically. The result of three independent assays and their standard deviation is shown.

3.4. Effect of Cmg1 on the RNA binding affinity of Prp43

The previously characterised G-patch cofactors of Prp43, Sqs1 and Spp382 (Tanaka *et al.*, 2007; Lebaron *et al.*, 2009) have been shown to enhance the unwinding activity of the helicase. However, other cofactors can also inhibit the activity of their associated helicases. After identifying the Prp43 - Cmg1 interaction, the next step was therefore to investigate the Prp43 enzyme activity in the presence of the newly identified binding partner. The unwinding activity of the RNA helicases is coupled to their RNA binding ability, so the influence of Cmg1 on the RNA binding affinity of Prp43 was analysed. Electromobility shift assays (EMSA) were performed with a radioactively labelled 11 nt long RNA and increasing amounts of Prp43 (0-500 nM) in absence or presence of full length Cmg1 (Figure 10a). Samples were analysed by native polyacrylamide gel electrophoresis (PAGE). Under the conditions when RNA is bound to an interaction partner it migrates more slowly in the gel and a band above the free RNA pool appears. The results presented in Figure 10a show that in the absence of cofactor the RNA stably associates with Prp43 at a protein concentration of 300 nM (lane 7). However, the presence of Cmg1 leads to stable RNA binding to Prp43 at a protein concentration of 50 nM (lane 12). Interestingly, Cmg1 alone does not bind RNA (lane 10). This is significant

Results

because the G-patch domain is often found in RNA-associated proteins and the Spp382 protein has previously been shown to bind to RNA (Aravind and Koonin, 1999; Tsai *et al.*, 2005).

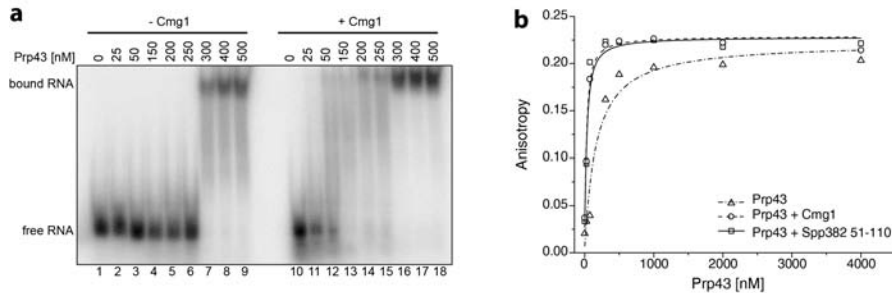


Figure 10: Cmg1 stimulates the RNA affinity of Prp43

a) An EMSA was performed using increasing amounts of Prp43 and a radioactively labelled 11 nt long RNA in absence (-) and presence (+) of Cmg1. Samples were analysed by native PAGE and RNA was visualised by exposing the dried gel to a phosphorimager screen. **b)** Anisotropy measurements of Prp43 (0-4 μ M) in the absence or presence of Cmg1 or Spp382 51-110. The mean values of at least three independent experiments and their fitted curves are shown.

To get a more quantitative analysis of Prp43's RNA affinity in the presence of Cmg1, anisotropy experiments were performed in collaboration with Mira Prior and Prof. Jörg Enderlein. Fluorescence anisotropy measurements are a tool to monitor the rotational correlation time of a molecule. Since this is connected to the size and molecular weight of a protein or RNA-protein complex, it can be used to accurately measure the RNA affinity of a protein. For these experiments Spp382 51-110 was chosen as a positive control, since this fragment, containing the G-patch domain, has been shown to increase Prp43's unwinding activity (Tanaka *et al.*, 2007; Christian *et al.*, 2014). The anisotropy of an 11 nt long Atto647 labelled RNA was measured in the absence or presence of Cmg1 or Spp382 51-110 and increasing amounts of Prp43. Each Prp43 concentration was measured at least three times and the mean values for each titration point were calculated. The curves were then fitted (Figure 10b) enabling the dissociation constant (K_d) for each complex to be determined (Table 14).

Table 14: Determined dissociation constants of the anisotropy measurements

Protein variants	K_d [nM]
Prp43	158 ± 70
Prp43 + Cmg1	20 ± 8
Prp43 + Spp382 51-110	24 ± 7

Results

Consistent with the EMSA data, the anisotropy increases as the concentration of Prp43 in the assay increases and addition of Cmg1 stimulates the RNA-affinity of Prp43. Remarkably, the titration curves in the presence of Cmg1 or Spp382 51-110 display almost the same stimulation and the calculated K_d -values are close (20 ± 8 nM for Cmg1 and 24 ± 7 nM for Spp382 51-110). When these constants are compared to the K_d -value of Prp43 alone (158 ± 70 nM), it becomes apparent that Cmg1 can increase the RNA-binding affinity of Prp43 approximately six-fold.

3.5. Prp43 ATPase activity in the presence of Cmg1

As Prp43 is an RNA-dependent ATPase and Cmg1 increases its RNA-binding affinity, the next experiments performed were ATPase assays to determine whether Cmg1 also has an influence on the ATP hydrolysis rate of Prp43. For the measurements the NADH-coupled ATPase assay described earlier was used. The reactions were carried out with increasing amounts of RNA (0-4.5 μ M), using Prp43 alone and also in the presence of Cmg1 or Spp382 51-110. Again, Spp382 51-110 functioned as a positive control and all experiments were performed at least three times. The maximal reaction velocity was calculated and plotted against the RNA concentration. The resulting titration curves are presented in Figure 11. The ATPase activity of Prp43 increased as the RNA concentration was raised confirming that it is an RNA-dependent ATPase. The ATPase activity of Prp43 was stimulated by the presence of Spp382 51-110 and, to greater extent, by Cmg1. This is in line with the calculated K_M values for the reactions (Table 15), which correlates with Prp43's RNA affinity. Thus, Prp43 alone has a high K_M value but addition of either Cmg1 or Spp382 lead to decreased K_M values (Table 15), meaning the G-patch proteins increase the Prp43 ATP hydrolysis rate at certain RNA concentrations. Furthermore, the rate constants (k_{cat}) of Prp43 alone and in presence of Spp382 51-110 are close, while surprisingly in the presence of Cmg1 it is increased (Table 15). To summarise, the fifth, previously uncharacterised G-patch protein from yeast was identified as a Prp43 cofactor. Cmg1 increases the Prp43 RNA-binding affinity as well as its ATPase activity.

Results

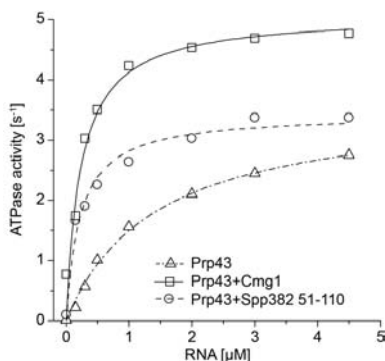


Figure 11: Cmg1 stimulates the ATPase activity of Prp43

The ATPase activity of Prp43 was monitored with an NADH-coupled ATPase assay. The decrease of the reduced β -nicotinamide adenine dinucleotide (NADH) and the increase of its oxidised version (NAD⁺) lead to a decrease of absorption at 340 nm. The assay was performed with 400 nM Prp43 in the absence, and 250 nM Prp43 in the presence, of 1 μ M cofactor (Cmg1 or Spp382 51-110) and indicated concentrations of 32 nt RNA (18S H29). The reaction velocities were calculated from the change in absorption and plotted against the RNA concentration. The ATP hydrolysis rates were analysed with the Origin software and calculated using the Michaelis-Menten equation.

Table 15: Determined Michaelis-Menten constants and rate constants of the ATPase assays

	K_M [μ M]	k_{cat} [s^{-1}]
Prp43	1.41 ± 0.14	3.61 ± 0.14
Prp43 + Cmg1	0.23 ± 0.05	5.09 ± 0.26
Prp43 + Spp382 51-110	0.22 ± 0.04	3.44 ± 0.13

3.6. Cmg1 cellular localisation

Prp43 is a multifunctional protein that has been shown to act in pre-mRNA splicing and in ribosome biogenesis. The G-patch proteins Pxr1 and Sqs1 are Prp43 cofactors in ribosome biogenesis and Spp382 works together with Prp43 in splicing (section 1.4). Accordingly, Pxr1 and Sqs1 are localised in the nucleolus and Spp382 is found in the nucleus. However, the function of the newly identified Prp43 cofactor Cmg1 was not known. To get insight into the role of Cmg1, its localisation was determined using fluorescence microscopy. In order to distinguish between the different cellular compartments, yeast strains were prepared with genomically RFP-tagged marker proteins for each compartment in combination with a genomically GFP-tagged Cmg1 protein. The strains were analysed for colocalisation of GFP and RFP tagged proteins

Results

with fluorescence microscopy. Figure 12a shows that Cmg1 is not present in endoplasmic reticulum (ER), golgi apparatus, endosome, pre-vacuole, peroxisomes, and P-bodies. However, in addition to distinct foci, a portion of Cmg1 was observed to co-localise with the cytoplasmic marker protein Ssa2. Surprisingly, a colocalisation between the Cmg1 foci and a mitotracker, a marker for mitochondria, was detected (Figure 12b), implying that Cmg1 is also localised to mitochondria. For this reason the protein expressed from the gene locus *YLR271W* was renamed in this study as *cytoplasmic and mitochondrial G-patch protein 1* (Cmg1).

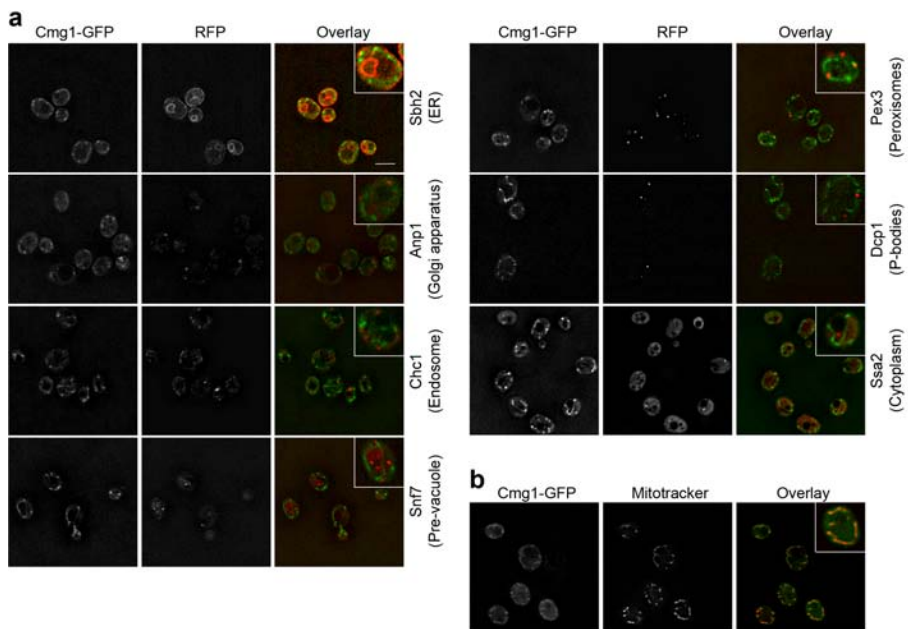


Figure 12: Cmg1 colocalisation with a mitotracker

a) Yeast strains with RFP-tagged marker proteins (Sbh2, endoplasmic reticulum; Anp1, golgi apparatus; Chc1, endosome; Snf7, pre-vacuole; Pex3, peroxisomes; Dcp1, P-bodies; and Ssa2, cytoplasm) for each compartment in combination with a genetically GFP-tagged Cmg1 protein were analysed using fluorescence microscopy. A magnified view of a single cell is given in the upper right-hand corner of each panel. **b)** Fluorescence microscopy of yeast cells with mitotracker stained mitochondria and GFP-tagged Cmg1 was performed as in (a). Scale bar represents 5 μm of main image.

3.7. Submitochondrial localisation of Cmg1

Mitochondria are essential for aerobic metabolism. They contain an outer mitochondrial membrane (OMM) and an inner mitochondrial membrane (IMM). The compartment surrounded by the inner membrane is called matrix and the space between the two membranes is named the intermembrane space (IMS). The IMM is folded and forms cristae, which contain enzymes of the respiratory chain whereas, the matrix contains ribosomes, granules and mitochondrial DNA. To confirm the localisation of Cmg1 at mitochondria (Figure 12b) and to answer the question of where within mitochondria Cmg1 is found, a mitochondrial sublocalisation assay was performed in collaboration with Dr. Markus Deckers and Prof. Peter Rehling. Isolated mitochondria were transformed into mitoplasts by hypotonic swelling in EM buffer or lysed in Triton X-100 and then treated with different concentrations of Proteinase K to degrade accessible proteins. The remaining proteins were analysed by Western blotting. Antibodies against ProteinA-tagged Cmg1 were used alongside antibodies against different mitochondrial proteins as submitochondrial markers. Tom70 is an OMM protein that faces the cytoplasm. In contrast, Tim21 is an IMM facing the IMS, while the IMM protein Tim44 is orientated toward the matrix. The marker protein Mic10 is a soluble protein of the IMS. The Western blots in Figure 13 show the digestion patterns of proteins localised in different mitochondrial compartments.

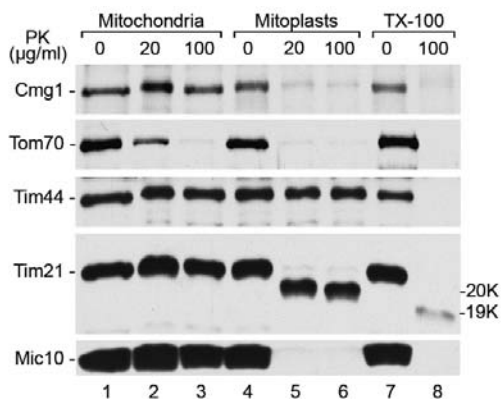


Figure 13: Submitochondrial localisation of Cmg1

Isolated mitochondria were prepared, converted to mitoplasts by hypotonic swelling in EM buffer or lysed in Triton X-100 and then treated with different concentration of Proteinase K. Protein samples were analysed by Western blotting. Antibodies against ProteinA-tagged Cmg1, Tom70 as cytoplasmic OMM protein, Tim21 as IMM protein facing the IMS, IMM protein Tim44 with matrix orientation, and IMS marker protein Mic10 were used.

Results

Tom70, as a cytoplasmic facing marker protein, has almost no signal in mitochondria treated with 100 µg/ml Proteinase K (Figure 13, lane 3). In contrast, Cmg1 is not degraded suggesting it is found within the mitochondria (Figure 13, lanes 1-3). Tim21 is truncated in the mitoplasts, because it spans the membrane so the part reaching in the IMS is degraded. Thus, the IMM proteins Tim44 and Tim21 are only fully degraded after total mitochondrial lysis (Figure 13, lane 8). Interestingly, Cmg1 shows the same profile as Mic10. Both proteins are present after Proteinase K digestion of intact mitochondria, but they are no longer detected in Proteinase K treated mitoplasts, where the protease reaches the IMS. This means Cmg1 is a mitochondrial IMS protein.

3.8. Analysis of mitochondrial metabolism upon *cmg1* deletion or overexpression

The identification of Cmg1 within mitochondria raised the question of the function of Cmg1 in these organelles. The main function of mitochondria is the production of cellular energy and one possibility is that Cmg1 is involved in mitochondrial metabolism. An important molecule in metabolism is glucose, which serves as a carbon and energy source and is catabolised during glycolysis in the cytoplasm and during the citric acid cycle in the mitochondrial matrix. Alternative carbon sources such as glycerol and lactate offer less accessible energy than glucose for a cell. Glycerol can enter the last steps of glycolysis and citric acid cycle, while lactate is only catabolised in the citric acid cycle. When glycerol or lactate is provided as carbon source for yeast growth, functional mitochondria are very important. If there is a defect in the respiratory chain, the cells lack energy and often grow slow or even die. This can be the case when mitochondrial import of tRNAs or molecules necessary for translation is impaired leading to decreased mitochondrial protein production. To test whether Cmg1 is involved in one of these processes the growth of a wild-type strain, a *cmg1* deletion strain, and a *Cmg1* overexpression strain were compared using glucose (yeast extract, peptone/tryptone, dextrose; YPD plates), glycerol (yeast extract, peptone/tryptone, glycerol; YPG plates) or lactate (yeast extract, peptone/tryptone, lactate; YPL plates) as carbon source. Serial dilution assays were performed and all plates were incubated for two days at 30 °C (Figure 14). The colonies on the YPD plate were bigger compared with the ones on the YPG or YPL plates, which is consistent with the higher energy available. Besides this, no strong differences in growth were observed between the three

Results

different yeast strains. This suggests that *Cmg1* is not required for mitochondrial energy production, protein expression or import of essential molecules.

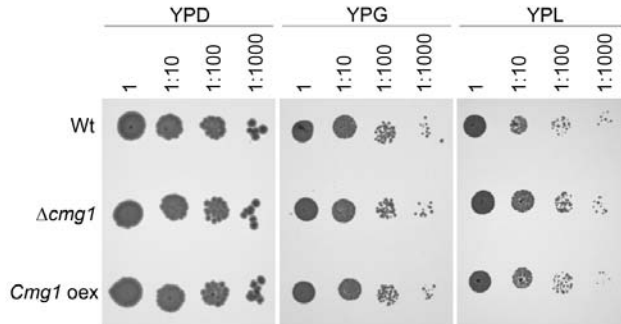


Figure 14: *Cmg1* is not required for mitochondrial metabolism

A serial dilution growth assay of wild-type (Wt), *cmg1* deletion ($\Delta cmg1$), and *Cmg1* overexpression (*Cmg1* oex) strains is shown. Saturated cultures of overnight grown yeast cells were diluted in YPD to an $OD_{600}=1$ followed by three serial dilutions 1:10. Diluted cultures were spotted on YPD, YPG or YPL plates. Plates were incubated for two days at 30°C.

3.9. Cell growth and survival in *cmg1* deletion and overexpression strains

The data suggest that *Cmg1* does not have an essential function in mitochondrial metabolism. Besides their function in cellular energy production mitochondria also play an important role in programmed cell death. When proapoptotic proteins of the Bcl-2 family are activated, the permeability of the OMM gets increased and cytochrome c, which is normally an IMS protein, is released from the mitochondria. Release of cytochrome c into the cytoplasm or the presence of reactive oxygen species (ROS) lead to activation of proteases called caspases that bring about the programmed cell death.

Although no significant growth defects were observed in serial dilution assay, a more sensitive growth analysis of the wild-type, *cmg1* deletion, and a *Cmg1* overexpression strains was performed to identify more subtle effects on growth. This approach revealed a reduced growth rate for the *Cmg1* overexpression strain, while the *cmg1* deletion strains grew like the wild-type strain (Figure 15a). The decreased growth rate of the *Cmg1* overexpression strain could suggest a role for the protein in apoptosis.

Results

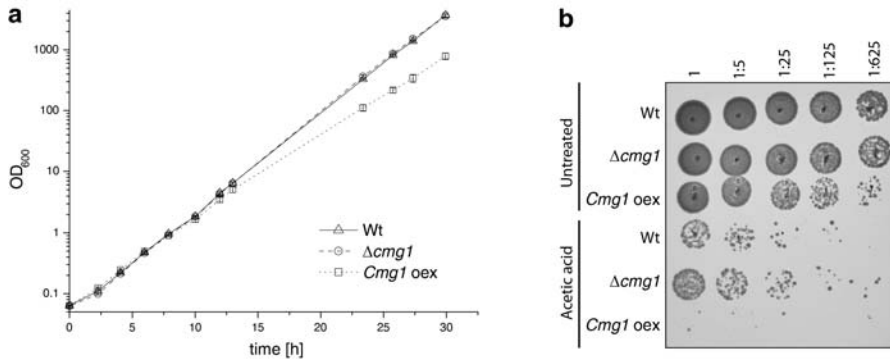


Figure 15: Cell growth and survival in *cmg1* deletion and overexpression strains
a) Shown are the growth curves of wild-type (Wt), *cmg1* deletion ($\Delta cmg1$), and *Cmg1* overexpression (*Cmg1* oex) strains, measured over 30 h and 30 °C. **b)** Survival assay of wild-type (Wt), *cmg1* deletion ($\Delta cmg1$), and a *Cmg1* overexpression (*Cmg1* oex) strains with or without 199 mM acetic acid treatment are shown. Four serial dilutions 1:5 were spotted on an YPD agar plate and incubated for two days.

It was therefore tested if *Cmg1* is a part of the apoptotic machinery and a wild-type, *cmg1* deletion, and a *Cmg1* overexpression strains were examined in a survival assay. Exponentially growing cultures with an OD₆₀₀ 0.5 were treated with acetic acid to induce apoptosis and treated and untreated cultures were incubated at 30 °C for a further 4 h. Finally, serial dilutions were spotted onto YPD agar plates and growth was monitored for two days (Figure 15b). The growth of the untreated samples is comparable to the results of the growth curves (Figure 15a), where the wild-type and *cmg1* deletion strains grow similarly, while the *Cmg1* overexpression strain displays decreased colony sizes. Interestingly, the *cmg1* deletion strain has slightly enhanced growth in comparison to the wild-type strain after acetic acid treatment (Figure 15b). Furthermore, there is hardly any growth visible for cells overexpressing the *Cmg1* protein after induction of apoptosis. Altogether, these data mean that the *Cmg1* is involved in cell survival and is potentially a new proapoptotic factor.

3.10. Relocalisation of *Cmg1* and *Prp43* under apoptotic conditions

During apoptosis cells undergo various physiological changes. One of these changes is that the outer mitochondrial membrane (OMM) becomes permeabilised. This has been shown to induce the release of some proapoptotic

Results

factors such as cytochrome c from the mitochondria into the cytoplasm (Garrido *et al.*, 2006). However, other apoptotic factors e.g. Bax and Bak are localised to mitochondria under apoptotic conditions (Ligr *et al.*, 1998; Westphal *et al.*, 2011). Furthermore, it is suggested that in human cells cytoplasmic calpain I can gain access to apoptotic mitochondria (Polster *et al.*, 2005; Cao *et al.*, 2007). The identification of Cmg1 as a potential new proapoptotic factor in mitochondria raised the question of whether this protein remains associated with mitochondria in apoptosis. Furthermore, the data show that Cmg1 is primarily localised to mitochondria but also that it interacts with Prp43. This leads to a second question of where Prp43 is localised under apoptotic conditions. For this reason a subcellular fractionation of yeast with and without previous apoptosis induction was performed to produce a cytoplasmic extract and enriched mitochondrial fraction. A cleared cell extract (E, also containing organelles) was prepared from a yeast strain overexpressing the Cmg1 protein treated with hydrogen peroxide or left untreated. A soluble cytoplasmic supernatant (S) was collected and an enriched mitochondrial pellet (P) was then prepared by sedimentation centrifugation through a sucrose cushion (section 2.2.18). Protein distribution in different fractions was analysed by Western blotting. A ProteinA antibody was used for detection of ProteinA-tagged Cmg1 and Prp43 was detected using an antibody against the endogenous protein. Antibodies against Pgc1 and Tom70 were taken as cytoplasmic and mitochondrial markers, respectively. Figure 16a shows that all four proteins are present in the total cell extract (E). The mitochondrial marker protein Tom70 is predominantly visible in the enriched mitochondria pellet (P). However, slight cytoplasmic contamination of the mitochondria enriched fraction can be seen as the Pgc1 signal is also weakly detected in these lanes. Under normal conditions Cmg1 was detectable in both the mitochondrial pellet and the cytoplasmic fraction, consistent with the microscopy data (Figure 12). Interestingly, upon induction of apoptosis Cmg1 is completely localised in the mitochondrial pellet. Under normal conditions the distribution of Prp43 is comparable to the Pgc1, but under apoptotic conditions it is distributed similar to the Tom70 signal. Excitingly, this means that Prp43 relocates from the cytoplasm to mitochondria upon induction of apoptosis. The finding that in apoptosis Prp43 is localised to mitochondria, where Cmg1 is located, raised the question if Prp43 recruitment to mitochondria depends on Cmg1. The subcellular fractionation experiment was therefore repeated with a *cmg1* deletion strain. Strikingly, the Western blots in Figure 16b show the same band pattern as in Figure 16a and Prp43 signal shifts from the cytoplasmic supernatant to the

Results

mitochondrial pellet with hydrogen peroxide treatment. Consequently, Cmg1 does not seem to be responsible for Prp43 relocalisation to mitochondria.

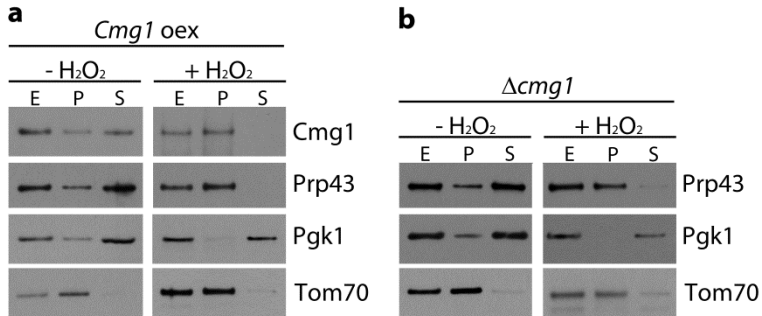


Figure 16: Cmg1 and Prp43 localisation to mitochondria in apoptosis

For mitochondrial localisation assay, mitochondria of **a)** *Cmg1* overexpression strain (*Cmg1* oex) and **b)** *cmg1* deletion ($\Delta cmg1$) without (-H₂O₂) or with (+H₂O₂) 100 mM hydrogen peroxide treatment were prepared. Samples of cell extract (E), enriched mitochondrial pellet (P), and cytoplasmic supernatant (S) were taken. All samples were precipitated with TCA. Samples were resuspended in SDS sample loading buffer and analysed by SDS-PAGE for Western blotting. Antibodies against Prp43, Pgk1 as cytoplasmic marker protein, and Tom70 as mitochondrial marker protein were used. Cmg1-TAP was detected by using an antibody against ProteinA.

3.11. Mitochondrial binding partners of Prp43 in apoptosis

Since Prp43 localises to mitochondria in apoptosis in the absence of Cmg1, the next aim was to find mitochondrial interaction partners of Prp43. For this reason a pull-down experiment using immobilised recombinant ProteinA tagged Prp43 or empty IgG sepharose beads and solubilised mitochondria was performed. For specific elution of complexes formed, the ProteinA-tag of Prp43 was cleaved by TEV protease. The elution and input samples were analysed by SDS-PAGE followed by coomassie staining. The visible bands were excised and sent for mass spectrometry to identify the corresponding peptides. Table 16 lists all mitochondrial proteins that were retrieved at significantly high levels with immobilised Prp43.

Results

Table 16: Mitochondrial Prp43 binding partners identified by mass spectrometry

Gene name	Score	Protein description
HSP60	674	Heat shock protein 60
HSP77	485	Heat shock protein SSC1
QCR2	322	Cytochrome b-c1 complex subunit 2
ODP2	209	Dihydropyridyllysine-residue acetyltransferase component of pyruvate dehydrogenase complex
PRX1	191	Mitochondrial peroxiredoxin PRX1
RIM1	156	Single-stranded DNA-binding protein RIM1
ODO2	128	Dihydropyridyllysine-residue succinyltransferase component of 2-oxoglutarate dehydrogenase complex
GRPE	57	GrpE protein homolog
ODPB	54	Pyruvate dehydrogenase E1 component subunit beta
QCR7	51	Cytochrome b-c1 complex subunit 7

Besides two heat shock proteins the highest score was detected for Qcr2 that is a complex III protein of the electron transport chain. A second protein of this complex Qcr7 was also found, suggesting that Prp43 may associate with complex III in the mitochondrial IMS during apoptosis. Other identified proteins were less likely to interact with Prp43 because they are located in the mitochondrial matrix or they had a low score. Complex III and complex IV are thought to form supercomplexes (Lapuente-Brun *et al.*, 2013). For this reason the pull-down experiment was repeated with mitochondrial lysate from wild-type yeast and cells in which either complex III ($\Delta cyt1$) or complex IV ($\Delta cox4$) were disrupted. If the Cyt1 protein is missing, the complex III fails to assemble and if a cell lacks Cox4 protein, it is complex IV deficient. The wild-type (Wt) strain functioned as positive control while incubated with TAP-Prp43 or as negative control (C) when incubated with empty beads. Precipitated input and elution samples of the different strains and controls were analysed by SDS-PAGE followed by Western blotting. The membrane was incubated with antibodies against the complex III protein Qcr8, the complex IV protein Cox2 and the complex V protein Atp5 (Figure 17). The input sample for the *cyt1* deletion strain displayed a reduced signal for Qcr8 and the *cox4* deletion strain a reduced signal for Cox2 as expected. In the negative control elution (C) no signal is detectable showing that any signals detected arise from interactions with Prp43. Incubation of mitochondrial lysate from wild-type cells supported the mass spectrometry findings as proteins of complex III and IV but not complex V were retrieved. No signal for Cox2 was detected in the elution of either complex III or IV deficient strains but Qcr8 was pulled down from the *cox4* deletion strain. Atp5 was also not detected in any of the elutions from the

Results

$\Delta cyt1$ and $\Delta cox4$ strains. Together, these results indicate that Prp43 interacts with complex III in absence of complex IV. In contrast, Cox2 of complex IV needs complex III for association with Prp43. Thus, it is proposed that Prp43 is bound to complex III in apoptosis.

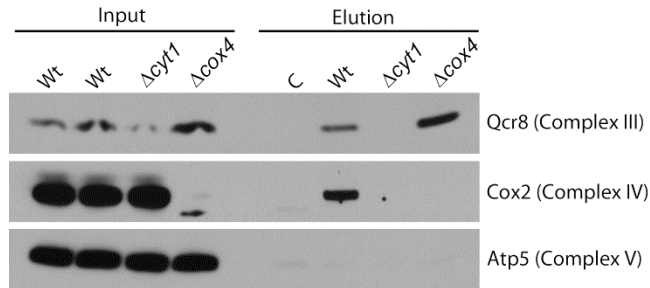


Figure 17: Prp43 associates with complex III

Shown are the Western blots of Co-IP of wild-type (Wt) strain, *cyt1* deletion strain ($\Delta cyt1$), and *cox4* deletion ($\Delta cox4$) strain mitochondrial lysate. TAP-Prp43 was used as bait protein. Wild-type functioned as positive control (Wt) while incubated with TAP-Prp43 or as negative control (C) while incubated with empty beads. Precipitated input and elution samples of the different strains and controls were analysed by SDS-PAGE and by Western blotting. The membrane was incubated with antibodies against complex III protein Qcr8, complex IV protein Cox2 and complex V protein Atp5.

3.12. Prp43 localisation in the complex III deficient strain

It was shown so far that Prp43 localises to mitochondria under apoptotic conditions (section 3.10) and new mitochondrial binding partners were identified (section 3.11). These results raised the question whether complex III is necessary for recruitment and/or tethering of Prp43 to the mitochondrial IMS in apoptosis. For this reason a subcellular fractionation of yeast cell lysates under apoptotic conditions were repeated with wild-type and a strain in which complex III ($\Delta cyt1$) is destabilised. A cleared cytoplasmic extract (E, also containing organelles) was prepared from each strain and a cytoplasmic supernatant and enriched mitochondrial pellet were then prepared by sedimentation centrifugation through a sucrose cushion (section 2.2.18). Protein distribution in different fractions was analysed by Western blotting. Prp43 was detected using an antibody against the endogenous protein. Antibodies against Pgk1 and Tom70 were taken as cytoplasmic and mitochondrial markers, respectively.

Results

The mitochondrial marker protein Tom70 is predominantly visible in the enriched mitochondria pellet (P; Figure 18) while the cytoplasmic marker Pgk1 is mostly present in the soluble cytoplasmic supernatant (S; Figure 18). Under apoptotic conditions, in the wild-type strain Prp43 is distributed similar to Tom70, but in the complex III destabilised strain Prp43 is mainly found in the soluble cytoplasmic fraction (S). Interestingly, this suggests that Prp43 is recruited to complex III in apoptosis and is tethered there.

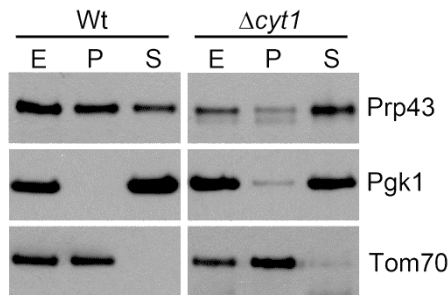


Figure 18: Prp43 is recruited to complex III under apoptotic conditions

For mitochondrial localisation assay, mitochondria of wild-type (Wt) and *cyt1* deletion ($\Delta 3$) strains without ($-H_2O_2$) or with ($-H_2O_2$) 100 mM hydrogen peroxide treatment were prepared. Samples of cell extract (E), enriched mitochondrial pellet (P), and cytoplasm (S) were taken. All samples were precipitated with TCA. Samples were resuspended in SDS sample loading buffer and analysed by SDS-PAGE for Western blotting. Antibodies against Prp43, Pgk1 as cytoplasmic marker protein, and Tom70 as mitochondrial marker protein were used.

3.13. Localisation of Prp43 upon G-patch protein overexpression

Prp43 is a multifunctional RNA helicase involved in ribosome biogenesis in the nucleolus and cytoplasm and in pre-mRNA splicing in the nucleus. Here, evidence is provided that Prp43 relocates to mitochondria in apoptosis. How Prp43 is distributed between these cellular pathways and compartments is therefore an interesting question. Prp43 has previously been shown to function with the G-patch protein Spp382 in splicing and the G-patch proteins Sqs1 and Pxr1 in ribosome biogenesis. The data in this study further show that Prp43 is stimulated by the G-patch protein Cmg1. This raises the possibility that these G-patch cofactors of Prp43 target the helicase to its different cellular functions. It was therefore investigated if overexpression of G-patch proteins can influence the localisation of Prp43. Different yeast strains all expressing plasmid encoded Nop1-RFP and endogenous Prp43-GFP but where expression of a

Results

particular G-patch protein was under the control of the Gal1 promoter were produced. A wild-type strain (without Gal1 promoter) served as a control (Wt). The localisation of Prp43 and Nop1 after induction of the Gal1 promoter was monitored and compared to the wild-type and the results are shown in Figure 19.

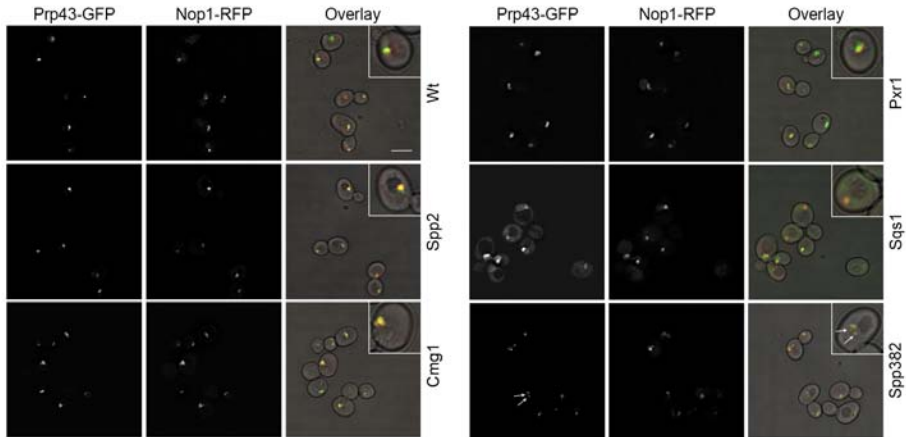


Figure 19: Prp43 relocalisation upon G-patch protein overexpression

Shown are fluorescence microscopy images of wild-type and *Spp2*, *Cmg1*, *Pxr1*, *Sqs1*, and *Spp382* Gal1 promoter inducible overexpression strains, containing Prp43-GFP and Nop1-RFP fusion proteins. Nop1 serves as a nucleolar marker. Shown are the images of the GFP, RFP and the overlay of both pictures. In the upper right corner of each overlay a magnified view of one cell is given. Scale bar represents 5 μm of the main image.

Under normal conditions both Prp43 and Nop1 are predominantly localised in the nucleolus (Henriquez *et al.*, 1990; Lebaron *et al.*, 2005). Comparison of localisation of Prp43 and Nop1 in the control strain to the *Spp2*, *Cmg1* and *Pxr1* overexpression strains revealed no changes. However, upon the overexpression of *Sqs1* or *Spp382* differences in the localisation of Prp43 but not Nop1 were observed. In addition to the nucleolar signal, a cytoplasmic Prp43-GFP signal is visible after *Sqs1* overexpression suggesting that Prp43 is relocalised to the cytoplasm. This is in line with the role of *Sqs1* in 20S pre-rRNA processing in the cytoplasm (Lebaron *et al.*, 2009; Pertschy *et al.*, 2009). In the case of *Spp382* overexpression Prp43 stays predominantly in the nucleolus, but nuclear speckles, which are indicated with arrows in Figure 19, are also visible. These spots likely correspond to splicing speckles in the nucleus, which is consistent with the role of *Spp382* as a splicing cofactor. Together these data show that

overexpression of cofactors can cause mislocalisation of the helicase to different cellular compartments.

3.14. G-patch proteins compete for Prp43 binding

The data so far show that the multifunctional DEAH-box protein Prp43 can be directed to different compartments of the cells by overexpression of its various G-patch protein cofactors. Interestingly, it was shown Sqs1 and Spp382 bind to the C-terminal part of Prp43 with their G-patch domains (Tsai *et al.*, 2005; Lebaron *et al.*, 2009; Christian *et al.*, 2014) and in this study, it was demonstrated that this is also the case for Cmg1. Together these data raise the possibility that the Prp43-interacting G-patch proteins compete for binding to the helicase. For this reason sequences encoding the five G-patch domains of Sqs1, Pxr1, Cmg1, and Spp2 were cloned into a vector enabling expression of MBP tagged fusion proteins that were subsequently purified from *E. coli*. The G-patch domain of Spp382 was also purified as a ProteinA fusion protein. In addition, Prp43 was expressed as a GFP fusion protein. The competition assay was performed as follows; Spp382 was bound to IgG sepharose and incubated with GFP-Prp43 and different concentrations of another G-patch protein. The unbound proteins were washed away, the IgG associated proteins were eluted and the fluorescence intensity of GFP was measured. If another G-patch protein interacts with Prp43 similarly or more strongly than Spp382 the amount of fluorescence measured will be decreased. Figure 20a shows the result of three independent measurements, normalised to the sample where no competitor was added (none). Addition of Spp2 does not influence the association of Prp43-GFP with Spp382, as would be expected for a protein that does not bind Prp43. The detected intensities show that Sqs1 competes with Spp382 for Prp43 binding and suggests that Prp43 has almost the same affinity for these proteins, since with 1:1 concentrations of the G-patch proteins the GFP signal is halved. Consistent with this, with increasing amounts of Sqs1 the GFP signal decreases. The Pxr1 G-patch domain similarly competes with Spp382 for Prp43 interaction and the effect is increased in the presence of higher amounts of Pxr1. In the case of Cmg1 competition, only minimal differences in the amount of Prp43-GFP associated with Spp382 could be observed. To examine the more minor effect of Cmg1 competition in more detail, a second assay was performed with pre-bound ProteinA-tagged Prp43 on IgG sepharose beads and RFP-Cmg1 1-85 as a signal output. In this case, direct competition between

Results

Cmg1 and the other G-patch protein domains could be monitored. To demonstrate the specificity of Prp43 interactions MBP was also included as a control.

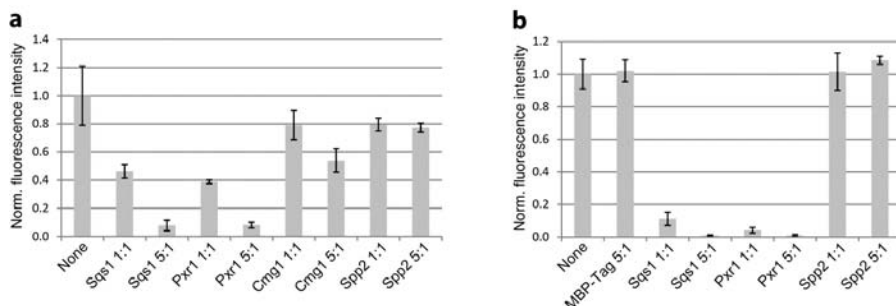


Figure 20: G-patch protein competition for Prp43 binding

a) Fluorescence based competition assay. The fluorescence intensities of GFP-Prp43 in the elution of ProteinA-Spp382 51-110 competing with MBP-Sqs1 705-767, MBP-Pxr1 1-82, MBP-Cmg1 1-85, and MBP-Spp2 92-157 are given. The results of three independent assays with empty beads value subtraction and their standard deviation are shown. **b)** Fluorescence based competition assay. The fluorescence intensities of RFP-Cmg1 competing with MBP, MBP-Sqs1 705-767, MBP-Pxr1 1-82, and MBP-Spp2 92-157 for interaction with ProteinA-Prp43 are given. The result of three independent assays with empty beads value subtraction and their standard deviation are shown.

The RFP signals of three independent measurements are given in Figure 20b. Neither MBP nor Spp2 affected the amount of Cmg1-RFP associated with Prp43. When Sqs1 or Pxr1 were included the fluorescence signals were dramatically reduced. This means that Sqs1 and Pxr1 bind to Prp43 with much higher affinity than Cmg1. Together these data show that the G-patch proteins compete for interaction with Prp43 and each have different affinities and in the order: Pxr1 > Sqs1 > Spp382 > Cmg1.

3.15. Overexpression of G-patch proteins affects precursor ribosomal RNA processing

The findings that G-patch proteins compete and their overexpression causes Prp43 mislocalisation suggests that changing the levels of individual G-patch proteins may affect Prp43 functions in its target pathways. Overexpression of G-patch proteins may influence the amount of Prp43 available for a particular process, potentially leading to defects in a pathway. To test this possibility, the effect of G-patch protein overexpression on the processing of pre-rRNA was studied. Total RNA was isolated from yeast wild-type and

Results

Spp2, *Cmd1*, *Pxr1*, *Sqs1*, and *Spp382* Gal1 promoter inducible overexpression strains grown in YPGal. *Spp2* served as negative control, because it does not interact with Prp43 and so no effect was expected. The RNA was separated by agarose-glyoxal gel electrophoresis, and analysed by Northern blotting using probes hybridising to different regions of the pre-rRNA transcript (p004 and p020; Figure 21a).

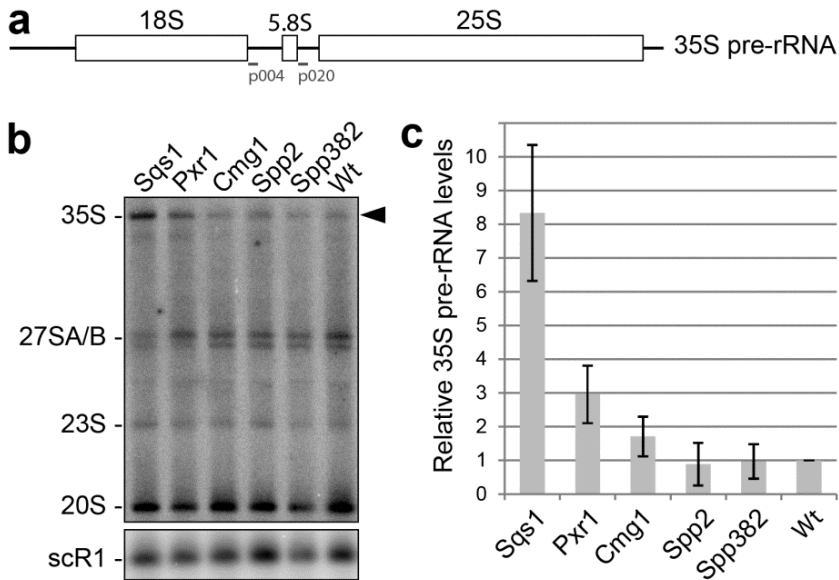


Figure 21: Influence of G-patch protein overexpression on ribosome biogenesis

a) Schematic representation of the 35S primary pre-rRNA transcript from yeast. The mature rRNAs are indicated by white boxes and the relative positions of probes that were used in Northern blotting are indicated in grey. **b)** Total RNA was isolated from wild-type (Wt) and G-patch protein overexpressing yeast strains (*Sqs1*, *Pxr1*, *Cmd1*, *Spp2*, and *Spp382*). After agarose-glyoxal gel electrophoresis Northern blotting was performed to detect rRNA precursors. **c)** The intensity of the 35S pre-rRNA signals was quantified using the ImageQuant software. The values were normalised to those for *scR1* RNA and wild-type level was set to one. Data of at least three experiments were taken and the standard deviation was calculated.

Together, these probes enable detection of the primary 35S transcript as well as the SSU pre-rRNAs (23S and 20S) and the LSU pre-rRNAs (27SA and 27SB). An additional probe, *scR1*, detects a small cytoplasmic RNA subunit of the signal recognition particle and was used as loading control. As shown in Figure 21b, overexpression of the G-patch proteins has minimal effect on the processing of the SSU pre-rRNAs, 23S and 20S. However, an accumulation of

Results

the early 35S pre-rRNA is clearly visible upon the overexpression of Sqs1 and Pxr1. Quantification of the results of at least three experiments show that overexpressing Sqs1 leads to an eight fold increase of 35S pre-rRNA. This supports the findings of (Pandit *et al.*, 2009) of a pre-rRNA processing defect upon Sqs1 overexpression. Interestingly, Pxr1 overexpression also leads to an accumulation of 35S pre-rRNA. Cmg1 overexpression also causes a minimal accumulation of 35S pre-rRNA while Spp2 and Spp382 overexpression does not influence 35S pre-rRNA levels. The accumulation of 35S pre-rRNA observed here is similar to the pre-rRNA processing defects detected in *prp43* mutant strains (Combs *et al.*, 2006; Leeds *et al.*, 2006) implying that the defects monitored here arise due to a lack of Prp43 available for particular steps in ribosome biogenesis. For example, the overexpression of the G-patch protein Sqs1 causes relocalisation of Prp43 to the cytoplasm (Figure 19), meaning less helicase can be recruited for early nucleolar steps of pre-rRNA processing.

4. DISCUSSION

A growing number of RNA helicases have been shown to play important roles in multiple cellular pathways, e.g. pre-mRNA splicing, ribosome synthesis, translation and RNA decay. How RNA helicases are recruited to their target pathways and how their activities in these processes are regulated has remained elusive. Protein cofactors are likely to be key players in RNA helicase recruitment and regulation but only a few helicase cofactors have been identified so far. Prp43 is a multifunctional RNA helicase that functions in the biogenesis of both the large and small ribosomal subunits, as well as at several stages of pre-mRNA splicing. Interestingly, Prp43 interacts with a specific group of cofactors, the G-patch proteins, and is regulated by them. Five G-patch proteins have been identified in the yeast *S. cerevisiae*. Three of these (Spp382, Sqs1 and Pxr1) have previously been shown to interact with and regulate Prp43 while the fourth (Spp2) interacts with the RNA helicase Prp2. At the beginning of this study the fifth G-patch protein (Cmg1/YLR271W) was uncharacterised.

4.1. Characterisation of the orphan G-patch protein Cmg1

Four of the yeast G-patch proteins are localised in the nucleolus (Pxr1 and Sqs1), in the nucleus (Spp2, Spp382, and Sqs1) and cytoplasm (Sqs1; Guglielmi and Werner, 2002; Huh *et al.*, 2003; Tsai *et al.*, 2005; Lebaron *et al.*, 2009; Pertschy *et al.*, 2009). In this study we found Cmg1 is localised in the cytoplasm as well as in the mitochondrial intermembrane space. Based on this observation, we renamed the protein to cytoplasmic and mitochondrial G-patch protein 1 (Cmg1). Interestingly, Cmg1 is the only G-patch protein that is localised in mitochondria. An overview of the localisation of the yeast G-patch proteins is given in Figure 22 (Exponential growth part). Interestingly, in other species G-patch proteins are also found in diverse sub-cellular localisations. In addition to several examples in the cytoplasm and nucleus, in human erythroleukaemia cells the G-patch protein CHERP is localised to the endoplasmic reticulum and in *Arabidopsis thaliana* the G-patch protein DRT111 is reported to be localised in the chloroplasts (Pang *et al.*, 1993; Laplante *et al.*, 2000). In yeast, the compartments of the cell in which the individual G-patch proteins are found are consistent with the pathways in which they function, e.g.

Discussion

Pxr1 is involved in ribosome biogenesis in the nucleolus. The broad range of organelles containing G-patch proteins implies that, like their helicase partners, they have roles in multiple cellular pathways. How the G-patch proteins are targeted to these different compartments is an important question. In the case of Pxr1, classical KK(E/D) motifs found in many nucleolar proteins were identified (Guglielmi and Werner, 2002). Similarly, an atypical nuclear localisation signal has been identified in Spp382 and its human homologue TFIP11 (Boon *et al.*, 2006; Tannukit *et al.*, 2009). How the mitochondrial fraction of Cmg1 is recruited to the IMS was therefore of interest. Most mitochondrial proteins are synthesised in the cytoplasm, targeted to the mitochondria and imported via the translocase of the outer membrane (TOM complex). Proteins imported using this pathway possess an N-terminal amphipathic α helical segment with a net positive charge and a length of 15 to 55 amino acids called the N-terminal presequence (Claros *et al.*, 1997; Dudek *et al.*, 2013). Several prediction programs (e.g. MitoProt, <http://ihg.gsf.de/ihg/mitoprot.html>; Claros and Vincens, 1996) could not identify such a sequence for Cmg1. Although poorly conserved sequences cannot be identified by these programmes, together with our observation that tagging Cmg1 at the N-terminal does not affect its mitochondrial localisation, this implies that Cmg1 is not imported into mitochondria via the classical TOM complex import pathway. However, alternative signals for protein import into mitochondria have also been described. C-terminal mitochondrial import signals have been suggested for the human APE1 protein and the yeast protein Him1p (Claros *et al.*, 1997; Lee *et al.*, 1999; Li *et al.*, 2010), although the functionality of these import signals has yet to be experimentally tested. Furthermore, hydrophobic internal import signals of proteins were discovered to play a role in mitochondrial protein targeting by interacting with Tom70 and Tom71 (Bolender *et al.*, 2008; Dudek *et al.*, 2013). Interestingly, small IMS proteins can also be imported via the MIA pathway. These proteins contain a mitochondrial IMS sorting signal (MISS) consisting of characteristic CX₃C or CX₉C twin motifs where C refers to a cysteine residue, which form disulphide bridges with the Mia40 protein in order to trap the proteins in the IMS (Bolender *et al.*, 2008; Stojanovski *et al.*, 2012; Dudek *et al.*, 2013). Cmg1 contains four cysteines but not in the characteristic sequence order of the MISS. So, how Cmg1 is imported to the mitochondrial IMS currently remains unknown.

Discussion

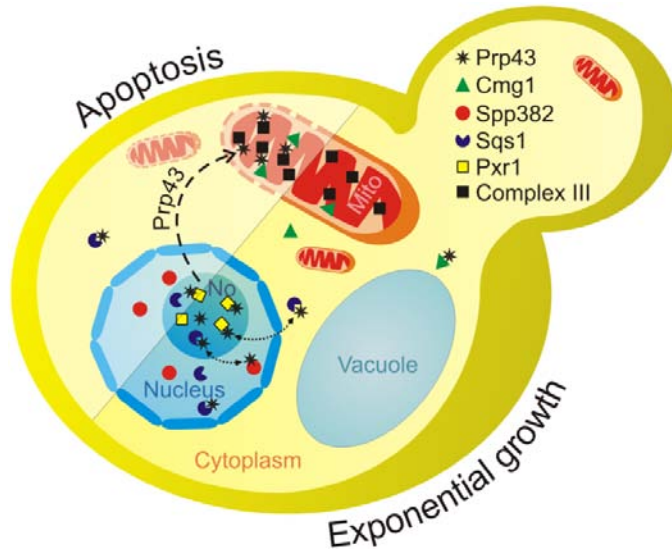


Figure 22: Scheme of Prp43 and G-patch protein localisation in exponential growth and apoptosis

In exponentially growing yeast cells, Prp43 is predominantly localised in the nucleolus (No) where it interacts with Sqs1 and Pxr1 during ribosome biogenesis. In the nucleus Prp43 interacts with Spp382 as component of the spliceosome. Only small amounts of Prp43 are in the cytoplasm where it is possibly associated with Sqs1 or Cmg1. Dotted arrows indicate G-patch protein competition for Prp43 binding. Under apoptotic conditions the OMM is permeabilised and Prp43 can enter the mitochondrial (Mito) IMS (dashed arrow) and binds complex III. Legend is given in the upper right.

Mitochondria function in several major cellular pathways such as, energy production and apoptosis. Our data showed that Cmg1 is not essential for mitochondrial metabolism. However, the *Cmg1* overexpression strain shows growth defects under normal conditions and reduced survival after induction of apoptosis, suggesting Cmg1 is a novel proapoptotic factor. In yeast, apoptosis can be triggered by exogenous signals such as heat stress, UV irradiation and toxic concentrations of various chemicals, as well as several endogenous cues including DNA damage and changes in the intracellular calcium concentration. Together, these signals cause an accumulation of reactive oxygen species (ROS) in the mitochondrial matrix and cytochrome c, which is normally anchored in the mitochondria by its interaction with cardiolipin, is then released into the cytoplasm through the permeabilised outer mitochondrial membrane (Guaragnella *et al.*, 2012; Côte-Real and Madeo, 2013). In yeast, this is dependent on the caspase Yca1 and leads to activation of effector caspase-like proteins, which cause DNA fragmentation bringing about cell death.

Discussion

Interestingly, we observed that the cytoplasmic pool of Cmg1 relocates to mitochondria under apoptotic conditions. It is possible for proteins to enter the mitochondrial IMS in apoptosis due to the permeabilised outer mitochondrial membrane but only a few yeast proteins that promote programmed cell death translocate to mitochondria under apoptotic conditions and examples include the proteins Mmi1 and Mcd1 (Rinnerthaler *et al.*, 2006; Yang *et al.*, 2008). Although novel proapoptotic factors, such as Cmg1, are being identified, their role in programmed cell death often remains elusive. In the case of the G-patch protein Cmg1, it is possible that its proapoptotic function involves an RNA helicase interaction partner.

Here, we identified the DEAH-box protein Prp43 as a Cmg1 interaction partner. Under normal growth conditions, the DEAH-box protein Prp43 is predominantly found in the nucleolus and the nucleus (Arenas and Abelson, 1997; Lebaron *et al.*, 2005; Bohnsack *et al.*, 2009). However, Prp43 is also exported to the cytoplasm with Sqs1 on the pre-40S ribosomal subunit (Lebaron *et al.*, 2005; Pertschy *et al.*, 2009). Since, without induction of apoptosis Cmg1 is also mainly cytosolic, it is likely that in exponentially growing yeast Prp43 and Cmg1 function together in the cytoplasm. However, elucidating the role of Cmg1-Prp43 complex in the cytoplasm is challenging. Our data show that, unlike other G-patch proteins, Cmg1 does not bind to RNA itself, so target RNAs cannot be identified using methods such as CRAC. This method has previously been applied to identify Prp43-associated RNAs (Bohnsack *et al.*, 2009). However, Cmg1 is naturally expressed at very low levels and approximately ten times more Prp43 is present in the cell (Ghaemmaghani *et al.*, 2003). This means that few Cmg1-Prp43 complexes will be present and their cytoplasmic targets will be hard to detect amongst the many nuclear targets of the multifunctional helicase Prp43. However, under apoptotic conditions Cmg1 is exclusively mitochondrial and cytoplasmic Prp43 is also relocalised to the mitochondria, indicating that the helicase and its cofactor may also function together in mitochondria in apoptosis.

4.2. Prp43 at mitochondria in apoptosis

A parallel study recently showed that the human homologue of Prp43, DHX15, is localised in the nucleus, cytosol and mitochondria under normal growth conditions (Mosallanejad *et al.*, 2014). How DHX15 is recruited to mitochondria and its function there were not elucidated, but the helicase was found to play an important role in the cellular response to RNA virus infection

Discussion

by triggering cytokine production and apoptosis through regulation of the NF- κ B and MAPK signalling pathways (Lu *et al.*, 2014; Mosallanejad *et al.*, 2014). In contrast, in yeast, Prp43 was not detected at mitochondria during exponential growth but was only recruited to mitochondria in apoptosis. Although a fraction of Cmg1 is localised to the mitochondria in steady-state growth, the recruitment of Prp43 to the mitochondrial IMS under apoptotic conditions was found to be independent of Cmg1. Interestingly, Prp43 was found to associate with complex III of the respiratory chain (Figure 22) and this interaction is required for the relocation of Prp43 to the mitochondria in apoptosis. Notably, complex III contains the Cor1 protein that has previously been shown to be involved in apoptosis in yeast (Büttner *et al.*, 2011), potentially suggesting a more general role for complex III in programmed cell death.

It is possible that Prp43 has an active role in mitochondria in apoptosis. Prp43 is required for snoRNA release from pre-ribosomes, intron-lariat release from spliceosome and spliceosomal disassembly (Martin *et al.*, 2002; Tsai *et al.*, 2005; Bohnsack *et al.*, 2009), suggesting that the helicase has a general function in the disassembly of RNP complexes. The disassembly of RNA-protein complexes can allow better access of nucleases and proteases to their targets and leading to enhanced degradation. Therefore, in apoptosis, some Prp43 protein may facilitate degradation of mitochondrial RNP complexes such as mitochondria-associated ribosomes, mRNPs or the imported cytosolic tRNA^{Lys} and precursor of the mitochondrial lysyl-tRNA synthetase complex (Tarassov *et al.*, 1995). However, these functions would be limited to the IMS and mitochondria-associated complexes, as Cmg1 and Prp43 likely not enter the mitochondrial matrix where the degradosome composed of the RNA helicase Suv3 and the RNase II-like protein Dss1 (Stepien *et al.*, 1992; Min *et al.*, 1993; Margossian *et al.*, 1996; Dziembowski *et al.*, 2003), might also be able to perform such functions in apoptosis. Data from the Bohnsack lab suggest, however, that rather than playing an active role at mitochondria, Prp43 is sequestered to the organelle during apoptosis. An UV cross-linking experiment was performed to analyse the RNA interactions of Prp43 with and without induction of apoptosis. This revealed that the majority of RNA interactions of Prp43 were lost after induction of apoptosis. This suggests that during apoptosis Prp43 is withdrawn from its RNA targets in pre-mRNA splicing and ribosome biogenesis, likely to inhibit these pathways.

4.3. Recruitment of helicases to their target sites

Prp43 is one of a growing number of RNA helicases that have been shown to have multiple cellular functions. Prp43 plays roles in the biogenesis of both ribosomal subunits and is also involved in pre-mRNA splicing and spliceosome quality control. Other examples include Dbp2 that is involved in ribosome biogenesis and RNA quality control/decay and Dbp5, which is implicated in RNA export and translation (Tseng *et al.*, 1998; Bond *et al.*, 2001; Gross *et al.*, 2007; Cloutier *et al.*, 2012). Furthermore, the human RNA helicase DDX5 is reported to function in transcription regulation, pre-mRNA splicing and RNA decay (Jurica *et al.*, 2002; Wilson *et al.*, 2004). Similarly, the bacterial RNA helicase CsdA is required for mRNA degradation and ribosome biogenesis (Moll *et al.*, 2002; Charollais *et al.*, 2004; Peil *et al.*, 2008; Palonen *et al.*, 2012). The existence of multifunctional helicases may enable cross-regulation of various cellular pathways. However, since these helicases have numerous RNA substrates; how to identify their targets and how they are recruited to them are key questions.

It is possible that some RNA helicases recognise specific sequence motifs or secondary structures within their substrate RNAs. So far only one example of a helicase that is recruited in this way has been identified and this is the *E. coli* DEAD-box protein DbpA and its *Bacillus subtilis* ortholog YxiN (Kossen and Uhlenbeck, 1999; Tsu *et al.*, 2001). In both species, the helicase has been shown to interact with helix 92 of the 23S rRNA. However, it is highly likely that other RNA helicases recruited in this way will be discovered as the RNA substrates and binding sites of a growing number of RNA helicases are being identified. Interestingly, it was recently shown that the human RNA helicase DDX1 is recruited to viral particles upon phosphorylation of the nucleocapsid (Wu *et al.*, 2014), suggesting that post-translational modification of the protein components of RNP complexes may also regulate recruitment of helicases to their RNA targets.

Another way in which helicases can be recruited to their substrates is by protein cofactors. Relatively few RNA helicase cofactors have been identified so far and direct evidence of their role in targeting helicases is often lacking. However, the DEAD-box RNA helicase cofactor Esf2 not only stimulates Dbp8 activity but is suggested to also recruit the helicase to its pre-rRNA target site (Granneman *et al.*, 2006). Furthermore, the nucleoporin Gle5/Nup159 acts as a cofactor of Dbp5 and is suggested to recruit the helicase to the nuclear pore complex for its function in remodelling RNA-protein complexes after export

(Montpetit *et al.*, 2011). Also, the NTR complex, composed of Ntr2 and the G-patch protein Spp382, has been shown to recruit Prp43 to the spliceosome (Tsai *et al.*, 2007).

4.4. Regulation of RNA helicases by cofactor competition

In addition to conferring substrate specificity on RNA helicases, protein cofactors can also regulate the ATPase and unwinding activity of RNA helicases. Different cofactors have been shown to affect all aspects of RNA helicase function, including RNA- and ATP-binding, RNA unwinding, ATP hydrolysis, and phosphate-, ADP-, and RNA-release (Karbstein, 2011; Linder and Jankowsky, 2011). The eIF4G cofactor increases the affinity of the DEAD-box helicase eIF4A for both ATP and RNA by causing a conformational change that reduces the distance between the two RecA-like domains (Oberer *et al.*, 2005; Schütz *et al.*, 2008). In contrast, binding of Upf2 reduces the RNA affinity of the SF1 helicase Upf1 but enhances its helicase activity by inducing structural rearrangements (Cheng *et al.*, 2007; Chakrabarti *et al.*, 2011). Furthermore, the interaction between the DEAD-box protein Dbp5 and its cofactor Gle1 is mediated by the inositol hexakisphosphate molecule and the complex shows increased substrate release (Montpetit *et al.*, 2011).

The best characterised class of RNA helicase cofactors are the G-patch proteins, which contain a conserved glycine-rich domain. The G-patch proteins PINX1 (human ortholog of Pxr1), Sqs1 and Spp382 have all been shown to stimulate the helicase and/or the ATPase activity of Prp43 (Tanaka *et al.*, 2007; Lebaron *et al.*, 2009; Chen *et al.*, 2014; Christian *et al.*, 2014), while Spp2 enhances the ATPase activity of Prp2 (Roy *et al.*, 1995), and here it was found that the G-patch protein Cmg1 increases the RNA-dependent ATPase activity and RNA-binding affinity of Prp43. The G-patch domains of Cmg1, Sqs1 and Spp382 were shown to mediate the interactions with Prp43 (this study; Tsai *et al.*, 2005; Lebaron *et al.*, 2009; Walbott *et al.*, 2010; Christian *et al.*, 2014) and mutation analysis of Pxr1 confirmed that the integrity of its G-patch domain is essential for its interaction with Prp43 (Chen *et al.*, 2014). All DEAH-box RNA helicases contain a common helicase core domain but have different N- and C-terminal extensions that are proposed to function as cofactor binding platforms (Cordin and Beggs, 2013). Here it was shown that deletion of either the N-terminal helix of Prp43 or 110 amino acid residues from the C-terminus

Discussion

abolishes interaction with Cmg1. For Sqs1 it was shown that its G-patch domain interacts with the C-terminal part of Prp43 and although Sqs1 can still interact with a C-terminally truncated version of Prp43 (Prp43 1-657), this interaction is not mediated by the G-patch domain (Walbott *et al.*, 2010). Similarly, Spp2 binds to the C-terminal domain of the RNA helicase Prp2 (Silverman *et al.*, 2004). Interestingly, all five G-patch proteins interact with the C-terminal domain of DEAH-box proteins while only certain G-patch proteins contact the N-termini of their helicase partners, perhaps suggesting that unique N-terminal sequences confer cofactor specificity.

The finding that four G-patch proteins all bind the C-terminal region of Prp43 raised the possibility that the cofactors compete for binding to the helicase. Consistent with this, we found that overexpression of individual G-patch proteins leads to mislocalisation of Prp43. An increase in Sqs1 levels causes accumulation of Prp43 in the cytoplasm, which is likely to correlate with the function of Sqs1 in the late steps of biogenesis of the small ribosomal subunit (Pertschy *et al.*, 2009). Furthermore, Sqs1 overexpression leads to accumulation of the 35S pre-rRNA. This pre-rRNA processing phenotype is also observed upon depletion of Prp43 (Bohnsack *et al.*, 2009), implying that Sqs1 overexpression causes withdrawal of the helicase from its early functions in ribosome biogenesis in the nucleolus. In line with this, overexpression of Sqs1 has also been shown to lead to defects in pre-mRNA splicing (Pandit *et al.*, 2009). Unsurprisingly, overexpression of the nucleolar G-patch protein Pxr1 does not cause mislocalisation of Prp43, however, accumulation of the 35S pre-rRNA was observed. This suggests that when Pxr1 is overexpressed, it competes for Prp43 binding and prevents association of the helicase with early pre-ribosomal complexes. Mislocalisation of Prp43 to nuclear foci upon overexpression of Spp382 was also observed and probably reflects recruitment of Prp43 to spliceosomes. Only minimal pre-rRNA processing defects were detected but it is possible that the effect observed would be stronger if both Spp382 and Ntr2 were overexpressed as, along with Prp43, these proteins form the trimeric NTR-complex and Ntr2, rather than Spp382, is responsible for recruitment of Prp43 to the spliceosome. A mild accumulation of 35S pre-rRNA was also observed upon overexpression of Cmg1 indicating that Cmg1 may also compete for interaction with Prp43 in the cytoplasm. Together, these data support a model of cofactor competition in which changes in the levels of G-patch proteins affect the localisation of Prp43 and its functions in its target pathways of ribosome biogenesis and pre-mRNA splicing.

Discussion

Competition between G-patch proteins may not only determine the steady-state distribution of Prp43 between different pathways as high-throughput analyses suggest that the expression levels of the G-patch proteins are altered in different conditions. For example, Cmg1 is overexpressed in oxidative and chemical stress (Gasch *et al.*, 2000; Guan *et al.*, 2012) and both Sqs1 and Pxr1 are overexpressed during sporulation (Brauer *et al.*, 2008; Borde *et al.*, 2009). Furthermore, the levels of Spp382 are reported to be increased by the unfolded protein response (Wyrick *et al.*, 1999; Thibault *et al.*, 2011) and Spp2 is overexpressed during starvation (Bradley *et al.*, 2009).

Analysis of the competition between G-patch proteins *in vitro* suggests that there exists a hierarchy of affinities for Prp43, as follows: Pxr1 > Sqs1 > Spp382 > Cmg1. The consensus motif that was used for the identification of these G-patch proteins was $h h x_3 G a x_2 G x G h G x_4 G$, which contains bulky and hydrophobic residues (h; I, L, V, M), an aromatic residue (a; F, Y, W), several positions of any residue (x_n) and six conserved glycines (G). A multiple sequence alignment of the G-patch domains of Sqs1, Pxr1, Spp382, Cmg1 and Spp2 (Figure 23) suggests a correlation between the conservation of the G-patch motif and the helicase affinity. All six glycine residues are present in the domains of Sqs1, Pxr1 and Spp382, which were best able to compete for Prp43 binding. Cmg1 contains only five of the six conserved glycine residues, while Spp2 has only four, which may explain the weaker, or lack of, binding to Prp43. Furthermore, Chen and co-workers showed that the leucine residues at positions 33, 44 and 67 of Pxr1 are required for the G-patch domain integrity implying that not only the glycine residues of this domain are important. Along this line, an interesting difference between Spp382, which appears to have relatively low affinity for Prp43, and Pxr1 and Sqs1, which are best able to compete for Prp43 binding, is the presence of a tyrosine instead of a tryptophan after the first glycine. However, to confirm the influence for specific residues on the affinity of each cofactor for the helicase further mutational and structural analysis would be required. In addition, since other regions of some G-patch proteins (e.g. Sqs1) have also been shown to contact Prp43, it would be interesting to compare these data to the relative affinities of the full-length G-patch proteins.

Discussion

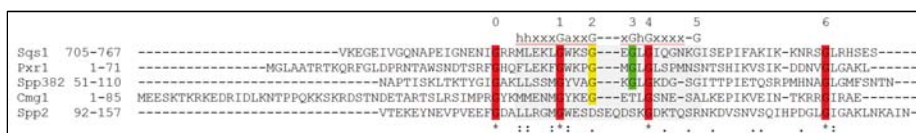


Figure 23: Alignment of yeast protein G-patch domains

Shown is an alignment of the five yeast G-patch protein domains used during this study. The grey box indicates the signature $hhx_3Gax_2GxGhGx_4G$ (h = bulky, hydrophobic residue: I, L, V, M; a = aromatic residue: F, Y, W; and x_n = n positions of any residues) used for a simple pattern search (Aravind and Koonin, 1999) and which is shown above the box. Numbers above sequences represent the glycines predicted from Aravind and Koonin (0 means not predicted). Red coloured glycines are found in all five G-patch proteins, yellow ones are present in four proteins and green glycines are only found in three G-patch proteins at the given position. Alignment was performed using the ClustalW2 software from EMBL-EBI homepage (McWilliam *et al.*, 2013). An asterisk (*) indicates positions, which have a single, fully conserved residue. A colon (:) indicates conservation between groups of strongly similar properties. A fullstop (.) indicates conservation between groups of weakly similar properties.

Besides the primary amino acid sequence, it is likely that additional levels of regulation, such as post-translational modifications can also influence G-patch proteins and therefore, their helicase partners. Numerous modifications are predicted for G-patch proteins, especially in higher eukaryotes. Indeed, phosphorylation of the human G-patch protein GPKOW has been shown to influence its RNA-binding affinity (Aksaas *et al.*, 2011) and the G-patch protein ZGPAT, which is involved in inhibition cell proliferation and survival, is ubiquitinated and degraded during HIV-1 infection (Maudet *et al.*, 2013). In addition, G-patch proteins may be regulated by multimerisation. Pandit and co-workers showed by using a yeast two-hybrid assays that the yeast G-patch proteins Sqs1 and Spp382 can interact directly (Pandit *et al.*, 2009). Further, a comprehensive yeast two-hybrid analysis of the factors found in human spliceosomal complexes suggest that the G-patch proteins GPKOW, RBM10, SUGP1 and RBM17 are able to multimerise with each other (Hegele *et al.*, 2012). However, not only heteromers of G-patch proteins have been identified. Dimerisation of yeast Pxr1 and human GPKOW have been suggested (Tarassov *et al.*, 2008; Gui *et al.*, 2012) and size-exclusion experiments performed in the Bohnsack lab suggest that Cmg1 may also forms homomultimers.

G-patch proteins are likely to represent the largest family of RNA helicase cofactors. Proteins containing the G-patch motif are not found in bacteria or archaea, but G-patch proteins are found throughout higher eukaryotes and are present in many retroviruses. Human homologues of the five G-patch proteins

Discussion

found in yeast have been identified (Sqs1 → GPATCH2; Spp382 → TFIP11; Pxr1 → PINX1; Spp2 → GPKOW). The roles of TFIP11 and GPKOW in human pre-mRNA splicing appear to be conserved from yeast (Yoshimoto *et al.*, 2009; Zang *et al.*, 2014). Similarly, PINX1 can substitute for Pxr1 in yeast (Guglielmi and Werner, 2002; Yoo *et al.*, 2009), but an additional function of the human protein as a telomerase inhibitor has also been shown (Zhou and Lu, 2001). Beside these five proteins, human cells contain approximately 20 additional G-patch proteins, which have so far been linked to various cellular processes including transcription, pre-mRNA splicing, tumour suppression and some are implicated in viral infection (Feng *et al.*, 2002; Jurica *et al.*, 2002; Li *et al.*, 2009; Sutherland *et al.*, 2010). The helicases that these cofactors interact with are mostly not known yet but it has been shown that human G-patch protein GPKOW binds to the RNA helicase DHX16 (homolog of yeast Prp2) and also that the G-patch protein RBM5 interacts, via its G-patch domain, with the human homolog of Prp43, DHX15 (Aksaas *et al.*, 2011; Niu *et al.*, 2012). The presence of a large number of G-patch proteins in higher eukaryotes implies that the cofactor competition model identified in yeast will also be highly relevant for the regulation of multifunctional helicases in humans.

4.5. Conclusions

In summary, the fifth G-patch in *S. cerevisiae*, Cmg1, was identified as a cofactor of the multifunctional RNA helicase Prp43. This protein was found to be localised in the cytoplasm and mitochondrial intermembrane space and to be a new proapoptotic factor. Furthermore, under apoptotic conditions, Prp43 is relocated to mitochondria where it interacts with complex III of the respiratory chain. Furthermore, overexpression of G-patch protein cofactors of Prp43 was shown to cause mislocalisation of the helicase and defects in its target pathway of ribosome biogenesis. The data therefore suggest cofactor competition as a novel mechanism for regulation of multifunctional RNA helicases.

5. REFERENCES

- Aksaas A K, Larsen A C, Rogne M, Rosendal K, Kvissel A-K, Skalhegg B S. (2011) G-patch domain and KOW motifs-containing protein, GPKOW; a nuclear RNA-binding protein regulated by protein kinase A. *Journal of Molecular Signaling* **6**: 10.
- Alcázar-Román A R, Tran E J, Guo S, Wentz S R. (2006) Inositol hexakisphosphate and Gle1 activate the DEAD-box protein Dbp5 for nuclear mRNA export. *Nature Cell Biology* **7**: 711–716.
- Anderson J S, Parker R P. (1998) The 3' to 5' degradation of yeast mRNAs is a general mechanism for mRNA turnover that requires the SKI2 DEVH box protein and 3' to 5' exonucleases of the exosome complex. *The EMBO Journal* **5**: 1497–1506.
- Aravind L, Koonin E V. (1999) G-patch: a new conserved domain in eukaryotic RNA-processing proteins and type D retroviral polyproteins. *Trends In Biochemical Sciences* **9**: 342–344.
- Arenas J E, Abelson J N. (1997) Prp43: An RNA helicase-like factor involved in spliceosome disassembly. *Biochemistry* **94**: 11798–11802.
- Bhaskaran H, Russell R. (2007) Kinetic redistribution of native and misfolded RNAs by a DEAD-box chaperone. *Nature* **7165**: 1014–1018.
- Bleichert F, Baserga S J. (2007) The Long Unwinding Road of RNA Helicases. *Molecular Cell* **3**: 339–352.
- Blum S, Mueller M, Schmid S R, Linder P, Trachsel H. (1989) Translation in *Saccharomyces cerevisiae*: initiation factor 4A-dependent cell-free system. *Proceedings of the National Academy of Sciences of the United States of America* **16**: 6043–6046.
- Bohnsack M T, Kos M, Tollervey D. (2008) Quantitative analysis of snoRNA association with pre-ribosomes and release of snR30 by Rok1 helicase. *EMBO Reports* **12**: 1230–1236.
- Bohnsack M T, Martin R, Granneman S, Ruprecht M, Schleiff E, Tollervey D. (2009) Prp43 Bound at Different Sites on the Pre-rRNA Performs Distinct Functions in Ribosome Synthesis. *Molecular Cell* **4**: 583–592.
- Bohnsack M T, Tollervey D, Granneman S. (2012) Identification of RNA helicase target sites by UV cross-linking and analysis of cDNA. *Methods in Enzymology* **511**: 275–288.
- Bolender N, Sickmann A, Wagner R, Meisinger C, Pfanner N. (2008) Multiple pathways for sorting mitochondrial precursor proteins. *EMBO Reports* **1**: 42–49.
- Bolger T A, Wentz S R. (2011) Gle1 is a multifunctional DEAD-box protein regulator that modulates Ded1 in translation initiation. *The Journal of biological Chemistry* **46**: 39750–39759.
- Bond A T, Mangus D A, He F, Jacobson A. (2001) Absence of Dbp2p alters both nonsense-mediated mRNA decay and rRNA processing. *Molecular and Cellular Biology* **21**: 7366–7379.
- Boon K-L, Auchynnikava T, Edwards-Gilbert G, Barrass J D, Droop A P, Dez C, Beggs J D. (2006) Yeast Ntr1/Spp382 Mediates Prp43 Function in Postsplisomes. *Molecular and Cellular Biology* **16**: 6016–6023.
- Borde V, Robine N, Lin W, Bonfils S, Geli V, Nicolas A. (2009) Histone H3 lysine 4 trimethylation marks meiotic recombination initiation sites. *The EMBO Journal* **2**: 99–111.
- Brachmann C B, Davies A, Cost G J, Caputo E, Li J, Hieter P, Boeke J D. (1998) Designer deletion strains derived from *Saccharomyces cerevisiae* S288C: a useful set of strains and plasmids for PCR-mediated gene disruption and other applications. *Yeast (Chichester, England)* **2**: 115–132.
- Bradley P H, Brauer M J, Rabinowitz J D, Troyanskaya O G. (2009) Coordinated concentration changes of transcripts and metabolites in *Saccharomyces cerevisiae*. *PLoS Computational Biology* **1**: e1000270.

References

- Brauer M J, Huttenhower C, Airoidi E M, Rosenstein R, Matese J C, Gresham D, Boer V M, Troyanskaya O G, Botstein D. (2008) Coordination of growth rate, cell cycle, stress response, and metabolic activity in yeast. *Molecular Biology of the Cell* **1**: 352–367.
- Büttner K, Nehring S, Hopfner K-P. (2007) Structural basis for DNA duplex separation by a superfamily-2 helicase. *Nature structural & molecular biology* **7**: 647–652.
- Büttner S, Ruli D, Vogtle F-N, Galluzzi L, Moitzi B, Eisenberg T, Kepp O, Habernig L, Carmona-Gutierrez D, Rockenfeller P, Laun P, Breitenbach M, Khoury C, Frohlich K-U, Rechberger G, Meisinger C, Kroemer G, Madeo F. (2011) A yeast BH3-only protein mediates the mitochondrial pathway of apoptosis. *The EMBO Journal* **14**: 2779–2792.
- Cao G, Xing J, Xiao X, Liou, Anthony K F, Gao Y, Yin X-M, Clark, Robert S B, Graham S H, Chen J. (2007) Critical role of calpain I in mitochondrial release of apoptosis-inducing factor in ischemic neuronal injury. *The Journal of Neuroscience* **35**: 9278–9293.
- Chakrabarti S, Jayachandran U, Bonneau F, Fiorini F, Basquin C, Domcke S, Le Hir H, Conti E. (2011) Molecular mechanisms for the RNA-dependent ATPase activity of Upf1 and its regulation by Upf2. *Molecular Cell* **6**: 693–703.
- Chamot D, Colvin K R, Kujat-Choy S L, Owtttrim G W. (2005) RNA structural rearrangement via unwinding and annealing by the cyanobacterial RNA helicase, CrhR. *The Journal of Biological Chemistry* **3**: 2036–2044.
- Charollais J, Dreyfus M, Iost I. (2004) CsdA, a cold-shock RNA helicase from *Escherichia coli*, is involved in the biogenesis of 50S ribosomal subunit. *Nucleic Acids Research* **9**: 2751–2759.
- Chen Y-L, Capeyrou R, Humbert O, Mouffok S, Kadri Y Al, Lebaron S, Henras A K, Henry Y. (2014) The telomerase inhibitor Gno1p/PINX1 activates the helicase Prp43p during ribosome biogenesis. *Nucleic Acids Research* **11**: 7330–7345.
- Cheng Z, Muhlrud D, Lim M K, Parker R, Song H. (2007) Structural and functional insights into the human Upf1 helicase core. *The EMBO Journal* **1**: 253–264.
- Cheung D, Hang-Cheong, Kung H-F, Huang J-J, Shaw P-C. (2012) PinX1 is involved in telomerase recruitment and regulates telomerase function by mediating its localization. *FEBS Letters* **19**: 3166–3171.
- Christian H, Hofele R V, Urlaub H, Ficner R. (2014) Insights into the activation of the helicase Prp43 by biochemical studies and structural mass spectrometry. *Nucleic Acids Research* **2**: 1162–1179.
- Claros M G, Brunak S, von Heijne G. (1997) Prediction of N-terminal protein sorting signals. *Current Opinion in Structural Biology* **3**: 394–398.
- Claros M G, Vincens P. (1996) Computational method to predict mitochondrially imported proteins and their targeting sequences. *European Journal of Biochemistry / FEBS* **3**: 779–786.
- Cloutier S C, Ma W K, Nguyen L T, Tran E J. (2012) The DEAD-box RNA Helicase Dbp2 Connects RNA Quality Control with Repression of Aberrant Transcription. *Journal of Biological Chemistry* **31**: 26155–26166.
- Combs D J, Nagel R J, Ares MJR, Stevens S W. (2006) Prp43p is a DEAH-box spliceosome disassembly factor essential for ribosome biogenesis. *Molecular and Cellular Biology* **2**: 523–534.
- Cordin O, Banroques J, Tanner N K, Linder P. (2006) The DEAD-box protein family of RNA helicases. *Gene* **367**: 17–37.
- Cordin O, Beggs J D. (2013) RNA helicases in splicing. *RNA Biology* **1**: 83–95.
- Cordin O, Hahn D, Beggs J D. (2012) Structure, function and regulation of spliceosomal RNA helicases. *Current Opinion in Cell Biology* **3**: 431–438.

References

- Cordin O, Tanner N K, Doere M, Linder P, Banroques J. (2004) The newly discovered Q motif of DEAD-box RNA helicases regulates RNA-binding and helicase activity. *The EMBO Journal* **13**: 2478–2487.
- Côrte-Real M, Madeo F. (2013) Yeast programmed cell death and aging. *Frontiers in Oncology* **3**: 283.
- Dominguez D, Altmann M, Benz J, Baumann U, Trachsel H. (1999) Interaction of Translation Initiation Factor eIF4G with eIF4A in the Yeast *Saccharomyces cerevisiae*. *Journal of Biological Chemistry* **38**: 26720–26726.
- Dudek J, Rehling P, van der Laan M. (2013) Mitochondrial protein import: common principles and physiological networks. *Biochimica et Biophysica Acta* **2**: 274–285.
- Dziembowski A, Piwowarski J, Hoser R, Minczuk M, Dmochowska A, Siep M, van der Spek H, Grivell L, Stepien P P. (2003) The yeast mitochondrial degradosome. Its composition, interplay between RNA helicase and RNase activities and the role in mitochondrial RNA metabolism. *The Journal of Biological Chemistry* **3**: 1603–1611.
- Fairman-Williams M E, Guenther U-P, Jankowsky E. (2010) SF1 and SF2 helicases: family matters. *Current Opinion in Structural Biology* **3**: 313–324.
- Feng X, Guo Z, Nourbakhsh M, Hauser H, Ganster R, Shao L, Geller D A. (2002) Identification of a negative response element in the human inducible nitric-oxide synthase (hiNOS) promoter: The role of NF-kappa B-repressing factor (NRF) in basal repression of the hiNOS gene. *Proceedings of the National Academy of Sciences of the United States of America* **22**: 14212–14217.
- Frazier A E, Taylor R D, Mick D U, Warscheid B, Stoepel N, Meyer H E, Ryan M T, Guiard B, Rehling P. (2006) Mdm38 interacts with ribosomes and is a component of the mitochondrial protein export machinery. *The Journal of Cell Biology* **4**: 553–564.
- Fromont-Racine M, Senger B, Saveanu C, Fasiolo F. (2003) Ribosome assembly in eukaryotes. *Gene* **313**: 17–42.
- Fuller-Pace F V. (2006) DExD/H box RNA helicases: multifunctional proteins with important roles in transcriptional regulation. *Nucleic Acids Research* **15**: 4206–4215.
- Garrido C, Galluzzi L, Brunet M, Puig P E, Didelot C, Kroemer G. (2006) Mechanisms of cytochrome c release from mitochondria. *Cell Death and Differentiation* **9**: 1423–1433.
- Gasch A P, Spellman P T, Kao C M, Carmel-Harel O, Eisen M B, Storz G, Botstein D, Brown P O. (2000) Genomic expression programs in the response of yeast cells to environmental changes. *Molecular Biology of the Cell* **12**: 4241–4257.
- Ghaemmaghami S, Huh W-K, Bower K, Howson R W, Belle A, Dephoure N, O'Shea E K, Weissman J S. (2003) Global analysis of protein expression in yeast. *Nature* **6959**: 737–741.
- Granneman S, Kudla G, Petfalski E, Tollervey D. (2009) Identification of protein binding sites on U3 snoRNA and pre-rRNA by UV cross-linking and high-throughput analysis of cDNAs. *Proceedings of the National Academy of Sciences of the United States of America* **24**: 9613–9618.
- Granneman S, Lin C, Champion E A, Nandineni M R, Zorca C, Baserga S J. (2006) The nucleolar protein Esf2 interacts directly with the DExD/H box RNA helicase, Dbp8, to stimulate ATP hydrolysis. *Nucleic Acids Research* **10**: 3189–3199.
- Gross T, Siepmann A, Sturm D, Windgassen M, Scarcelli J J, Seedorf M, Cole C N, Krebber H. (2007) The DEAD-box RNA helicase Dbp5 functions in translation termination. *Science (New York, N.Y.)* **5812**: 646–649.
- Guan Q, Haroon S, Bravo D G, Will J L, Gasch A P. (2012) Cellular memory of acquired stress resistance in *Saccharomyces cerevisiae*. *Genetics* **2**: 495–505.
- Guaragnella N, Zdravlečić M, Antonacci L, Passarella S, Marra E, Giannattasio S. (2012) The role of mitochondria in yeast programmed cell death. *Frontiers in Oncology* **2**: 70.

References

- Guglielmi B, Werner M. (2002) The Yeast Homolog of Human PinX1 Is Involved in rRNA and Small Nucleolar RNA Maturation, Not in Telomere Elongation Inhibition. *Journal of Biological Chemistry* **38**: 35712–35719.
- Gui B, Han X, Zhang Y, Liang J, Wang D, Xuan C, Yu Z, Shang Y. (2012) Dimerization of ZIP promotes its transcriptional repressive function and biological activity. *The International Journal of Biochemistry & cell biology* **6**: 886–895.
- He Y, Andersen G R, Nielsen K H. (2010) Structural basis for the function of DEAH helicases. *EMBO Reports* **3**: 180–186.
- Hegele A, Kamburov A, Grossmann A, Sourlis C, Wowro S, Weimann M, Will C L, Pena V, Luhrmann R, Stelzl U. (2012) Dynamic protein-protein interaction wiring of the human spliceosome. *Molecular Cell* **4**: 567–580.
- Henras A K, Soudet J, G erus M, Lebaron S, Caizergues-Ferrer M, Mougin A, Henry Y. (2008) The post-transcriptional steps of eukaryotic ribosome biogenesis. *Cellular and Molecular Life Sciences* **15**: 2334–2359.
- Henriquez R, Blobel G, Aris J P. (1990) Isolation and sequencing of NOP1. A yeast gene encoding a nucleolar protein homologous to a human autoimmune antigen. *The Journal of Biological Chemistry* **4**: 2209–2215.
- Henry Y, Wood H, Morrissey J P, Petfalski E, Kearsley S, Tollervey D. (1994) The 5' end of yeast 5.8S rRNA is generated by exonucleases from an upstream cleavage site. *The EMBO Journal* **10**: 2452–2463.
- Herrmann G, Kais S, Hoffbauer J, Shah-Hosseini K, Br uggenolte N, Schober H, F asi M, Sch ar P. (2007) Conserved interactions of the splicing factor Ntr1/Spp382 with proteins involved in DNA double-strand break repair and telomere metabolism. *Nucleic Acids Research* **7**: 2321–2332.
- Hilbert M, Kebbel F, Gubaev A, Klostermeier D. (2011) eIF4G stimulates the activity of the DEAD box protein eIF4A by a conformational guidance mechanism. *Nucleic Acids Research* **6**: 2260–2270.
- Huh W-K, Falvo J V, Gerke L C, Carroll A S, Howson R W, Weissman J S, O'Shea E K. (2003) Global analysis of protein localization in budding yeast. *Nature* **6959**: 686–691.
- Jankowsky E. (2011) RNA helicases at work: binding and rearranging. *Trends in Biochemical Sciences* **1**: 19–29.
- Jankowsky E, Bowers H. (2006) Remodeling of ribonucleoprotein complexes with DExH/D RNA helicases. *Nucleic Acids Research* **15**: 4181–4188.
- Jankowsky E, Putnam A. (2010) Duplex unwinding with DEAD-box proteins. *Methods in Molecular Biology (Clifton, N.J.)* **587**: 245–264.
- Jensen T Heick, Boulay J, Rosbash M, Libri D. (2001) The DECD box putative ATPase Sub2p is an early mRNA export factor. *Current Biology* **21**: 1711–1715.
- Jia H, Wang X, Anderson J T, Jankowsky E. (2012) RNA unwinding by the Trf4/Air2/Mtr4 polyadenylation (TRAMP) complex. *Proceedings of the National Academy of Sciences of the United States of America* **19**: 7292–7297.
- Johnson S J, Jackson R N. (2013) Ski2-like RNA helicase structures: common themes and complex assemblies. *RNA Biology* **1**: 33–43.
- Jurica M S, Licklider L J, Gygi S R, Grigorieff N, Moore M J. (2002) Purification and characterization of native spliceosomes suitable for three-dimensional structural analysis. *RNA (New York, N.Y.)* **4**: 426–439.
- Karbstein K. (2011) Inside the 40S ribosome assembly machinery. *Current Opinion in Chemical Biology* **5**: 657–663.

References

- Koodathingal P, Novak T, Piccirilli J A, Staley J P. (2010) The DEAH Box ATPases Prp16 and Prp43 Cooperate to Proofread 5' Splice Site Cleavage during Pre-mRNA Splicing. *Molecular Cell* **3**: 385–395.
- Kos M, Tollervey D. (2005) The Putative RNA Helicase Dbp4p Is Required for Release of the U14 snoRNA from Preribosomes in *Saccharomyces cerevisiae*. *Molecular Cell* **1**: 53–64.
- Kossen K, Uhlenbeck O C. (1999) Cloning and biochemical characterization of *Bacillus subtilis* YxiN, a DEAD protein specifically activated by 23S rRNA: delineation of a novel sub-family of bacterial DEAD proteins. *Nucleic Acids Research* **19**: 3811–3820.
- Kötter P, Weigand J E, Meyer B, Entian K-D, Suess B. (2009) A fast and efficient translational control system for conditional expression of yeast genes. *Nucleic Acids Research* **18**: e120.
- Kressler D, Hurt E, Bassler J. (2010) Driving ribosome assembly. *Biochimica et Biophysica Acta* **6**: 673–683.
- Kudlinski D, Schmitt A, Christian H, Ficner R. (2012) Structural analysis of the C-terminal domain of the spliceosomal helicase Prp22. *Biological Chemistry* **10**: 1131–1140.
- Kufel J, Dichtl B, Tollervey D. (1999) Yeast Rnt1p is required for cleavage of the pre-ribosomal RNA in the 3' ETS but not the 5' ETS. *RNA (New York, N.Y.)* **7**: 909–917.
- Laemmli U K. (1970) Cleavage of structural proteins during the assembly of the head of bacteriophage T4. *Nature* **5259**: 680–685.
- Lafontaine D L, Tollervey D. (2001) The function and synthesis of ribosomes. *Nature reviews. Molecular Cell Biology* **7**: 514–520.
- Laplante J M, O'Rourke F, Lu X, Fein A, Olsen A, Feinstein M B. (2000) Cloning of human Ca²⁺ homeostasis endoplasmic reticulum protein (CHERP): regulated expression of antisense cDNA depletes CHERP, inhibits intracellular Ca²⁺ mobilization and decreases cell proliferation. *The Biochemical Journal* **1**: 189–199.
- Lapiente-Brun E, Moreno-Loshuertos R, Acin-Perez R, Latorre-Pellicer A, Colas C, Balsa E, Perales-Clemente E, Quiros P M, Calvo E, Rodriguez-Hernandez M A, Navas P, Cruz R, Carracedo A, Lopez-Otin C, Perez-Martos A, Fernandez-Silva P, Fernandez-Vizarra E, Enriquez J A. (2013) Supercomplex assembly determines electron flux in the mitochondrial electron transport chain. *Science (New York, N.Y.)* **6140**: 1567–1570.
- Lebaron S, Froment C, Fromont-Racine M, Rain J-C, Monsarrat B, Caizergues-Ferrer M, Henry Y. (2005) The splicing ATPase prp43p is a component of multiple preribosomal particles. *Molecular and Cellular Biology* **21**: 9269–9282.
- Lebaron S, Papin C, Capeyrou R, Chen Y-L, Froment C, Monsarrat B, Caizergues-Ferrer M, Grigoriev M, Henry Y. (2009) The ATPase and helicase activities of Prp43p are stimulated by the G-patch protein Pfa1p during yeast ribosome biogenesis. *The EMBO Journal* **24**: 3808–3819.
- Lee C M, Sedman J, Neupert W, Stuart R A. (1999) The DNA helicase, Hmi1p, is transported into mitochondria by a C-terminal cleavable targeting signal. *The Journal of Biological Chemistry* **30**: 20937–20942.
- Leeds N B, Small E C, Hiley S L, Hughes T R, Staley J P. (2006) The splicing factor Prp43p, a DEAH box ATPase, functions in ribosome biogenesis. *Molecular and Cellular Biology* **2**: 513–522.
- Li M, Zhong Z, Zhu J, Xiang D, Dai N, Cao X, Qing Y, Yang Z, Xie J, Li Z, Baugh L, Wang G, Wang D. (2010) Identification and characterization of mitochondrial targeting sequence of human apurinic/aprimidinic endonuclease 1. *The Journal of Biological Chemistry* **20**: 14871–14881.
- Li R, Zhang H, Yu W, Chen Y, Gui B, Liang J, Wang Y, Sun L, Yang X, Zhang Y, Shi L, Li Y, Shang Y. (2009) ZIP: a novel transcription repressor, represses EGFR oncogene and suppresses breast carcinogenesis. *The EMBO Journal* **18**: 2763–2776.

References

- Liang X-H, Fournier M J. (2006) The helicase Has1p is required for snoRNA release from pre-rRNA. *Molecular and Cellular Biology* **20**: 7437–7450.
- Ligr M, Madeo F, Fröhlich E, Hilt W, Fröhlich K U, Wolf D H. (1998) Mammalian Bax triggers apoptotic changes in yeast. *FEBS Letters* **438**:61-65.
- Linder P, Jankowsky E. (2011) From unwinding to clamping — the DEAD box RNA helicase family. *Nature Reviews Molecular Cell Biology* **8**: 505–516.
- Linder P, Lasko P F, Ashburner M, Leroy P, Nielsen P J, Nishi K, Schnier J, Slonimski P P. (1989) Birth of the D-E-A-D box. *Nature* **6203**: 121–122.
- Linder P, Slonimski P P. (1988) Sequence of the genes TIF1 and TIF2 from *Saccharomyces cerevisiae* coding for a translation initiation factor. *Nucleic Acids Research* **21**: 10359.
- Long E O, Dawid I B. (1980) Repeated genes in eukaryotes. *Annual Review of Biochemistry* **49**: 727–764.
- Longtine M S, McKenzie A 3rd, Demarini D J, Shah N G, Wach A, Brachat A, Philippsen P, Pringle J R. (1998) Additional modules for versatile and economical PCR-based gene deletion and modification in *Saccharomyces cerevisiae*. *Yeast (Chichester, England)* **10**: 953–961.
- Lu H, Lu N, Weng L, Yuan B, Liu Y-J, Zhang Z. (2014) DHX15 Senses Double-Stranded RNA in Myeloid Dendritic Cells. *Journal of Immunology (Baltimore, Md. : 1950)* **3**: 1364–1372.
- Margossian S P, Li H, Zassenhaus H P, Butow R A. (1996) The DExH box protein Suv3p is a component of a yeast mitochondrial 3'-to-5' exoribonuclease that suppresses group I intron toxicity. *Cell* **2**: 199–209.
- Martin A, Schneider S, Schwer B. (2002) Prp43 Is an Essential RNA-dependent ATPase Required for Release of Lariat-Intron from the Spliceosome. *Journal of Biological Chemistry* **20**: 17743–17750.
- Martin R, Straub A U, Doebele C, Bohnsack M T. (2013) DExD/H-box RNA helicases in ribosome biogenesis. *RNA Biology* **1**: 4–18.
- Matera A Gregory, Wang Z. (2014) A day in the life of the spliceosome. *Nature reviews. Molecular Cell Biology* **2**: 108–121.
- Maudet C, Sourisce A, Dragin L, Lahouassa H, Rain J-C, Bouaziz S, Ramirez B Cecilia, Margottin-Goguet F. (2013) HIV-1 Vpr induces the degradation of ZIP and sZIP, adaptors of the NuRD chromatin remodeling complex, by hijacking DCAF1/VprBP. *PLoS one* **10**: e77320.
- Mayas R M, Maita H, Semlow D R, Staley J P. (2010) Spliceosome discards intermediates via the DEAH box ATPase Prp43p. *Proceedings of the National Academy of Sciences* **22**: 10020–10025.
- McWilliam H, Li W, Uludag M, Squizzato S, Park Y Mi, Buso N, Cowley A Peter, Lopez R. (2013) Analysis Tool Web Services from the EMBL-EBI. *Nucleic Acids Research Web Server issue*: W597-600.
- Mick D U, Wagner K, van der Laan M, Frazier A E, Perschil I, Pawlas M, Meyer H E, Warscheid B, Rehling P. (2007) Shy1 couples Cox1 translational regulation to cytochrome c oxidase assembly. *The EMBO Journal* **20**: 4347–4358.
- Min J, Heuert R M, Zassenhaus H P. (1993) Isolation and characterization of an NTP-dependent 3'-exoribonuclease from mitochondria of *Saccharomyces cerevisiae*. *The Journal of Biological Chemistry* **10**: 7350–7357.
- Moll I, Grill S, Grundling A, Blasi U. (2002) Effects of ribosomal proteins S1, S2 and the DeaD/CsdA DEAD-box helicase on translation of leaderless and canonical mRNAs in *Escherichia coli*. *Molecular Microbiology* **5**: 1387–1396.
- Montpetit B, Thomsen N D, Helmke K J, Seeliger M A, Berger J M, Weis K. (2011) A conserved mechanism of DEAD-box ATPase activation by nucleoporins and InsP6 in mRNA export. *Nature* **7342**: 238–242.

References

- Mosallanejad K, Sekine Y, Ishikura-Kinoshita S, Kumagai K, Nagano T, Matsuzawa A, Takeda K, Naguro I, Ichijo H. (2014) The DEAH-box RNA helicase DHX15 activates NF-kappaB and MAPK signaling downstream of MAVS during antiviral responses. *Science Signaling* **323**: ra40.
- Myong S, Cui S, Cornish P V, Kirchhofer A, Gack M U, Jung J U, Hopfner K-P, Ha T. (2009) Cytosolic viral sensor RIG-I is a 5'-triphosphate-dependent translocase on double-stranded RNA. *Science (New York, N.Y.)* **5917**: 1070–1074.
- Nag A, Steitz J A. (2012) Tri-snRNP-associated proteins interact with subunits of the TRAMP and nuclear exosome complexes, linking RNA decay and pre-mRNA splicing. *RNA Biology* **3**: 334–342.
- Nissen P, Hansen J, Ban N, Moore P B, Steitz T A. (2000) The structural basis of ribosome activity in peptide bond synthesis. *Science (New York, N.Y.)* **5481**: 920–930.
- Niu Z, Jin W, Zhang L, Li X. (2012) Tumor suppressor RBM5 directly interacts with the DEXD/H-box protein DHX15 and stimulates its helicase activity. *FEBS Letters* **7**: 977–983.
- Oberer M, Marintchev A, Wagner G. (2005) Structural basis for the enhancement of eIF4A helicase activity by eIF4G. *Genes & Development* **18**: 2212–2223.
- Palonen E, Lindstrom M, Somervuo P, Johansson P, Bjorkroth J, Korkeala H. (2012) Requirement for RNA helicase CsdA for growth of *Yersinia pseudotuberculosis* IP32953 at low temperatures. *Applied and Environmental Microbiology* **4**: 1298–1301.
- Pandit S, Lynn B, Rymond B C. (2006) Inhibition of a spliceosome turnover pathway suppresses splicing defects. *Proceedings of the National Academy of Sciences of the United States of America* **37**: 13700–13705.
- Pandit S, Paul S, Zhang L, Chen M, Durbin N, Harrison, S M W, Rymond B C. (2009) Spp382p Interacts with Multiple Yeast Splicing Factors, Including Possible Regulators of Prp43 DEXD/H-Box Protein Function. *Genetics* **1**: 195–206.
- Pang Q, Hays J B, Rajagopal I (1993) Two cDNAs from the plant *Arabidopsis thaliana* that partially restore recombination proficiency and DNA-damage resistance to *E. coli* mutants lacking recombination-intermediate-resolution activities. *Nucleic Acids Research* **7**: 1647–1653.
- Peil L, Virumae K, Remme J. (2008) Ribosome assembly in *Escherichia coli* strains lacking the RNA helicase DeaD/CsdA or DbpA. *The FEBS Journal* **15**: 3772–3782.
- Pena V, Jovin S M, Fabrizio P, Orłowski J, Bujnicki J M, Lührmann R, Wahl M C. (2009) Common design principles in the spliceosomal RNA helicase Brr2 and in the Hel308 DNA helicase. *Molecular Cell* **4**: 454–466.
- Pertschy B, Schneider C, Gnadig M, Schafer T, Tollervey D, Hurt E. (2009) RNA Helicase Prp43 and Its Co-factor Pfa1 Promote 20 to 18 S rRNA Processing Catalyzed by the Endonuclease Nob1. *Journal of Biological Chemistry* **50**: 35079–35091.
- Polster B M, Basanez G, Etxebarria A, Hardwick J Marie, Nicholls D G. (2005) Calpain I induces cleavage and release of apoptosis-inducing factor from isolated mitochondria. *The Journal of Biological Chemistry* **8**: 6447–6454.
- Powis K, Schrul B, Tienson H, Gostimskaya I, Breker M, High S, Schuldiner M, Jakob U, Schwappach B. (2013) Get3 is a holdase chaperone and moves to deposition sites for aggregated proteins when membrane targeting is blocked. *Journal of Cell Science Pt 2*: 473–483.
- Pyle A M. (2008) Translocation and unwinding mechanisms of RNA and DNA helicases. *Annual Review of Biophysics* **37**: 317–336.
- Rinnerthaler M, Jarolim S, Heeren G, Palle E, Perju S, Klinger H, Bogengruber E, Madoe F, Braun R J, Breitenbach-Koller L, Breitenbach M, Laun P. (2006) MMI1 (YKL056c, TMA19), the yeast orthologue of the translationally controlled tumor protein (TCTP) has apoptotic functions and interacts with both microtubules and mitochondria. *Biochimica et Biophysica Acta* **5-6**: 631–638.

References

- Rodríguez-Galan O, García-Gómez J J, de la Cruz, J. (2013) Yeast and human RNA helicases involved in ribosome biogenesis: current status and perspectives. *Biochimica et Biophysica Acta* **8**: 775–790.
- Roy J, Kim K, Maddock J R, Anthony J G, Woolford, J L Jr. (1995) The final stages of spliceosome maturation require Spp2p that can interact with the DEAH box protein Prp2p and promote step 1 of splicing. *RNA (New York, N.Y.)* **4**: 375–390.
- Sambrook J, Fritsch E F, Maniatis T. (1989) *Molecular Cloning: A Laboratory Manual*.
- Schütz P, Bumann M, Oberholzer A Erich, Bieniossek C, Trachsel H, Altmann M, Baumann U. (2008) Crystal structure of the yeast eIF4A-eIF4G complex: an RNA-helicase controlled by protein-protein interactions. *Proceedings of the National Academy of Sciences of the United States of America* **28**: 9564–9569.
- Silverman E J, Maeda A, Wei J, Smith P, Beggs J D, Lin R-J. (2004) Interaction between a G-Patch Protein and a Spliceosomal DEXD/H-Box ATPase That Is Critical for Splicing. *Molecular and Cellular Biology* **23**: 10101–10110.
- Singleton M R, Dillingham M S, Wigley D B. (2007) Structure and mechanism of helicases and nucleic acid translocases. *Annual Review of Biochemistry*: 23–50.
- Sloan K E, Leisegang M S, Doebele C, Ramirez A S, Simm S, Safferthal C, Kretschmer J, Schorge T, Markoutsas S, Haag S, Karas M, Ebersberger I, Schleiff E, Watkins N J, Bohnsack M T. (2015) The association of late-acting snoRNPs with human pre-ribosomal complexes requires the RNA helicase DDX21. *Nucleic Acids Research* **1**: 553–564.
- Small E C, Leggett S R, Winans A A, Staley J P. (2006) The EF-G-like GTPase Snu114p regulates spliceosome dynamics mediated by Brr2p, a DEXD/H box ATPase. *Molecular Cell* **3**: 389–399.
- Steinmetz E J, Conrad N K, Brow D A, Corden J L. (2001) RNA-binding protein Nrd1 directs poly(A)-independent 3'-end formation of RNA polymerase II transcripts. *Nature* **6853**: 327–331.
- Stepien P P, Margossian S P, Landsman D, Butow R A. (1992) The yeast nuclear gene *suv3* affecting mitochondrial post-transcriptional processes encodes a putative ATP-dependent RNA helicase. *Proceedings of the National Academy of Sciences of the United States of America* **15**: 6813–6817.
- Stojanovski D, Bragoszewski P, Chacinska A. (2012) The MIA pathway: a tight bond between protein transport and oxidative folding in mitochondria. *Biochimica et Biophysica Acta* **7**: 1142–1150.
- Sutherland L C, Wang K, Robinson A G. (2010) RBM5 as a putative tumor suppressor gene for lung cancer. *Journal of Thoracic Oncology* **3**: 294–298.
- Tanaka N, Aronova A, Schwer B. (2007) Ntr1 activates the Prp43 helicase to trigger release of lariat-intron from the spliceosome. *Genes & Development* **18**: 2312–2325.
- Tanaka N, Schwer B. (2006) Mutations in PRP43 that uncouple RNA-dependent NTPase activity and pre-mRNA splicing function. *Biochemistry* **20**: 6510–6521.
- Tanner N, Cordin O, Banroques J, Doère M, Linder P. (2003) The Q Motif A Newly Identified Motif in DEAD Box Helicases May Regulate ATP Binding and Hydrolysis. *Molecular Cell* **1**: 127–138.
- Tannukit S, Crabb T L, Hertel K J, Wen X, Jans D A, Paine M L. (2009) Identification of a novel nuclear localization signal and speckle-targeting sequence of tuftelin-interacting protein 11, a splicing factor involved in spliceosome disassembly. *Biochemical and Biophysical Research Communications* **3**: 1044–1050.
- Tarassov I, Entelis N, Martin R P. (1995) Mitochondrial import of a cytoplasmic lysine-tRNA in yeast is mediated by cooperation of cytoplasmic and mitochondrial lysyl-tRNA synthetases. *The EMBO Journal* **14**: 3461–3471.

References

- Tarassov K, Messier V, Landry C R, Radinovic S, Serna M, Mercedes M, Shames I, Malitskaya Y, Vogel J, Bussey H, Michnick S W. (2008) An in vivo map of the yeast protein interactome. *Science (New York, N.Y.)* **5882**: 1465–1470.
- Teng X, Hardwick J M. Reliable Method for Detection of Programmed Cell Death in Yeast *Methods in Molecular Biology* **559**: 335–42.
- Thibault G, Ismail N, Davis T W. (2011) The unfolded protein response supports cellular robustness as a broad-spectrum compensatory pathway. *Proceedings of the National Academy of Sciences of the United States of America* **51**: 20597–20602.
- Treco D A, Lundblad V. (2001) Preparation of yeast media. *Current Protocols in Molecular Biology* **23**: 13.1.1–13.1.7.
- Tsai R-T, Fu R-H, Yeh F-L, Tseng C-K, Lin Y-C, Huang Y-H, Cheng S-C. (2005) Spliceosome disassembly catalyzed by Prp43 and its associated components Ntr1 and Ntr2. *Genes & Development* **24**: 2991–3003.
- Tsai R-T, Tseng C-K, Lee P-J, Chen H-C, Fu R-H, Chang K-j, Yeh F-L, Cheng S-C. (2007) Dynamic Interactions of Ntr1-Ntr2 with Prp43 and with U5 Govern the Recruitment of Prp43 To Mediate Spliceosome Disassembly. *Molecular and Cellular Biology* **23**: 8027–8037.
- Tseng S S, Weaver P L, Liu Y, Hitomi M, Tartakoff A M, Chang T H. (1998) Dbp5p, a cytosolic RNA helicase, is required for poly(A)+ RNA export. *The EMBO Journal* **9**: 2651–2662.
- Tsu C A, Kossen K, Uhlenbeck O C. (2001) The Escherichia coli DEAD protein DbpA recognizes a small RNA hairpin in 23S rRNA. *RNA (New York, N.Y.)* **5**: 702–709.
- Ursic D, Himmel K L, Gurley K A, Webb F, Culbertson M R. (1997) The yeast SEN1 gene is required for the processing of diverse RNA classes. *Nucleic Acids Research* **23**: 4778–4785.
- van der Feltz C, Anthony K, Brilot A, Pomeranz Krummel D A. (2012) Architecture of the spliceosome. *Biochemistry* **16**: 3321–3333.
- Venema J, Tollervey D. (1999) Ribosome synthesis in Saccharomyces cerevisiae. *Annual Review of Genetics* **33**: 261–311.
- Vukotic M, Oeljeklaus S, Wiese S, Vogtle F N, Meisinger C, Meyer H E, Ziesenis A, Katschinski D M, Jans D C, Jakobs S, Warscheid B, Rehling P, Deckers M. (2012) Rcf1 mediates cytochrome oxidase assembly and respirasome formation, revealing heterogeneity of the enzyme complex. *Cell Metabolism* **3**: 336–347.
- Walbott H, Mouffok S, Capeyrou R, Lebaron S, Humbert O, van Tilbeurgh H, Henry Y, Leulliot N. (2010) Prp43p contains a processive helicase structural architecture with a specific regulatory domain. *The EMBO Journal* **13**: 2194–2204.
- Warner J R. (1999) The economics of ribosome biosynthesis in yeast. *Trends in Biochemical Sciences* **11**: 437–440.
- Watkins N J, Bohnsack M T. (2012) The box C/D and H/ACA snoRNPs: key players in the modification, processing and the dynamic folding of ribosomal RNA. *Wiley Interdisciplinary Reviews: RNA* **3**: 397–414.
- Westphal D, Dewson G, Czabotar P E, Kluck R M. (2011) Molecular biology of Bax and Bak activation and action. *Biochimica et Biophysica Acta* **4**: 521–531.
- Will C L, Lührmann R. (2011) Spliceosome structure and function. *Cold Spring Harbor Perspectives in Biology* **7**
- Wilson B J, Bates G J, Nicol S M, Gregory D J, Perkins N D, Fuller-Pace F V. (2004) The p68 and p72 DEAD box RNA helicases interact with HDAC1 and repress transcription in a promoter-specific manner. *BMC Molecular Biology* **5**: 11.
- Woodman I L, Bolt E L. (2011) Winged helix domains with unknown function in Hel308 and related helicases. *Biochemical Society Transactions* **1**: 140–144.

References

- Woolford J L Jr, Baserga S J (2013) Ribosome biogenesis in the yeast *Saccharomyces cerevisiae*. *Genetics* **3**: 643–681.
- Wu C-H, Chen P-J, Yeh S-H. (2014) Nucleocapsid phosphorylation and RNA helicase DDX1 recruitment enables coronavirus transition from discontinuous to continuous transcription. *Cell Host & Microbe* **4**: 462–472.
- Wyrick J J, Holstege F C, Jennings E G, Causton H C, Shore D, Grunstein M, Lander E S, Young R A. (1999) Chromosomal landscape of nucleosome-dependent gene expression and silencing in yeast. *Nature* **6760**: 418–421.
- Xie J, Beickman K, Otte E, Rymond B C. (1998) Progression through the spliceosome cycle requires Prp38p function for U4/U6 snRNA dissociation. *The EMBO Journal* **10**: 2938–2946.
- Yang H, Ren Q, Zhang Z. (2008) Cleavage of Mcd1 by caspase-like protease Esp1 promotes apoptosis in budding yeast. *Molecular Biology of the Cell* **5**: 2127–2134.
- Yang Q, Fairman M E, Jankowsky E. (2007) DEAD-box-protein-assisted RNA structure conversion towards and against thermodynamic equilibrium values. *Journal of Molecular Biology* **4**: 1087–1100.
- Yang Q, Jankowsky E. (2005) ATP- and ADP-dependent modulation of RNA unwinding and strand annealing activities by the DEAD-box protein DED1. *Biochemistry* **41**: 13591–13601.
- Yean S L, Lin R J. (1991) U4 small nuclear RNA dissociates from a yeast spliceosome and does not participate in the subsequent splicing reaction. *Molecular and Cellular Biology* **11**: 5571–5577.
- Yoneyama M, Fujita T. (2008) Structural mechanism of RNA recognition by the RIG-I-like receptors. *Immunity* **2**: 178–181.
- Yoo J E, Oh B-K, Park Y N. (2009) Human PinX1 Mediates TRF1 Accumulation in Nucleolus and Enhances TRF1 Binding to Telomeres. *Journal of Molecular Biology* **5**: 928–940.
- Yoshimoto R, Kataoka N, Okawa K, Ohno M. (2009) Isolation and characterization of post-splicing lariat-intron complexes. *Nucleic Acids Research* **3**: 891–902.
- Young C L, Khoshnevis S, Karbstein K. (2013) Cofactor-dependent specificity of a DEAD-box protein. *Proceedings of the National Academy of Sciences of the United States of America* **29**: E2668-76.
- Zang S, Lin T-Y, Chen X, Gencheva M, Newo, Alain N S, Yang L, Rossi D, Hu J, Lin S-B, Huang A, Lin R-J. (2014) GPKOW is essential for pre-mRNA splicing in vitro and suppresses splicing defect caused by dominant-negative DHX16 mutation in vivo. *Bioscience Reports* **6**: e00163
- Zhang L, Xu T, Maeder C, Bud L-O, Shanks J, Nix J, Guthrie C, Pleiss J A, Zhao R. (2009) Structural evidence for consecutive Hel308-like modules in the spliceosomal ATPase Brr2. *Nature Structural & Molecular Biology* **7**: 731–739.
- Zhou X Z, Lu K P. (2001) The Pin2/TRF1-Interacting Protein PinX1 Is a Potent Telomerase Inhibitor. *Cell* **3**: 347–359

PUBLICATION

Part of this work is being published:

Heininger, A.U., Hackert, P., Andreou, A.Z., Boon, K.L., Memet, I., Prior, M., Clancy, A., Schmidt, B., Urlaub, H., Schleiff, E., Sloan, K.E., Deckers, M., Lührmann, R., Enderlein, J., Klostermeier, D., Rehling, P., Bohnsack, M.T. (2016) Protein cofactor competition regulates the action of a multifunctional RNA helicase in different pathways. *RNA Biol*, *in press*. DOI: 10.1080/15476286.2016.1142038

ACKNOWLEDGMENTS

I want to thank...

... my supervisor Prof. Dr. Markus T. Bohnsack for his excellent supervision and support, the inspiring discussions and the experience that I could gain in his group during my PhD work. Furthermore, I want to thank him for the social group events.

... my Thesis committee Prof. Dr. Markus T. Bohnsack, Prof. Dr. Jörg Enderlein and Prof. Dr. Jörg Stülke for supervision.

... Prof. Dr. Jörg Enderlein, Prof. Dr. Dagmar Klostermeier, Prof. Dr. Peter Rehling, Dr. Bernhard Schmidt, Prof. Dr. Henning Urlaub, Dr. Markus Deckers, Dr. Mira Prior, Dr. Alexandra Andreou, PhD Nuno Raimundo, and Olaf Bernhard for their collaboration, support and the useful conversations.

... Prof. Dr. Blanche Schwappach and the whole department of the Molecular Biology for the support and a great time in the labs.

... Philipp Hackert for his collaboration, discussions, and help during this work.

... Dr. Katherine Sloan for the inspiring discussions, support and proofreading.

... Gabriela Brodtkorb for the interesting conversations and her help with administration.

... Dr. Roman Martin, Lukas Brüning, Philipp Hackert, Dr. Carmen Döbele, Jens Kretschmer, Ahmed Warda, Dr. Katherine Sloan, and Dr. Sara Haag for a great time in the lab, the interesting conversations and the pleasant lunchtimes.

... Lukas & Svenja, Roman & Hasret, Carmen, and Jens for the great time outside of the lab.

... my family: my brother Matthias, Carina, Julian, Sophia, Franz, Margit, Yvonne and the big rest for the distractions at the right time. Especial thanks goes to my parents, Wolfgang and Martina, for the enduring support and encouragement. Thank you!!

... my husband, Johannes. Thousand words wouldn't be enough to thank you, but four words to explain it: You are my saviour!

CURRICULUM VITAE

Personal information

Date and place of birth: 03.06.1986 in Aschaffenburg
Family status: married
Birth name: Straub

Doctoral thesis **Georg August University of Göttingen**

Since 01/11/2012 Topic: *Characterisation of the yeast RNA helicase Prp43*

Academic studies **Biochemistry (Diploma)**
Goethe University Frankfurt am Main
Final grade: 1.3

01/11/2010 - 01/08/2011 **Diploma thesis**
Topic: *Probing the mechanisms of transmembrane communication by EnvZ_{Ec} with Cys-based reactivity studies*

26/10/2010 **Oral Diploma examination, grade: 1.4**

10/2008 - 31/07/2011 **Advanced study period**
Main subjects: Biochemistry, Biophysical chemistry
Subsidiary subject: Neurobiology

10/2006 - 09/2008 **Basic study period**

School education

09/1997 - 07/2006 **Friedrich-Dessauer-Gymnasium, Aschaffenburg**

Practical experience

Since 07/2012 **Biochemist** at Centre of Biochemistry and Molecular cell biology
Department: Molecular Biology
University Medical Centre Göttingen
(*Characterisation of RNA helicases in dependence of cofactors*)

08/2011 - 06/2012 **Biochemist** at Institute of Molecular Biosciences
Department: Molecular cell biology of plants
University of Frankfurt a.M.
(*Characterisation of protein-RNA interactions during ribosome biogenesis*)

11/2010 - 07/2011	Researcher at the Institute of Biochemistry I, Department of Molecular Biochemistry <i>(Signal-transduction in the two-component system of E. coli)</i>
06/2010 - 07/2010	Internship at Institute of Biochemistry I, Department of Pathobiochemistry University Medical Centre Frankfurt a.M. <i>(Regulation of protein expression in kidney cells)</i>
04/2010 - 05/2010	Internship at Institute of Biochemistry, Department of Molecular membrane biology and neurobiology University of Frankfurt a.M. <i>(Behaviour and habituation of C. elegans strains containing Channelrhodopsin-2 expressing mechanoreceptor cells)</i>
09/2007	Internship at the central laboratory Medical Centre Aschaffenburg-Alzenau <i>Clinical chemistry, Immunology und Haematology</i>

Publications	<p>Martin R, Straub A U, Doebele C, Bohnsack M T. (2013) DExD/H-box RNA helicases in ribosome biogenesis. <i>RNA Biology</i> 1: 4–18.</p> <p>Heininger, A.U., Hackert, P., Andreou, A.Z., Boon, K.L., Memet, I., Prior, M., Clancy, A., Schmidt, B., Urlaub, H., Schleiff, E., Sloan, K.E., Deckers, M., Lührmann, R., Enderlein, J., Klostermeier, D., Rehling, P., Bohnsack, M.T. (2016) Protein cofactor competition regulates the action of a multifunctional RNA helicase in different pathways. <i>RNA Biol</i>, <i>in press</i>.</p>
---------------------	--

RNA helicases have many important roles in cell metabolism and are involved in numerous pathways, e.g. translation, pre-mRNA splicing and biogenesis. Interestingly, an increasing number of RNA helicases have been shown to be required for more than one cellular pathway. Therefore, protein cofactors have been suggested to recruit multifunctional RNA helicases to their substrates and regulate their activity. The best characterised family of helicase cofactors are G-patch proteins, which all contain a glycine-rich domain. This work focuses on the characterisation of the yeast RNA helicase Prp43 and its G-patch protein cofactors. Additionally, a new G-patch protein cofactor of Prp43 was identified and characterised. Together, the data suggest that protein cofactors can regulate the distribution and activity of RNA helicases in different pathways.



ISBN: 978-3-86395-237-2

Universitätsverlag Göttingen